

**EFFECTS OF INTERNAL MELTING AND
BUOYANCY ON MELT BAND EVOLUTION:
IMPLICATIONS FOR MID-OCEAN RIDGE
MELT TRANSPORT**

A Thesis Submitted to the College of Graduate and Postdoctoral Studies
In Partial Fulfillment of the Requirements
For the Degree of Master of Science
In the Department of Geological Sciences
University of Saskatchewan
Saskatoon

By

ZOË VESTRUM

I would like to dedicate this thesis to my loving family, particularly my grandfather, Abraham Klassen, and my aunt, Sheryn Clamp, both of whom encouraged my studies and passed away during the course of this research.

PERMISSION TO USE

In presenting this thesis/dissertation in partial fulfillment of the requirements for a Postgraduate degree from the University of Saskatchewan, I agree that the Libraries of this University may make it freely available for inspection. I further agree that permission for copying of this thesis/dissertation in any manner, in whole or in part, for scholarly purposes may be granted by the professor or professors who supervised my thesis/dissertation work or, in their absence, by the Head of the Department or the Dean of the College in which my thesis work was done. It is understood that any copying or publication or use of this thesis/dissertation or parts thereof for financial gain shall not be allowed without my written permission. It is also understood that due recognition shall be given to me and to the University of Saskatchewan in any scholarly use which may be made of any material in my thesis/dissertation.

DISCLAIMER

Reference in this thesis/dissertation to any specific commercial products, process, or service by trade name, trademark, manufacturer, or otherwise, does not constitute or imply its endorsement, recommendation, or favoring by the University of Saskatchewan. The views and opinions of the author expressed herein do not state or reflect those of the University of Saskatchewan, and shall not be used for advertising or product endorsement purposes.

Requests for permission to copy or to make other uses of materials in this thesis/dissertation in whole or part should be addressed to:

Head of the Department of Geological Sciences
114 Science Place
University of Saskatchewan
Saskatoon, Saskatchewan S7N 5E2 Canada

OR

Dean
College of Graduate and Postdoctoral Studies
University of Saskatchewan
116 Thorvaldson Building, 110 Science Place
Saskatoon, Saskatchewan S7N 5C9 Canada

Acknowledgements

I would like to first and foremost acknowledge the continuous support of my supervisor, Professor Butler. His mentorship and insight has been invaluable in the completion of this research.

I am grateful for the support of my research group, particularly Todd LeBlanc, who has been with me every step of the way. I am also thankful for the support of many dedicated women of science, including: Susan James, Brittany Laing, Lavie Nguyen, Joyce McBeth, Teddi Herring, Moriah Rempel, and Meagan Gilbert.

Abstract

This study analyses a two-phase porous medium whose permeability and solid viscosity are dependent on porosity. It has been established experimentally and numerically that when such a medium is subjected to shear, the porosity rearranges into stripes of high and low porosity known as melt bands (*Holtzman et al. 2003; Katz et al. 2006; Butler 2009*). This study uses linear theory and numerical simulations to analyze the formation of melt bands with ongoing melting and buoyancy forces. This is the first study to use analytical methods to isolate the effects of internal melting on melt bands. This study first looks at a square geometry with a simple shear stress regime to look at the effects different parameters have on the bands. The second model is used to validate the results of the first model as an analogue for the movement under the Mid-Ocean Ridge by implementing a more complex geometry based on the stream function from *Spiegelman and McKenzie (1987)*. Both numerical and analytical results for the square geometry showed that the internal melting and strain-rate exponent, which increases the viscosity's dependence on strain rate, both decrease the growth of the bands. The results showed that internal melting increases the effects of the strain-rate exponent on the angle of maximum growth (deviating it symmetrically about 45°), but the effect is small. While buoyancy was shown to cause oscillations which are dampened by the addition of internal melting, the growth of bands is not affected. The presence of ongoing melting when bulk viscosity is constant decreases the growth rate and therefore decreases the expected magnitude of the melt bands. However, when bulk viscosity is dependent on porosity and strain-rate, the internal melting has a marginal effect on the formation of the bands. This means that the melt bands in the upper mantle may still be a viable solution for: channeling melt towards mid-ocean ridges, acting to induce seismic anisotropy, and acting as pathways of enhanced electrical conductivity.

Table of contents

Dedication	i
Permission to Use	ii
Acknowledgements	iii
Abstract	iv
Table of Contents	v
List of figures	ix
1 Introduction	1
1.1 Creation and Transportation of Melt in the Upper Mantle	1
1.2 Melt Bands	3
1.2.1 Experimental Evidence	3
1.2.2 As Conduits for Flow	4
1.3 Significance of this study	5
2 Methodology	7
2.1 General Continuum Modeling	7
2.2 Deriving Governing Equations	7
2.3 Analytical Solutions	7
2.4 Numerical Solutions	8
2.5 Summary	8
3 The Mathematical System Governing Two-Phase Flow	9
3.1 Conservation of Mass for Solid	9
3.2 Force Balance of Fluid	10
3.3 Force Balance of Solid	10

3.4	Porosity Transformation	10
3.5	Viscosity and Permeability	11
3.6	Parameter Values	11
3.7	Summary	12
4	Effects of Buoyancy and Internal Melting on the Evolution of Melt Bands	13
4.1	Model Setup	13
4.1.1	Background Velocity and Pressure	13
4.1.2	Initial Conditions	14
4.1.3	Boundary Conditions	15
4.1.4	Numerical Geometry	15
4.2	Linear Theory	16
4.2.1	Growth-Rate	16
4.2.2	Oscillation Frequency	17
4.3	Numerical Results	18
4.3.1	Amplitude	19
4.3.2	Angle Analysis	21
4.3.3	Oscillation Frequency	22
4.4	Discussion	23
4.5	Conclusions	24
5	Quantifying the Error Introduced by Density Variation	25
5.1	Model Setup	25
5.1.1	Background Velocity and Pressure	25
5.1.2	Initial and Boundary Conditions as well as Numerical Geometry	26
5.2	Linear Theory	26
5.2.1	Variable Bulk Viscosity	26
5.2.2	Constant Bulk Viscosity	27
5.2.3	Comparison of Analytical Solutions	28
5.2.4	Without Applied Shear	30
5.3	Numerical Results	31
5.3.1	Amplitude	31
5.3.2	Oscillation Frequency	34
5.4	Discussion	34
5.5	Conclusions	35

6	Computational Analysis of Two-Phase Corner-Flow	36
6.1	Model Setup	36
6.1.1	Background Velocity and Pressure	36
6.1.2	Initial Conditions	37
6.1.3	Streamline Geometry	38
6.1.4	Boundary Conditions	38
6.2	Results	39
6.3	Discussion	41
6.4	Conclusions	42
7	Conclusions	43
	References	45
	Appendix A Derivations	50
A.1	Conservation of Mass	50
A.1.1	Fluid	51
A.1.2	Solid	52
A.1.3	Total	54
A.2	Force Balance	54
A.2.1	Fluid Force Balance	57
A.2.2	Solid Force Balance	58
	Appendix B Non-Dimensionalization	62
B.1	Conservation of Mass of Solid	62
B.2	Fluid Force Balance with Conservation of Total Mass	63
B.3	Solid Force Balance	63
	Appendix C Analytical Solution : Excluding Density Variation in Non-Buoyancy	
	Terms	65
C.1	Zeroth Order	66
C.1.1	Background Porosity	66
C.1.2	Zeroth Order Viscosity and Permeability	67
C.1.3	Zeroth Order Governing Equations	68
C.2	First Order	69
C.2.1	Linearizing First Order Viscosity and Permeability	70
C.2.2	First Order Governing Equations	72
C.2.3	Bringing It All Together	78

Appendix D Analytical Solution : Isotropic Expansion	80
D.1 Zeroth Order	81
D.1.1 Fluid Force Balance	81
D.1.2 Conservation of Solid Mass	81
D.1.3 Viscosity and Permeability	82
D.1.4 Solid Force Balance	83
D.2 First Order	84
D.2.1 Viscosity and Permeability	84
D.2.2 Conservation of Solid Mass	87
D.2.3 Fluid Force Balance	90
D.2.4 Solid Force Balance	91
D.2.5 Bringing It All Together	94
D.3 Growth Rate	94
D.3.1 Variable Bulk Viscosity	95
D.3.2 Constant Bulk Viscosity	95
D.4 Oscillation Frequency	97
D.4.1 Variable Bulk Viscosity	97
D.4.2 Constant Bulk Viscosity	97

List of figures

1.1	Google Earth Diagram of the Mid-Atlantic Ridge	1
1.2	Illustration of Hypothesized Melt Transport Mechanisms	3
1.3	Experimental Results of Melt Bands from Holtzman and Kohlstedt	4
1.4	Melt Bands Illustration	6
4.1	Simple Shear Stress and Strain Diagram	14
4.2	Initial Porosity Fields	15
4.3	Simple Geometry Schematic	15
4.4	Analytical Growth-Rate for Various Angles	17
4.5	Analytical Frequency at Different Strains for Varying Melt Rate and Strain-Rate Exponents	18
4.6	Numerical Solution for Simple Shear with Internal Melting	19
4.7	Amplitude Comparison for Various Parameters	20
4.8	Amplitude Comparison for Different Strain-Rate Exponents and Melt Rates	21
4.9	Comparison of Angular Distribution for Various Analytical and Numerical Solutions	22
4.10	Oscillation Frequency Comparison for Analytical and Numerical Solutions	23
5.1	Comparison of Analytical Growth Rates	29
5.2	Comparison of Analytical Frequencies	30
5.3	Amplitude Comparison for Models Including Density Difference for Various Strain-Rate Exponents and Melt Rates	31
5.4	Amplitude Comparison for Models Including Density Difference and a Constant Bulk Viscosity for Various Strain-Rate Exponents and Melt Rates	32
5.5	Amplitude Comparison for Isotropic Expansion Models with No Applied Shear	33
5.6	Parameter Comparison for Analytical and Numerical Results without Applied Shear	33

5.7	Oscillation Frequency Comparison for Analytical and Numerical Solutions with Density Variation and Variable Bulk Viscosity	34
6.1	Background Pressure Ridge	37
6.2	Geometric setup of the corner flow model	38
6.3	Boundary Conditions for the Corner Flow Model	38
6.4	Porosity results for Mid-Ocean Ridge Geometry	39
6.5	Band Amplitude over time for Regions under the Mid-Ocean Ridge	41
A.1	Physics Potato	50

Chapter 1

Introduction

1.1 Creation and Transportation of Melt in the Upper Mantle

Decompression melting occurs continuously as mantle upwells, rapidly decreasing the lithostatic pressure but retaining heat, creating partial melt. How this melt is transported from the mantle to the surface is not well understood (*Keller et al., 2017*). This phenomenon is typical of Mid-Ocean Ridges (figure 1.1) which are divergent oceanic tectonic plate boundaries. The ‘spine’ where the plates are diverging laterally and melt comes to surface is known as the ridge axis. The upper mantle beneath the Mid-Ocean Ridge consists of peridotites which are composed primarily of olivine and pyroxenes: clinopyroxene and orthopyroxene, with small amounts of garnet, spinel, or plagioclase (*Gill, 2010*). Pyroxenes comprise the majority of melt, first clinopyroxene is depleted, then orthopyroxene, leaving

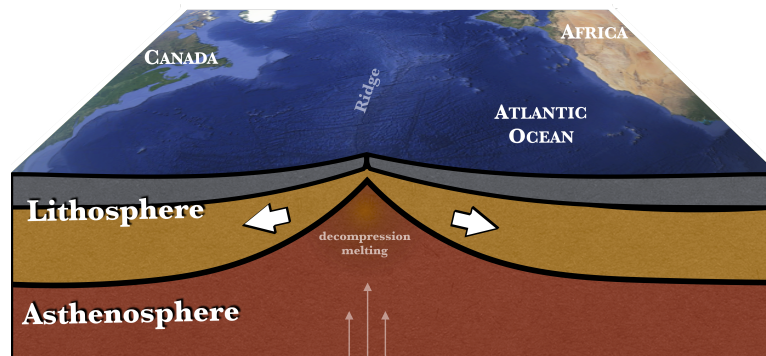


Fig. 1.1 Satellite image of the Mid-Atlantic Ridge from Google Earth with a schematic diagram illustrating the structures beneath the surface based on information from *Kearey et al., 2009*. Diagram not to scale. (Google Earth image ©2018 Google)

solidus olivine (Box 5.4 in *Gill*, 2010). The amount of melt present in the upper mantle beneath the Mid-Ocean Ridge is small. *Hammond and Toomey* (2003) found it to be between 0.1% and 0.7% by analysing seismic velocity anisotropy and heterogeneity under the East Pacific Rise.

There are certain observations that are not explained by our current understanding of the Mid-Ocean Ridge. The vulcanism associated with this margin is localized to within a kilometre of the ridge axis according to bathymetric and seismic data (*Vera et al.*, 1990). Melt must be rapidly transported from depth in order to preserve certain isotopes, Thorium 230 and Radium 226, which are present at the surface (*Kelemen et al.*, 1997). Melt is observed in seismic data at approximately sixty kilometres depth and up to a hundred kilometres from the ridge axis (*Forsyth et al.*, 1998). And significant elastic anisotropy is present in seismic data (*Wolfe and Silver*, 1998). Through these observations a mechanism is required to rapidly concentrate melt laterally to the ridge crest.

Several theories have been proposed to explain these observations. *Spiegelman and McKenzie* (1987) suggested that the tensional stress caused by the solid matrix being pulled by the diverging plates would create a pressure gradient causing fluid to flow towards the ridge axis (see figure 1.2b), but this explanation requires a compaction length, which describes how easily fluid flows through the medium, that is significant compared with the system size which requires that the viscosity of the mantle beneath mid-ocean ridges to be unrealistically large. *Sparks and Parmentier* (1991) theorized that melt may travel vertically, due to buoyancy force, to the base of the impermeable layer, which forms at the depth where the melt reaches its solidus temperature, then form a decompaction, dilation boundary layer where it could drain laterally to the ridge crest (see figure 1.2c). *Morgan* (1987) proposed strain created by the spreading mechanism of the Mid-Ocean Ridge could create anisotropic permeability which would allow the fluid to flow more easily through the solid matrix. This study looks at a high porosity channel system which is formed by a series of interconnected melt bands beneath a ridge axis (see figure 1.2a) as a possible explanation for: the concentration at the axis, rapid transport, large collection area, and elastic anisotropy. This solution was first proposed by *Katz et al.* (2006) who first argued that these bands were well oriented to channel melt towards the ridge axis.

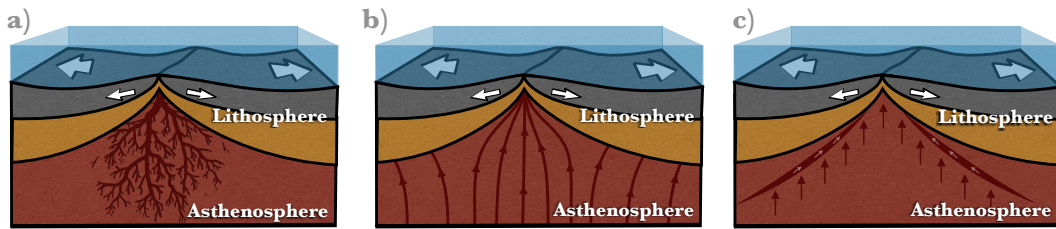


Fig. 1.2 Illustration of hypothesized melt transport mechanisms at the Mid-Ocean Ridge: a) high-porosity channel network illustration based on results found in Braun and Kelemen (2002) b) streamline illustration inspired by the results from Spiegelman and McKenzie (1987) c) dilation boundary layer with melt flow direction indicated by arrows as described by Sparks and Parmentier (1991)

1.2 Melt Bands

Consider a saturated porous material whose permeability and solid viscosity are dependent on porosity. Both the fluid and the solid materials are incompressible meaning they have a constant density, but when combined they become compressible. This means that the pressure changes the ratio of solids to fluids in a given volume. If such a material is subjected to shear at a rate slow enough that fractures do not form, the porosity will rearrange into stripes of highs and lows. This rearrangement is caused by the instability in the porosity due to the permeability and solid viscosity's dependence on porosity. This phenomenon is known as melt bands and these were first predicted theoretically by *Stevenson* (1989).

This instability was later investigated numerically by *Richardson* (1998) who found that porosity aligned in stripes along the principle stress axis. He proposed that this channelling could possibly concentrate melt at the axis of Mid-Ocean Ridges.

1.2.1 Experimental Evidence

Experiments have been performed to investigate the formation of these bands when applying shear stress using synthetic rock aggregates analogous to the peridotites found in the upper mantle beneath the Mid-Ocean Ridge (*Holtzman et al.* 2003; *Holtzman and Kohlstedt* 2007). *Holtzman and Kohlstedt* (2007) performed a series of experiments on a column of approximate peridotite using a shear deformation apparatus which had a temperature of 1523 K. Some images of the results of their experiments are seen in figure 1.3. The porosity variations can be seen in the contrast of the image: the darker areas show high porosity and the lighter areas show low porosity. The high stress scenario (figure 1.3a), which had an

applied stress of 83MPa and a duration of 35.4 minutes, shows thin (up to $15\mu\text{m}$), parallel bands. The intermediate stress scenario (figure 1.3b), which had an applied stress of 57MPa and a duration of 112.8 minutes, shows thicker (up to $50\mu\text{m}$), more interconnected bands. The low stress scenario (figure 1.3c), which had an applied stress of 28MPa and a duration of 370.8 minutes, shows much thicker (up to $75\mu\text{m}$) and highly interconnected bands. All these bands rotate clockwise and form approximately 25° from the principle compressive-stress axis which is 45° clockwise from horizontal in figure 1.3.

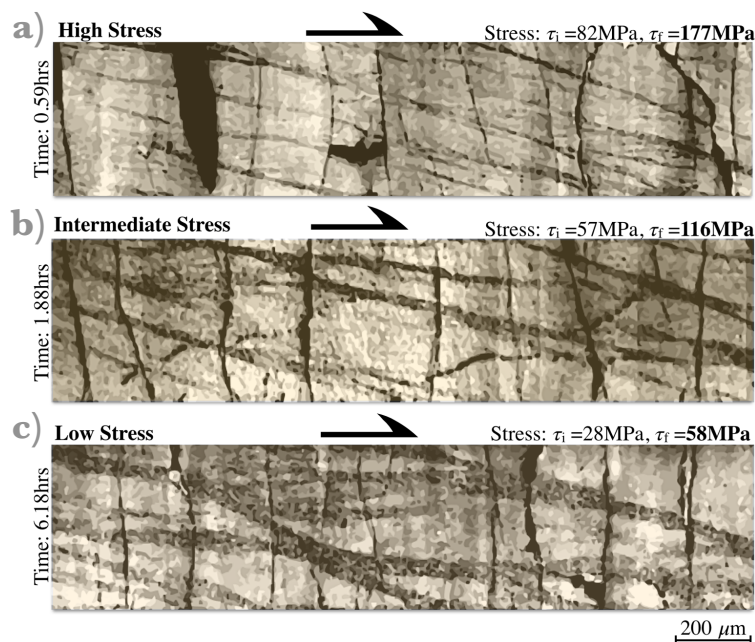


Fig. 1.3 Reflected light scans of three samples of original porosity of 4%. The rocks in the experiments were put under varying levels of shear stress for corresponding amounts of time. (modified from Holtzman and Kohlstedt (2007))

1.2.2 As Conduits for Flow

Many numerical studies have been done on the formation and evolution of melt bands (Richardson, 1998; Katz *et al.*, 2006; Katz, 2010; Katz and Takei, 2013; Butler, 2009; Butler, 2012). It has been well established that in a simple shear environment with strain-rate independent viscosity the growth of these bands is exponential and the fastest growth rate is parallel to the principle stress direction, which is 45° from horizontal for simple shear. A typical strain of 3 is experienced by mantle material during Mid-Ocean Ridge corner flow within 100km of the ridge axis with a maximum strain of 4 near the ridge axis (Butler, 2009).

The strain required to make bands of a sufficient amplitude channel melt is dependent on the initial porosity perturbation. The addition of viscosity's dependence on strain-rate decreases the growth rate of the bands and distributes the orientation symmetrically about the principle stress axis (*Katz et al.*, 2006; *Butler*, 2009). Anisotropic viscosity lowers the orientation of the growth of bands (*Butler*, 2012; *Katz and Takei*, 2013). The bulk viscosity decreases the bands' growth and is poorly constrained in the upper mantle (*Butler*, 2009). The bulk viscosity has been argued to be larger than the shear viscosity (*Katz and Takei*, 2013), in this case the bands will not have sufficient amplitude to affect melt movement in the upper mantle. Melt bands could contribute to elastic anisotropy present in the upper mantle (*Wolfe and Silver*, 1998; *Hess*, 1964; *Hammond and Toomey*, 2003) as seismic waves travel faster along planes of weakness, i.e. the bands of high porosity, than they do cutting across them.

The main motivation of this research is to determine whether melt bands are a viable solution for the transportation of melt to the base of the crust with the addition of internal melting.

1.3 Significance of this study

Geophysical observations support regions of porosity in the upper mantle with fluids migrating through the pore space (*Toomey et al.*, 1998; *Evans et al.*, 1999). Experimental and computational studies have shown that mantle material with two phases, fluid and solid, develop variations in porosity when subjected to shear (figure 1.4). The consequences of the ongoing decompression melting in the upper mantle has not previously been taken into account in theoretical and numerical calculations. Melt bands are analyzed to look at porosity distribution changes in a two phase flow as a viable way to transport the melt from the upper mantle to the crust, resulting in volcanism. Modelling these changes in porosity is essential for understanding some important mechanisms of the Earth.

There are two conflicting results for melt bands including buoyancy. *Katz et al.* (2006) proposed, supported by results from a simplified numerical model which assumed an angle relative to the principle stress direction, that melt bands could be a source of converging flows at the Mid-Ocean Ridge axes. But *Katz* (2010) included buoyancy, internal melting, and a corner flow geometry and found an absence of melt bands. Whereas *Butler's* (2009) shear simulation included buoyancy but also produced melt bands. The objective of this research is to find a more accurate representation of a Mid-Ocean Ridge: to ascertain the orientation of bands relative to the ridge axis and determine whether bands form in the presence of buoyancy and internal melting. A previous study by *Gebhardt and Butler* (2016) found that the orientation of the melt bands was not conducive to channeling melt towards the mid-ocean ridge.

The following chapters will outline the methods used, the mathematical model governing this system, analytical results for simple-shear, as well as numerical results from two models: a simple geometry model investigating the effects of internal melting and buoyancy in the growth of the bands and a model with more complex geometry. This research shows that although melt bands grow oriented away from the ridge axis, they still form with buoyancy. In a constant bulk viscosity case, internal melting decreases the amplitude of the bands. But when bulk viscosity is dependent on porosity and strain-rate, internal melting has a minimal effect on the formation of bands.

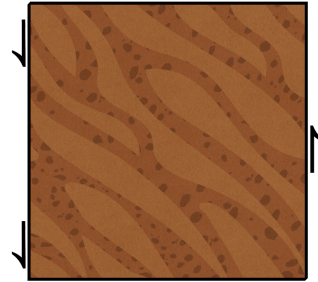


Fig. 1.4 Melt bands illustration inspired by the experimental results from *Holtzman and Kohlstedt* (2007) (figure 1.3)

Chapter 2

Methodology

2.1 General Continuum Modeling

There are three things needed in modelling:

- 1 Partial Differential Equations (PDEs)** translate physical systems into mathematics, which can be numerically approximated in computer code
- 2 Boundary Conditions** explain what happens at the edges of the model.
- 3 Initial Conditions** gives the model values at the beginning.

These are all part of the PDE problem and are used to create both analytical and numerical solutions.

2.2 Deriving Governing Equations

The first thing needed are PDEs which translate physical laws into modelling space. This is done by taking known laws such as conservation of momentum and mass, then manipulating this equation to find either a specific analytical solution, or the equations are put into a form where a numerical approximation can be made. The system is simplified using non-dimensionalization. The units are removed using scaling parameters.

2.3 Analytical Solutions

Analytical solutions use symbolic manipulation to obtain a function which is the expected outcome of the governing system. These solutions are important for validating certain

aspects of numerical models as analytical solutions can only be found in certain cases. One approximate technique for making progress analytically, known as perturbation theory, involves linearizing the system and finding a variation, or perturbation, from a known background state.

2.4 Numerical Solutions

Since an exact analytical solution cannot be found for this instability, an approximation is made by discretizing the system, then solving numerically using COMSOL[®] which is a computational modelling software that uses the finite element method. This method uses linear combinations of basis functions to numerically evaluate the behaviour of the PDEs.

2.5 Summary

Using the methodology described in this chapter combined with the mathematical system described in Chapter 3 the effects of internal melting, strain-rate exponent and buoyancy were investigated in the analytical solutions found in Appendix A and C as well as the numerical solutions in Chapters 4, 5 and 6.

Chapter 3

The Mathematical System Governing Two-Phase Flow

This chapter summarizes the mathematical system. The equations governing compacting two-phase systems were derived in Appendix A based on the original derivations in *McKenzie* (1984) and *Scott and Stevenson* (1984) with the addition of internal melting. These equations are non-dimensionalized in Appendix B using a length scale equal to the compaction length which is defined as $\delta_c = \sqrt{\eta_0 \kappa_0 / \mu}$ where η_0 is the initial solid viscosity, κ_0 is the initial permeability, and μ is the fluid viscosity. This system has length scales that are sufficiently greater than the compaction length in order to ensure that the fluid does not flow easily in the system. The compaction length of the mantle could range from 100m to 10km (*Holtzman et al.*, 2003).

3.1 Conservation of Mass for Solid

Mass cannot be created or destroyed. The change in the mass of solid inside a control volume is equal to the amount of solid material leaving the system and the amount solid being melted. The dimensionless conservation of solid mass equation is expressed as (Eq B.6):

$$\frac{\partial \phi}{\partial t} = \nabla \cdot [(1 - \phi)\vec{U}] - \Gamma \quad (3.1)$$

where ϕ is porosity, \vec{U} is the dimensionless solid velocity field, t is strain, i.e. dimensionless time, and Γ is dimensionless melt rate per unit volume. This equation means that the change in porosity over time ($\frac{\partial \phi}{\partial t}$) is equal to the amount of solid material leaving the system through the boundary ($\nabla \cdot [(1 - \phi)\vec{U}]$) combined with the amount of fluid becoming solid ($-\Gamma$).

3.2 Force Balance of Fluid

The forces in the system must be balanced in order to ensure no acceleration because of the sufficiently large fluid viscosity, albeit considerably smaller than the solid viscosity, combined with small pore sizes. Fluid force balance is defined in Darcy's Law which requires that the forces on the fluid are dominated by the drag on the walls. This is combined with conservation of fluid mass, which puts it in terms of solid velocity and porosity. The pressure was transformed to : $p = p_{fluid} + ((1 - \phi_{bac})\rho_s + \phi_{bac}\rho_f)gy$. The porosity was also transformed to a background porosity, $\phi_{bac} = \Gamma t + \phi_0$, which increases with time due to the background melting. The non-dimensionalized fluid force balance equation is given by (Eq B.11):

$$\nabla \cdot [\vec{U} - \kappa \nabla p] = -\frac{w_0}{U_0}(1 - \phi_{bac})\nabla \cdot \kappa \hat{j} + \Gamma \frac{\Delta\rho}{\rho_l} \quad (3.2)$$

where p is dimensionless pressure, κ is dimensionless permeability, and w_0 is the percolation velocity caused by the buoyancy force which is defined as $w_0 = \frac{g\Delta\rho\delta_c^2}{\eta_0}$ where $\Delta\rho$ is the difference in density between solid and fluid, g is acceleration due to gravity, and U_0 is the characteristic velocity.

3.3 Force Balance of Solid

Solid force balance assumes the inertia is negligible because of the high solid viscosity and relates the stress tensor to the pressure and buoyancy. The dimensionless version is given by equation (B.15):

$$\nabla p = \nabla \cdot [\eta(\nabla \vec{U} + (\nabla \vec{U})^T)] + \nabla(\zeta - \frac{2}{3}\eta)\nabla \cdot \vec{U} + \frac{w_0}{U_0}(\phi - \phi_{bac})\hat{j} \quad (3.3)$$

where ζ is the dimensionless bulk viscosity and η is the dimensionless solid viscosity.

3.4 Porosity Transformation

A transformation from *Butler (2017)* is introduced to the numerical models to ensure porosity stays within possible values, i.e. between zero and one. This transformation is defined as

$$\phi = \frac{1}{2}(1 + \tanh(\phi_c)). \quad (3.4)$$

where ϕ_c is the corrected porosity.

3.5 Viscosity and Permeability

The dimensionless solid viscosity, η , is defined by *Mei et al.* (2002) as

$$\eta = e^{\frac{\alpha(\phi-\phi_0)}{n_v}} \left[\sqrt{2} \left(\left(\frac{\partial U}{\partial x} \right)^2 + \left(\frac{\partial V}{\partial y} \right)^2 + \frac{1}{2} \left(\frac{\partial U}{\partial y} + \frac{\partial V}{\partial x} \right)^2 \right)^{\frac{1}{2}} \right]^{\frac{(1-n_v)}{n_v}}, \quad (3.5)$$

where α is assumed to be a constant parameters. The expression inside the square brackets denotes the second invariant of the strain-rate tensor, i.e. the strain-rate dependent term, whereas the exponential relates viscosity with porosity. If viscosity is strain-rate independent, then n_v is one, which gives the equation

$$\eta = e^{\alpha(\phi-\phi_0)} \quad (3.6)$$

where ϕ_0 is the initial porosity.

The dimensionless permeability, κ , is related to porosity by a simplified form of the Cozeny-Carman relationship, defined in *Carman* (1939), and is written as

$$\kappa = \left(\frac{\phi}{\phi_0} \right)^\beta \quad (3.7)$$

where β is a parameter exponent which dictates the permeability's dependence on porosity.

3.6 Parameter Values

The parameters α and β are taken to be -25 (*Mei et al.*, 2002) and 3 (*Wark and Watson*, 1998) respectively. Initial porosity ϕ_0 should be between 0.1% and 0.7% (*Hammond and Toomey* 2003), the simulations were run with initial porosity values of 1% and 5%. The initial porosity perturbation, $\Delta\phi$, was taken to be $\phi_0 \cdot 10^{-3}$. The bulk viscosity, ζ , of mantle materials is poorly constrained and was proposed by *Katz and Takei* (2013) to be linearly dependent on the solid viscosity: $\zeta = 5/3\eta$. This study uses two bulk viscosity models, a porosity and strain-rate dependent bulk viscosity $\zeta = \zeta_r \eta$ and constant value bulk viscosity $\zeta = \zeta_r$. The initial solid viscosity η_0 ranges from 10^{19} Pa s to 10^{21} Pa s (*Spiegelman and McKenzie* 1987). The compaction length is defined as $\delta_c = \sqrt{\eta_0 \kappa_0 / \mu}$ and ranges from 100m to 10km for the upper mantle (*Holtzman et al.*, 2003). The percolation velocity, given by $w_0 = \frac{g\Delta\rho\delta_c^2}{\eta_0}$, is between $1.6 \cdot 10^{-5}$ mm/yr and 158 mm/yr for $\Delta\rho = 500$ kg/m³ (*Guillot and Sator* 2007) and g is equal to 10 m/s². The characteristic velocity U_0 of spreading ridges range from 3 mm/yr to 30 mm/yr (*Spiegelman and McKenzie* 1987).

Melt productivity with depth is given by

$$\frac{dF}{dy} = \frac{(\partial T/\partial y)_a - (\partial T/\partial y)_s}{T\Delta S/C_p + (\partial F/\partial T)^{-1}} \quad (3.8)$$

(Morgan, 2001), where T is temperature, y is depth, and $\partial F/\partial T$ is isobaric melt productivity which is poorly constrained with values ranging between 0.01%/K and 0.6%/K (Hirschmann *et al.*, 1999). C_p is the heat capacity $C_p = (439.37 - 3734.1T^{-0.5} + (0.31702 \cdot 10^9)T^{-3})$ J/mol K (Berman, 1988). ΔS is entropy of fusion which is between 44 and 65 J/mol K (Richet *et al.*, 1993). $(\partial T/\partial y)_s$ is the solidus temperature-depth gradient which has typical values between 2.6 to 3.6 K/km (Morgan, 2001) and $(\partial T/\partial y)_a$ is the adiabatic temperature-depth gradient which is equal to $-vgT/C_p$ (Morgan, 2001) where v is the thermal expansion coefficient $v = 2.56 \cdot 10^{-5} + (T - 300)1.59 \cdot 10^{-8}$ (Katsura *et al.*, 2010). The melt productivity with depth is found to range from $2 \cdot 10^{-5}$ %/m to $7.5 \cdot 10^{-4}$ %/m. The dimensionless melt rate per unit volume is given by $\Gamma = (dF/dy)\delta_c$ and ranges from $2 \cdot 10^{-5}$ to 0.075 for temperatures between 1000 to 1550K (Lange *et al.*, 2009) and the range of parameter values outlined above.

3.7 Summary

This chapter outlined the mathematical framework that will be used to build numerical models in Chapters 4, 5 and 6 as well as analytical models in Appendix C and D.

Chapter 4

Effects of Buoyancy and Internal Melting on the Evolution of Melt Bands

4.1 Model Setup

The stress field, boundary conditions, initial conditions and geometry used for the idealized, simple-shear model are outlined below.

4.1.1 Background Velocity and Pressure

Instead of applying stress at the boundaries, a particular background velocity and pressure field is introduced:

$$\vec{U} = \vec{U}_{bac} + \vec{U}_1 \quad \text{and} \quad p = p_{bac} + p_1$$

where the subscript *bac* denotes the background state and the subscript 1 denotes the perturbation. This reduces the systems dependence on the boundary conditions and spreads the stress consistently throughout the volume. For the linear theory, the perturbation velocity and pressure are the first order perturbation expansion about the background state, whereas the numerics evaluate the perturbation velocity and pressure as the total variation from the background state.

This section focuses on simple shear, which is a specific stress regime where the strain-rate field is spatially constant and the velocity is divergence-less with only one non-zero, non-constant component. For this model the background solid velocity field and pressure are taken to be

$$U_{bac} = 0, \quad V_{bac} = x, \quad \text{and} \quad p_{bac} = 0.$$

This background velocity field is oriented such that the movement from the velocity field and the buoyancy force are in the same direction, i.e. vertical. Previous studies used a horizontal velocity field which was perpendicular to the buoyancy force which in turn made all the boundaries inlet-outlet boundaries. For the vertical shear system, material being moved by both buoyancy and shear will enter and leave the system exclusively through the top and bottom boundaries, which can be well represented by periodic boundaries.

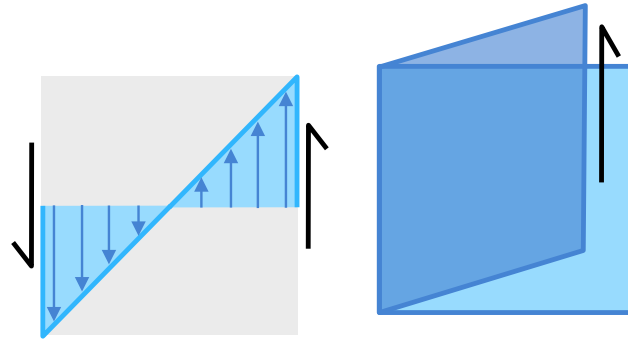


Fig. 4.1 Illustrations of the mechanics of simple shear stress (left) and strain (right)

4.1.2 Initial Conditions

The initial conditions for the system set U_1 , V_1 and p_1 to zero. This means the velocity and pressure are equal to their background fields. There were two types of initial conditions used for the porosity: waveform and random (figure 4.2). The waveform porosity field is given by $\phi = \phi_0 + \Delta\phi [\cos(k_{x_0}x + k_{y_0}y)]$ where $\Delta\phi$ is the maximum deviation from ϕ_0 and k_{x_0} , k_{y_0} are initial wave numbers which are both chosen to be equal to 4π meaning the porosity perturbations are plane waves at 45° with a period of $1/\sqrt{8}$. The random porosity field is given by $\phi = \phi_0 + \Delta\phi [\text{rand}(x,y)]$ where $\text{rand}(x,y)$ is a random function in x and y .

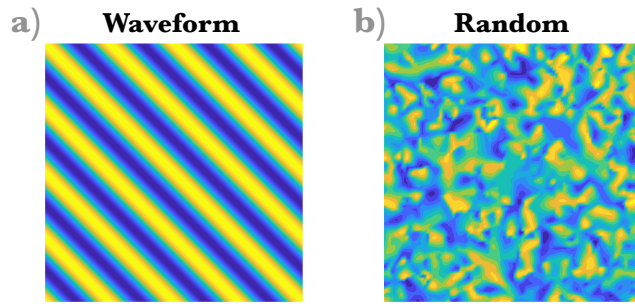


Fig. 4.2 Contour plots of the initial porosity fields with waveform on the left and random on the right.

4.1.3 Boundary Conditions

The boundary conditions used in this section were periodic for the top and bottom boundaries with a Dirichlet (constant value) boundary at the sides for velocity and porosity with values of $U_1 = 0$, $V_1 = 0$, and $\phi = \phi_{bac}$. The pressure is constrained in the centre of the geometry and periodic on all sides.

4.1.4 Numerical Geometry

The geometry used in this model is a simple square. The area of interest is a smaller two-by-two square at the centre of a ten-by-ten square (figure 4.3). This decreases the artifacts caused by the boundary conditions.

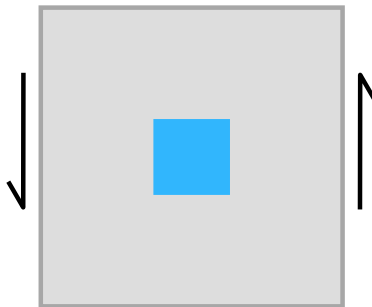


Fig. 4.3 Geometry set up for the numerical model with the area of interest, a two-by-two square in blue, far from the boundaries

4.2 Linear Theory

The analytical solution for growth-rate and oscillation frequency was derived in Appendix C using linear theory, which linearizes the system in order to approximate how the system changes over time. The porosity field is analyzed as plane waves (*Spiegelman, 2003*) with amplitude $s(t)$, angular frequency $\omega(t)$, and wave numbers $k_x(t)$ and $k_y(t)$ in the x and y directions. This puts the porosity in the form

$$\phi = \phi_0 + \Gamma t + \Delta\phi \exp [i(k_x(t)x + k_y(t)y - \omega(t)) + s(t)]. \quad (4.1)$$

This allows amplitude ($s(t)$), frequency ($\omega(t)$), and orientation ($\tan^{-1}(k_x(t)/k_y(t))$) information to be derived from the porosity field.

4.2.1 Growth-Rate

The analytical growth-rate (Eq C.96) is found to be

$$\frac{\partial s}{\partial t} = \frac{-6(1 - \phi_0 - \Gamma t)\alpha e^{\frac{\alpha\Gamma t}{n_v}} \kappa_0 k_x k_y (k_x^2 + k_y^2)^2}{n_v(3\psi + \kappa_0(k_x^2 + k_y^2))(4e^{\frac{\alpha\Gamma t}{n_v}}((k_x^4 + k_y^4)(1 + \sigma) + k_x^2 k_y^2(2 + \sigma)) + 3\psi\zeta)} \quad (4.2)$$

where $\kappa_0 = \left(\frac{\Gamma t}{\phi_0} + 1\right)^\beta$, $\sigma = \frac{(1-n_v)}{n_v}$, and $\psi = (k_x^2 + k_y^2)^2 + (k_x^2 - k_y^2)^2\sigma$. This expression simplifies to those previously derived without internal melting (*Katz et al. 2006 ; Butler 2009*) when Γ is set to zero. For the strain-rate independent viscosity case ($n_v = 1$), equation 4.2 simplifies to

$$\frac{\partial s}{\partial t} = \frac{6k_x k_y \left(\frac{\Gamma t}{\phi_0} + 1\right)^\beta (1 - \phi_0 - \Gamma t)\alpha e^{\alpha\Gamma t}}{3 + \left(\frac{\Gamma t}{\phi_0} + 1\right)^\beta (k_x^2 + k_y^2)(4e^{\alpha\Gamma t} + 3\zeta)}. \quad (4.3)$$

Observe that the entire equation is multiplied by the term $e^{\alpha\Gamma t}$. Since α is negative this term will decrease the growth rate with the presence of internal melting. This mechanism is caused by the viscosity being exponentially dependent on porosity. This means an increase in the background porosity due to the internal melting will in turn decrease the background viscosity. This decrease results in a decrease in the viscosity's affect on porosity, therefore decreasing the effect of the instability and the formation of bands.

The magnitude of the growth-rate is seen, in figure 4.4a-b, to significantly decrease with internal melting (increase in Γ). Although the angle of maximum growth is changing with strain-rate dependence of viscosity and internal melting (figure 4.4c), the distribution of

the growth-rate does not change with melting as significantly as strain-rate dependence of viscosity. This is shown by the overall shape of the curves in figure 4.4a-b. The angle of maximum growth is altered by the viscosity's dependence on strain-rate, as seen in figure 4.4. It is split symmetrically about 45 degrees which agrees with *Katz et al.* (2006) and *Butler* (2009). The internal melting does not affect the angle for the strain-rate independent case, but increases the splitting for the cases with $n_v > 1$.

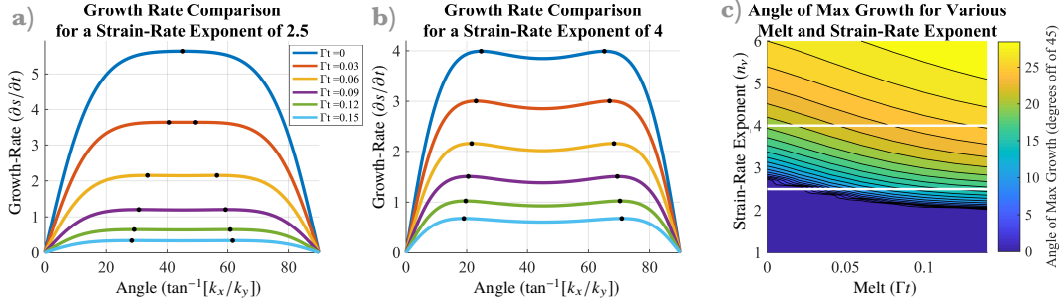


Fig. 4.4 Plots exploring the analytical solution for growth-rate at various angles. a) and b) are plots of growth-rate for a) $n_v = 2.5$ and b) $n_v = 4$ at various angles for different values of melt. The black dots show the angle at which max growth occurs for each curve. c) Contour map of the angle of maximum growth for strain-rate exponent and melt with the line of $n_v = 2.5$ is highlighted in white

4.2.2 Oscillation Frequency

The oscillation frequency (Eq C.98), which describes how the porosity changes at a point over time due to the buoyancy force, is given by the imaginary part of the linearized solution to the governing equations. This is expressed as

$$i \frac{\partial \omega}{\partial t} = 3k_y(1 - \phi_0 - \Gamma t) \frac{w_0}{U_0} \frac{\kappa_0((k_x^2 + k_y^2)^2 + (k_y^4 - k_x^4)\sigma) - \kappa_1 \psi(1 - \phi_0 - \Gamma t)}{3\psi + \kappa_0(k_x^2 + k_y^2)(4e^{\frac{\alpha \Gamma t}{n_v}}((k_x^4 + k_y^4)(1 + \sigma) + k_x^2 k_y^2(2 + \sigma)) + 3\psi \zeta)} \quad (4.4)$$

where ω is the oscillation frequency, $\kappa_1 = \left(\frac{\Gamma t}{\phi_0} + 1\right)^{\beta-1} \frac{\beta}{\phi_0}$. The strain-rate independent viscosity case ($n_v = 1$) simplifies to

$$i \frac{\partial \omega}{\partial t} = 3k_y(1 - \phi_0 - \Gamma t) \frac{w_0}{U_0} \frac{\left(\frac{\Gamma t}{\phi_0} + 1\right)^\beta - \kappa_1(1 - \phi_0 - \Gamma t)}{3 + \left(\frac{\Gamma t}{\phi_0} + 1\right)^\beta (k_x^2 + k_y^2)(4e^{\frac{\alpha \Gamma t}{n_v}} + 3\zeta)}. \quad (4.5)$$

The internal melting is found to decrease the oscillation frequency of the bands, as shown in figure 4.5. The effect of the melt-rate increases with strain which is due to the accumulation of melt due to the solid fraction term $(1 - \phi_0 - \Gamma t)$. This effect is usually quite small since Γt is generally much less than 1 and this term multiplies the entire right-hand side of the equation, meaning that as the solid is melting, it is decreasing the solid fraction and in turn decreasing the oscillation frequency. This is the opposite effect that strain-rate dependent viscosity has on the bands, and ultimately decreases the effect of buoyancy on the bands.

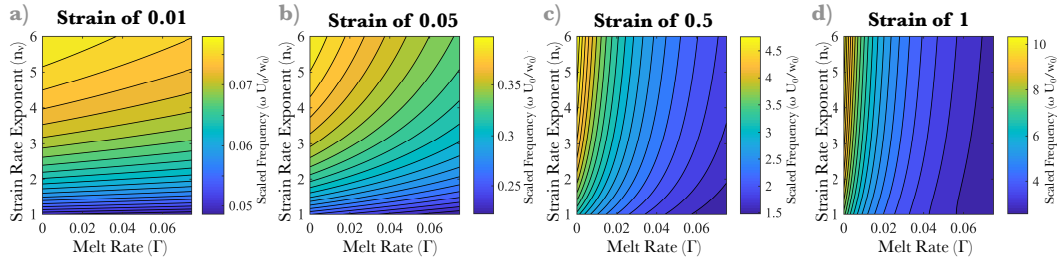


Fig. 4.5 Contour plot of the analytical frequency at various strains for different melt rates and strain-rate exponents

4.3 Numerical Results

Numerical solutions were created for various parameters, focusing on how the strain-rate exponent, melt and buoyancy changed the amplitude, orientation and oscillation frequency.

The numerical results from two models, strain-rate independent ($n_v = 1$) and dependent ($n_v = 6$), whose initial porosity was random (figure 4.2) are shown in figure 4.6. The porosity fields are shown in figure 4.6a-e.i with the strain-rate independent case in figure 4.6b-c.i and dependent case in figure 4.6d-e.i. The angular distribution found by Fourier transforming the corresponding porosity fields are shown in figure 4.6a-e.ii. The angular distribution of the initial condition (figure 4.6a.ii) is random. The distribution of the strain-rate independent cases (figure 4.6b-c.ii) show a predominant 45 degree orientation. This agrees with the analytical solution (figure 4.4), for small amounts of strain. Then existing bands are rotated to smaller angles by the background flow at larger strains. The distributions of the strain-rate dependent case (figure 4.6d-e.ii) shows a bi-modal distribution which also agrees with the analytical solution (figure 4.4).

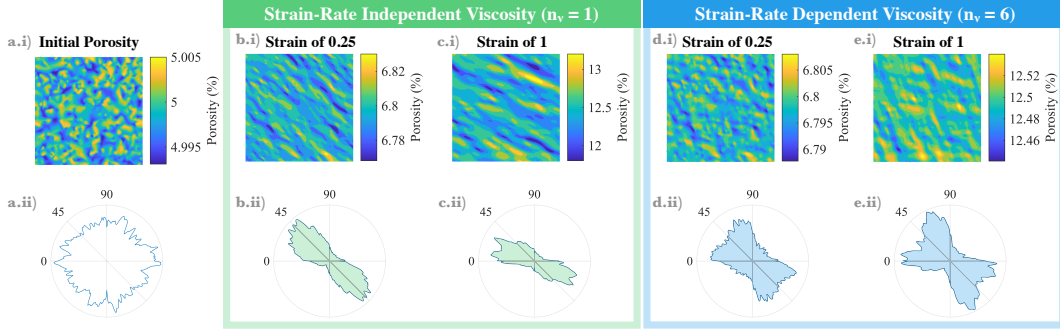


Fig. 4.6 Numerical solutions at various strains for strain-rate dependent and independent cases with internal melting rate ($\Gamma = 0.075$). i) Contour plots of porosity. ii) Angular distribution plots of the related porosity field.

4.3.1 Amplitude

This comparison is done by numerically integrating the analytical growth-rate then comparing this curve to the average normalized porosity,

$$s_{num} = \frac{1}{2} \ln \int \left(\frac{\phi - \phi_{bac}}{\Delta\phi} \right)^2 dA, \quad (4.6)$$

to find the amplitude of the numerical solution (Butler, 2009). The analytical solution was found to fit the numerics for variations in volumetric melt rate, Γ , and strain-rate exponent, n_v , (figure 4.8), initial porosity, ϕ_0 , bulk viscosity, ζ , parameters α and β , and initial wave numbers: k_{x_0} and k_{y_0} (figure 4.7). The amplitude curves of analytical solution and numerical solutions with random and waveform initial conditions for various internal melting and strain-rate exponents are shown in figure 4.8. The analytical solution and numerical solution for waveform initial condition correlate almost exactly, whereas the numerical solution with the random initial condition is parallel to the analytical solution at small strains, meaning they have the same growth rate. Some of the numerical solutions for various melt rates (figure 4.8a) did not run to a strain of 2. This is due to the fact that the porosity difference was large enough to make the minimum porosity zero, making the model divergent. Figure 4.8 shows that either increasing internal melting (figure 4.8a) or strain-rate exponent (figure 4.8b) decreases the amplitude of the bands. The slope of the analytical and waveform numerical solutions are negative after a strain of one, this is because the bands have been rotated past 90 degrees and are decaying. The curves for the random initial condition do not exhibit the same decay since they do not have predominant, pre-existing bands that the waveform initial condition do. For the random initial condition, there is a range of band angles and so there

will usually be some that are at a good orientation for growth. For the large melting rate case, it can be seen that the amplitude eventually saturates. By comparing the curves in figure 4.8a with no internal melting and internal melting of 0.075 at a strain of one, the addition of melting is shown to decrease the band amplitude approximately 30% for the analytical solution and 50% for the random initial condition model.

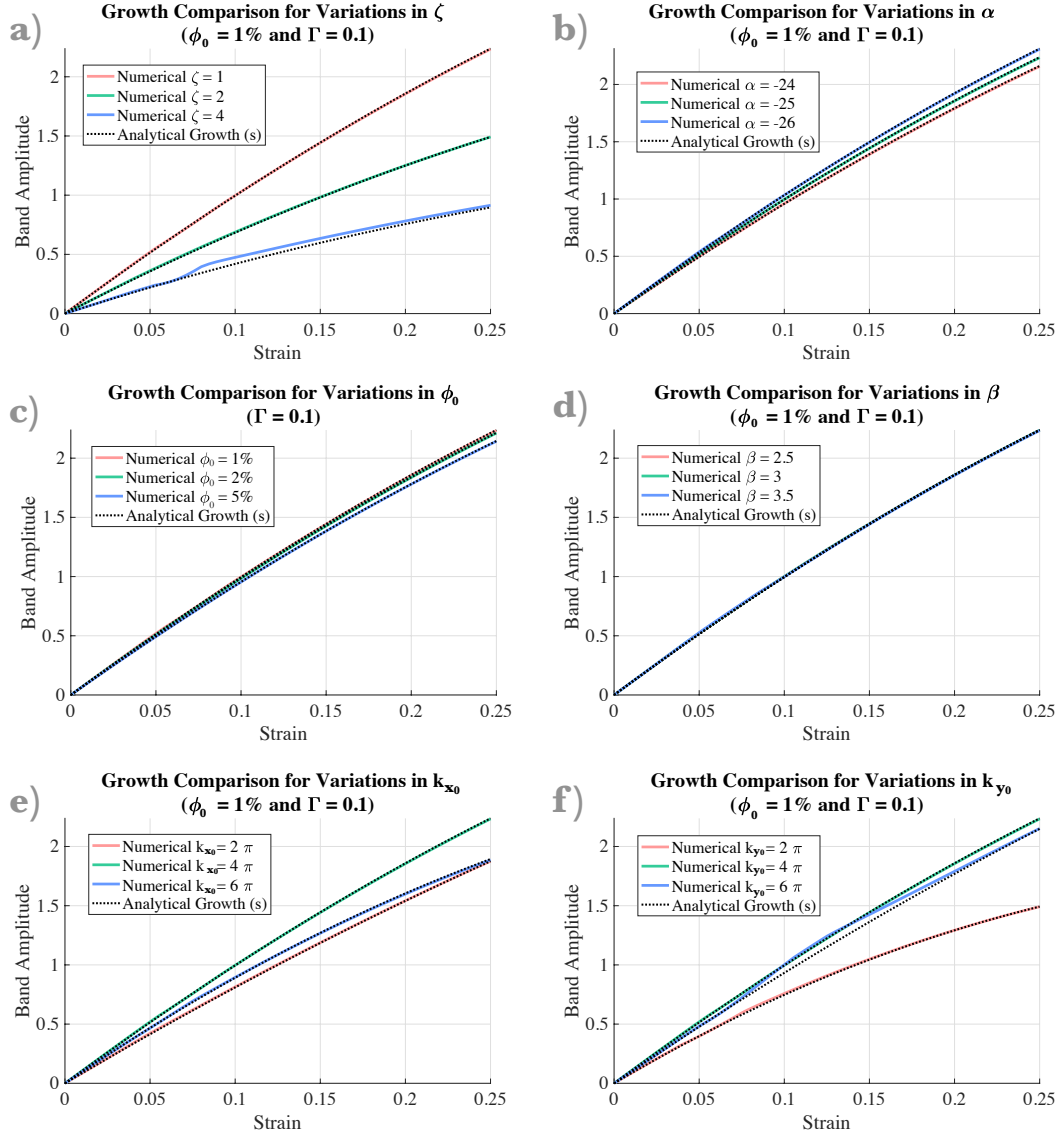


Fig. 4.7 Amplitude comparison of analytical and numerical solutions for various input parameters. All solutions were run with a waveform initial condition, strain-rate independent viscosity, and internal melting.

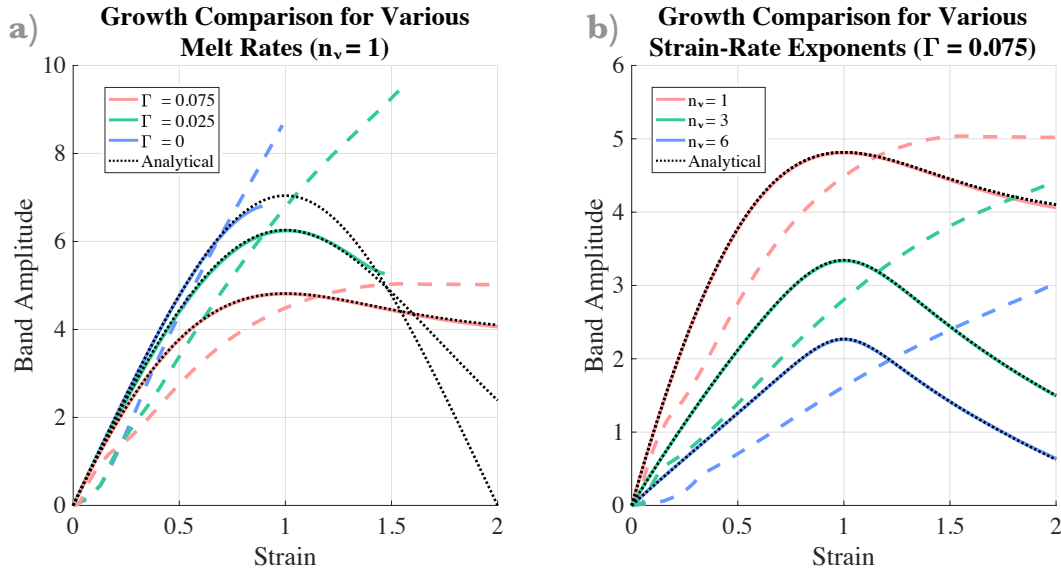


Fig. 4.8 a) Amplitude comparison for different values of melt rate. b) Amplitude comparison for different strain-rate exponents. Coloured lines are numerical results with dashed lines computed with a random initial porosity and solid line with a waveform initial porosity.

4.3.2 Angle Analysis

It is not only amplitude but also orientation of the bands which is vital in determining whether these bands could transport melt to the ridge axis. The results from the angle analysis are shown in figure 4.9 with analytical results shown in a-d and the numerical results shown in e-h. The numerical results are obtained by taking the Fourier transform of the porosity field to get the angular distribution (figure 4.6 ii) for each solution at each strain and compiling this data into a contour plot (figure 4.9 e-h). The angle distribution for numerical results compared to analytical are consistent for larger values of strain, but the alignment of the bands occurs at later strain for the numerical model. Overall the angle of the bands formed in the analytical and numerical solutions are in reasonable agreement.

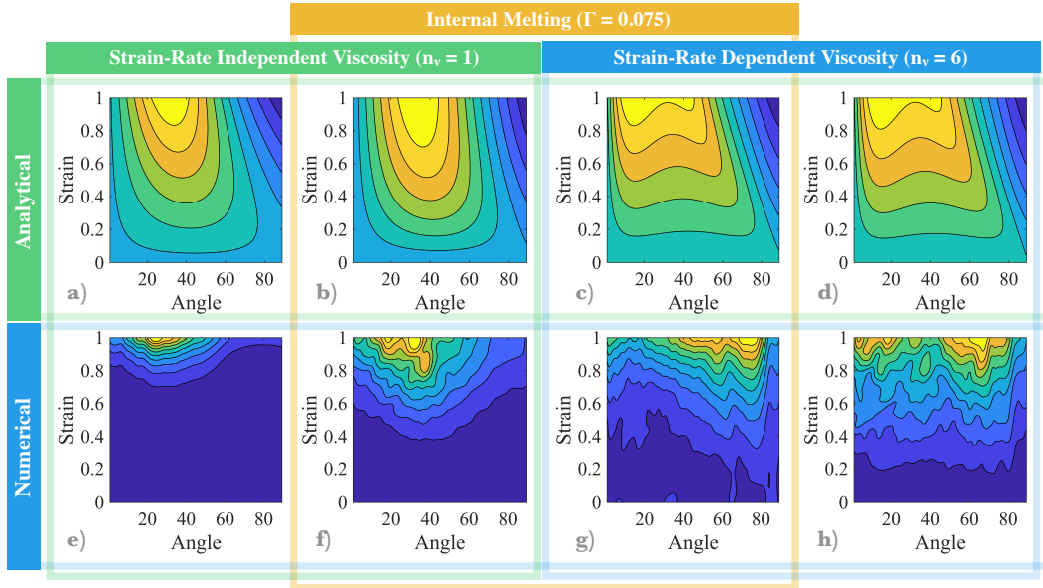


Fig. 4.9 Contour plots of the analytical and numerical solutions for angular distribution over strain for strain-rate independent and dependent viscosity both with and without internal melting. The analytical solution was numerically integrated from the growth-rate equation. The numerical solution uses a three point moving average along different strain values. The angular distribution is normalized between 0 and 1 then are plotted with a contour interval of 0.1.

4.3.3 Oscillation Frequency

The oscillation frequency describes the effects of the upward motion of the fluid due to buoyancy on the porosity at a given point over time. The analytical porosity at a point is given by: $\phi = \exp(s) \cos(\omega)$ and can be directly compared to numerical results from a model whose initial porosity is a waveform (figure 4.2a) and porosity is evaluated at the centre point using the normalization: $\phi_{norm} = (\phi - \phi_0 - \Gamma t) / \Delta\phi$. Results for different internal melting rates are plotted in figure 4.10 with the numerical solution plotted in solid lines and analytical solution in dashed. These solutions are in excellent agreement. The frequency of these curves decrease with internal melting as seen by the increase in distance between the peaks of the curves. Models with applied buoyancy force were run for longer strain and the bands persisted with negligible effect on the growth-rate.

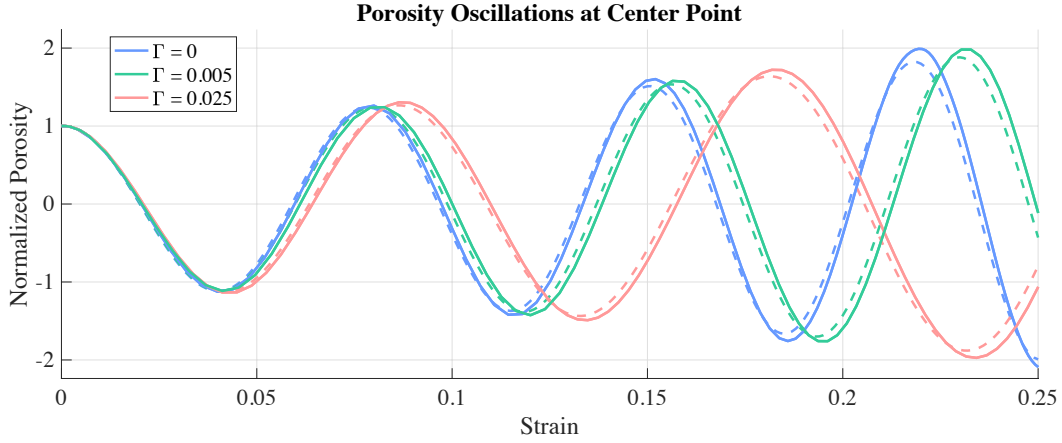


Fig. 4.10 Comparison of analytical porosity, plotted using dashed lines, and normalized numerical porosity, the solid lines, at the centre point of the model with waveform initial porosity for various values of melt rate with $n_v = 6$, $w_0/U_0 = 10$ and $\phi_0 = 1\%$.

4.4 Discussion

The effect of buoyancy on the bands is disputed. A study by *Katz* (2010) found an absence of melt bands when including buoyancy and internal melting. He theorized that this absence was due to the buoyancy force on the bands, which contradicts a previous study by *Butler* (2009). This research found that the buoyancy force causes the oscillation frequency with no effect on growth. Growth is shown to be significantly decreased by the presence of internal melting. This is due to the internal melting increasing the background porosity, decreasing the background viscosity and in turn the viscosity's affect on porosity, which lessens the effect of the instability, decreasing the growth of the bands. Internal melting decreases the band amplitude by at most 30% for the analytical solution and 50% for the numerical solutions with a random initial condition. Internal melting is likely the cause of the lack of bands in *Katz's* (2010) model. His model had an average melting rate of approximately $0.5 \text{ kg/m}^3/\text{yr}$ (figure 7a in *Katz*, 2010) which is between 0.5 and 50 in this dimensionless system. This internal melting rate is considerably larger than those used in this study. This, according to the analytical model, would result in a decrease in maximum band amplitude of 80% to 99%.

The orientation of the bands is strongly dictated by the viscosity's dependence on strain rate which changes the angle of maximum growth and direction ongoing strain which rotates existing bands. This is in agreement with *Katz et al.* (2006) as well as *Butler* (2009) and

(2010). The internal melting slightly increases the effect of the strain-rate exponent, but the effect is almost negligible.

4.5 Conclusions

The numerical and analytical results for growth and oscillation frequency of the bands are in excellent agreement, the orientation is also in reasonable agreement. This means that the analytical solution derived in this study is a reasonable approximation of the mathematical system described in Chapter 3. The numerical results for growth with a random initial condition deviates since they do not have the pre-existing bands assumed in the analytical solution. This random initial condition makes the growth occur for longer as there is a range of band angles some of which have good orientation for growth.

The internal melting and strain-rate exponent were shown to decrease the growth of the bands. The strain-rate exponent alters the angle of maximum growth, deviating symmetrically about 45° , and internal melting slightly increases this effect. Buoyancy was shown to cause oscillations of the bands; this effect was dampened by the presence of internal melting, but the amplitude remained unaffected. Since the introduction of internal melting decreases the growth rate, therefore the expected magnitude of the melt bands decreased. These bands may be less significant for channeling melt towards mid-ocean ridges, contributing to seismic anisotropy, and acting as pathways of enhanced electrical conductivity than originally thought.

Chapter 5

Quantifying the Error Introduced by Density Variation

5.1 Model Setup

The model used in this section is similar to the previous chapter with the inclusion of a density variation between solid and fluid as well as porosity and strain-rate dependent bulk viscosity. The model specifications are outlined below.

5.1.1 Background Velocity and Pressure

The assumption that density variation is zero with exception of buoyancy force ignores the isotropic expansion that occurs when solid melts into fluid. This is due to the solid being more dense than the fluid, so when it melts the fluid must expand since mass is constant.

The derivation of the analytical solution for density variation with variable bulk viscosity and constant bulk viscosity cases are found in Appendix D. The background velocity field is found to be

$$U_{bac} = \Gamma \frac{\Delta\rho}{\rho_l} x, \quad \text{and} \quad V_{bac} = \Gamma \frac{\Delta\rho}{\rho_l} y + x,$$

with a corresponding background porosity of

$$\phi_{bac} = \phi_0 + \Gamma t \left[\frac{\Delta\rho}{\rho_l} (1 - \phi_0) + 1 \right].$$

5.1.2 Initial and Boundary Conditions as well as Numerical Geometry

The initial conditions, boundary conditions and numerical geometry used in this model are the same as the previous chapter. See sections: 4.1.2 for initial conditions, 4.1.3 for boundary conditions, and 4.1.4 for numerical geometry.

5.2 Linear Theory

The analytical solutions including density variation for constant and variable bulk viscosity are derived in Appendix D using the same method as the previous chapter, linear theory. The wave numbers are found to be $k_x = \exp[-\Gamma t \Delta \rho / (2\rho_l)](k_{x0} + k_{y0}t)$ and $k_y = k_{y0} \exp[-\Gamma t \Delta \rho / (2\rho_l)]$. The results for growth rate and oscillation frequency are outlined below.

5.2.1 Variable Bulk Viscosity

The growth rate found for the variable bulk viscosity case, $\zeta = \zeta_r \eta$, with strain-rate dependent viscosity (Eq D.100) is given by

$$\frac{\partial s}{\partial t}_{\zeta=\zeta_r \eta} = - \frac{\frac{\alpha}{n_v} \eta_{bac} \kappa_{bac} k^4 (6k_x k_y + \Gamma \frac{\Delta \rho}{\rho_l} k^2 (1 + 3\zeta_r)) (1 - \phi_{bac})}{d_r} - \Gamma \frac{\Delta \rho}{\rho_l} \quad (5.1)$$

where the denominator is expressed as

$$d_r = \frac{1-n_v}{n_v} \left(2\eta_{bac} \Gamma \frac{\Delta \rho}{\rho_l} \kappa_{bac} k_x k_y k^4 (4 + 3\zeta_r) + (k_x^6 + k_y^6) \psi_r + 3k_y^4 + k_x^2 k_y^2 (\sigma_r - 6) + k_x^4 (3 + \sigma_r) \right) + k^4 (3 + \eta_{bac} \kappa_{bac} k^2 (4 + 3\zeta_r)) \quad (5.2)$$

and where $\sigma_r = \eta_{bac} \kappa_{bac} k_y^2 (8 - 3\zeta_r + (\Gamma \frac{\Delta \rho}{\rho_l})^2 (3 + 9\zeta_r))$ and $\psi_r = \eta_{bac} \kappa_{bac} (4 + (\Gamma \frac{\Delta \rho}{\rho_l})^2 + 3(1 + (\Gamma \frac{\Delta \rho}{\rho_l})^2) \zeta_r)$. For the strain rate independent viscosity case, $n_v = 1$, this simplifies to

$$\frac{\partial s}{\partial t}_{\zeta=\zeta_r \eta} = - \frac{\alpha \eta_{bac} \kappa_{bac} (6k_x k_y + \Gamma \frac{\Delta \rho}{\rho_l} k^2 (1 + 3\zeta_r)) (1 - \phi_{bac})}{3 + \eta_{bac} \kappa_{bac} k^2 (4 + 3\zeta_r)} - \Gamma \frac{\Delta \rho}{\rho_l}. \quad (5.3)$$

Observe that because of the bulk viscosity's dependence on shear viscosity the second term in the denominator is multiplied by the background viscosity, η_{bac} . This means that as long as this term is significantly larger than 3, the background viscosity, which is dependent on the melt rate, cancels. This decreases the growth rate's overall dependence on melt rate.

The oscillation frequency of the variable bulk viscosity case with strain rate dependent viscosity (Eq D.110) is given by

$$\frac{\partial \omega}{\partial t}_{\zeta=\zeta_r, \eta} = \frac{w_0}{U_0} (1 - \phi_{bac}) \frac{n_f}{d_r} \quad (5.4)$$

where the numerator is

$$n_f = 3\kappa_{bac} k_y k^4 - \kappa_{bac} \frac{1-n_v}{n_v} (k_x^4 - k_y^4) (3k_y + \Gamma \frac{\Delta \rho}{\rho_l} k_x (1 + 3\zeta_r)) + 3\kappa_1 k_y (k^4 + \frac{1-n_v}{n_v} (k_x^2 - k_y^2)^2) (\phi_{bac} - 1) \quad (5.5)$$

The strain-rate independent case is expressed as

$$\frac{\partial \omega}{\partial t}_{\zeta=\zeta_r, \eta} = 3k_y (1 - \phi_{bac}) \frac{w_0}{U_0} \frac{\kappa_{bac} + \kappa_1 (\phi_{bac} - 1)}{3 + \eta_{bac} \kappa_{bac} k^2 (4 + 3\zeta_r)}. \quad (5.6)$$

The entire equation is multiplied by the amount of buoyancy force w_0 which is constant as well as the vertical wave number k_y and the solid fraction $(1 - \phi_{bac})$ which both decrease with time due to the internal melting. This means the oscillation frequency decreases overtime due to the internal melting.

5.2.2 Constant Bulk Viscosity

The growth rate for the constant bulk viscosity case with strain-rate dependent viscosity (Eq D.105) is found to be

$$\frac{\partial s}{\partial t}_{\zeta=C} = - \frac{\frac{\alpha}{n_v} \eta_{bac} \kappa_{bac} k^4 (6k_x k_y + \Gamma \frac{\Delta \rho}{\rho_l} k^2) (1 - \phi_{bac})}{d_c} - \Gamma \frac{\Delta \rho}{\rho_l} \quad (5.7)$$

where the denominator is given by

$$d_c = \frac{1-n_v}{n_v} (8\eta_{bac} \Gamma \frac{\Delta \rho}{\rho_l} \kappa_{bac} k_x k_y k^4 + (k_x^6 + k_y^6) \Psi_c + k_x^2 k_y^2 (\sigma_c - 6) + k_x^4 (3 + \sigma_c) + 3k_y^4) + k^4 (3 + k^2 \kappa_{bac} (4\eta_{bac} + 3\zeta)) \quad (5.8)$$

and where $\sigma_c = \kappa_{bac} k_y^2 (\eta_{bac} (8 + 3(\Gamma \frac{\Delta \rho}{\rho_l})^2) - 3\zeta)$ and $\Psi_c = \kappa_{bac} (\eta_{bac} (4 + (\Gamma \frac{\Delta \rho}{\rho_l})^2) + 3\zeta)$. When the shear viscosity is strain rate independent, $n_v = 1$, this simplifies to

$$\frac{\partial s}{\partial t}_{\zeta=C} = - \frac{\alpha \eta_{bac} \kappa_{bac} (1 - \phi_{bac}) (6k_x k_y + \Gamma \frac{\Delta \rho}{\rho_l} k^2)}{3 + \kappa_{bac} k^2 (4\eta_{bac} + 3\zeta)} - \Gamma \frac{\Delta \rho}{\rho_l}. \quad (5.9)$$

Conversely to the variable bulk viscosity case, the background viscosity is not multiplying the entire second term in the denominator and is generally much smaller than the bulk viscosity, the background viscosity does not cancel. This means since the growth rate is dependent on the background viscosity which is dependent on melt rate, the growth rate will be more affected by melt rate than the variable bulk viscosity case.

The oscillation frequency for the constant bulk viscosity case with strain-rate dependent viscosity (Eq D.113) is given by

$$\frac{\partial \omega}{\partial t}_{\zeta=C} = (1 - \phi_{bac}) \frac{w_0 n_o}{U_0 d_c} \quad (5.10)$$

where the numerator is

$$n_o = 3\kappa_{bac} k_y k^4 - \kappa_{bac} \frac{1-n_v}{n_v} (\Gamma \frac{\Delta \rho}{\rho_l} k_x + 3k_y)(k_x^4 - k_y^4) + 3\kappa_1 k_y (k^4 + \frac{1-n_v}{n_v} (k_x^2 - k_y^2)^2)(\phi_{bac} - 1). \quad (5.11)$$

The strain-rate independent case has the oscillation frequency of

$$\frac{\partial \omega}{\partial t}_{\zeta=C} = 3k_y (1 - \phi_{bac}) \frac{w_0}{U_0} \frac{\kappa_{bac} + \kappa_1 (\phi_{bac} - 1)}{3 + \kappa_{bac} k^2 (4\eta_{bac} + 3\zeta)}. \quad (5.12)$$

Similarly to the variable bulk viscosity model the oscillation frequency is multiplied by the gravity force, vertical wave number and solid fraction, which means the oscillation frequency also decreases with time due to internal melting in this case.

5.2.3 Comparison of Analytical Solutions

Plots of the analytical solutions of growth rate outlined above as well as the solution from the previous chapter are shown in figure 5.1 for strain-rate dependent and independent viscosity. The density variation with variable bulk viscosity case (figure 5.1 a and e) show almost no effect from the melting. Internal melting shows a small increase in amplitude with variable bulk viscosity for both strain-rate dependent and independent viscosity regardless of density variation (figure 5.1 a, b, e and f). For the constant bulk viscosity models, density variation has almost no effect on growth in the strain-rate independent case (figure 5.1 c-d). Whereas in the strain-rate dependent case the melt has less effect on the density variation case (figure 5.1 g) than the density variation free case (figure 5.1 h).

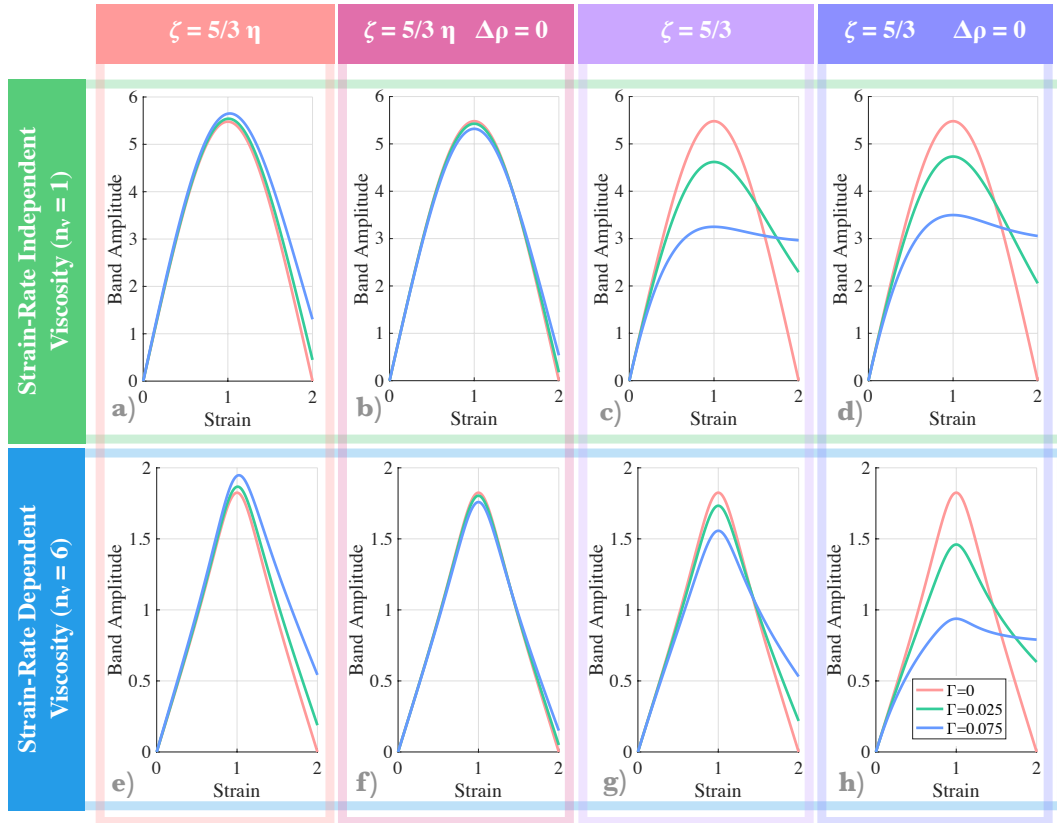


Fig. 5.1 Plots of various analytical solutions for a variety of melt rates with an initial band angle of 45° . a) and e) include density variation as well as variable bulk viscosity $\zeta = 5/3\eta$. b) and f) have no density difference with variable bulk viscosity $\zeta = 5/3\eta$. c) and g) include density variation with a constant bulk viscosity $\zeta = 5/3$. d) and h) are solutions from Chapter 4, derived in Appendix C, which assumes no density difference and a constant bulk viscosity of $\zeta = 5/3$. a-d) have strain rate independent viscosity, $n_v = 1$, and e-h) have strain-rate dependent viscosity, $n_v = 6$.

Analytical solutions of porosity oscillations for the strain-rate dependent viscosity case from this chapter and the previous chapter are plotted in figure 5.2. The inclusion of density variations for non-gravity terms are shown to decrease the oscillation frequency as seen by the blue and green lines compared to the red line which is the solution from the previous chapter. The constant bulk viscosity model has a lower frequency than the variable bulk viscosity model.

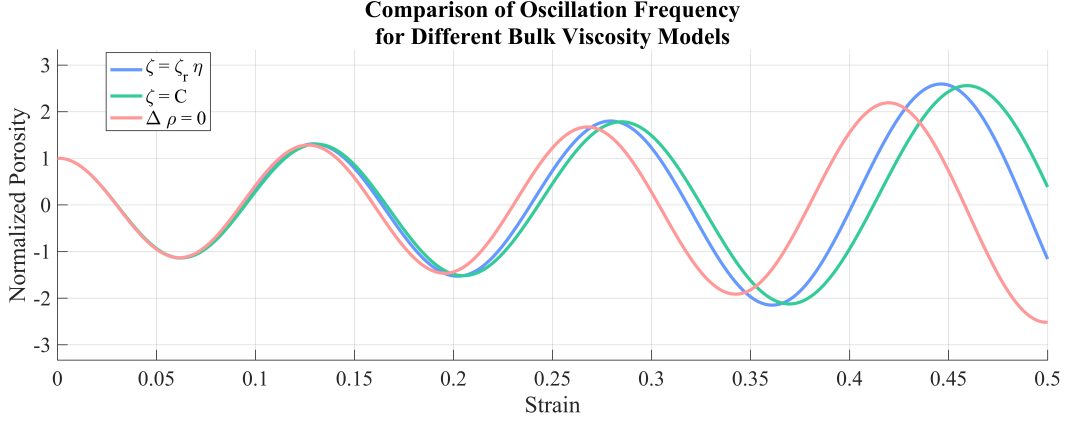


Fig. 5.2 Plots of analytical solutions for variable and constant bulk viscosity as well as the solution from the previous chapter for a melt rate of 0.025 with an initial band angle of 45° and strain-rate exponent of 6.

5.2.4 Without Applied Shear

The system is also solved for the situation when no shear is applied, i.e. $U_{bac} = U_{melt}$, in order to isolate the effects of isotropic expansion. Both cases are evaluated for strain-rate independent viscosity. The growth rate for variable bulk viscosity case (Eq D.103) is given by

$$\frac{\partial s}{\partial t}_{\zeta=\zeta_r\eta} = \Gamma \frac{\Delta\rho}{\rho_l} \left(\frac{\alpha\eta_{bac}\kappa_{bac}k^2(1+3\zeta_r)(\phi_{bac}-1)}{3+\eta_{bac}\kappa_{bac}k^2(4+3\zeta_r)} - 1 \right). \quad (5.13)$$

Similarly to the applied shear model, the background viscosity cancels. This means that the first term in the brackets is much greater than one making the growth rate always positive.

The growth rate for constant bulk viscosity (Eq D.108) is expressed as

$$\frac{\partial s}{\partial t}_{\zeta=C} = \Gamma \frac{\Delta\rho}{\rho_l} \left(\frac{\alpha\eta_{bac}\kappa_{bac}k^2(\phi_{bac}-1)}{3+\kappa_{bac}k^2(4\eta_{bac}+3\zeta)} - 1 \right). \quad (5.14)$$

Since the background viscosity does not cancel, similar to the applied shear solution, and is typically much less than one at later times. The first term in the brackets can be less than one at later times making the growth rate negative.

Both variable and constant bulk viscosity cases have isotropic growth rates. This is shown by the presence of k , instead of independent directions of k_x and k_y .

5.3 Numerical Results

Numerical models were run to verify the analytical solutions for density variation with variable and constant bulk viscosity cases, with and without applied shear.

5.3.1 Amplitude

Variable Bulk Viscosity

Numerical and analytical results were found for the variable bulk viscosity case with density variation and were plotted in figure 5.3. The melt rate increases the band amplitude slightly (figure 5.3a) which is contradictory to the other models (figure 5.4a and figure 4.8a). The strain-rate exponent still significantly decreases the amplitude (figure 5.3b).

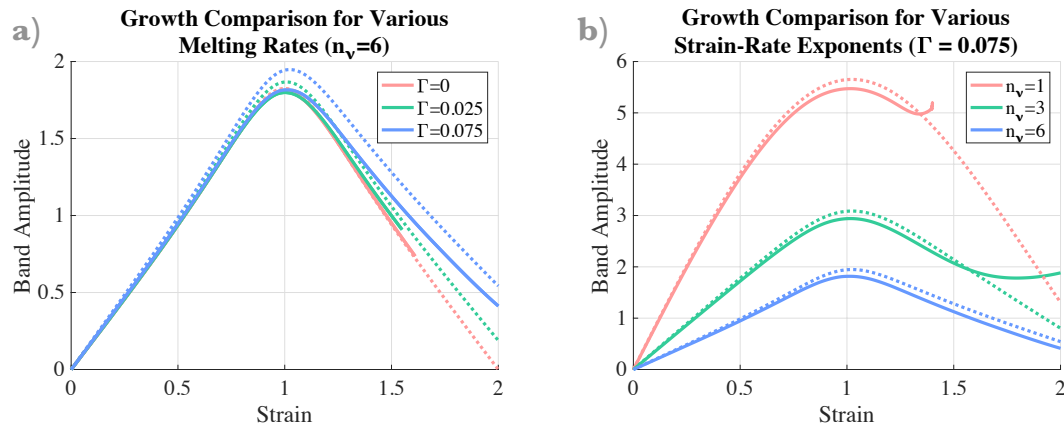


Fig. 5.3 Amplitude comparisons for models with a bulk viscosity of $\zeta = 5/3\eta$ and density variation. a) Compares amplitudes for different values of melt rate. b) Compares amplitudes for different strain-rate exponents. The dotted lines are analytical results and solid lines are numerical results with a waveform initial porosity.

Constant Bulk Viscosity

Comparison of analytical and numerical results for the constant bulk viscosity case with density variation are shown in figure 5.4. These results are in excellent agreement. The melt rate has little effect on the band amplitude as shown by proximity of the plots in figure 5.4a). The strain-rate exponent still has a significantly effect on the amplitude of the bands (figure 5.4b).

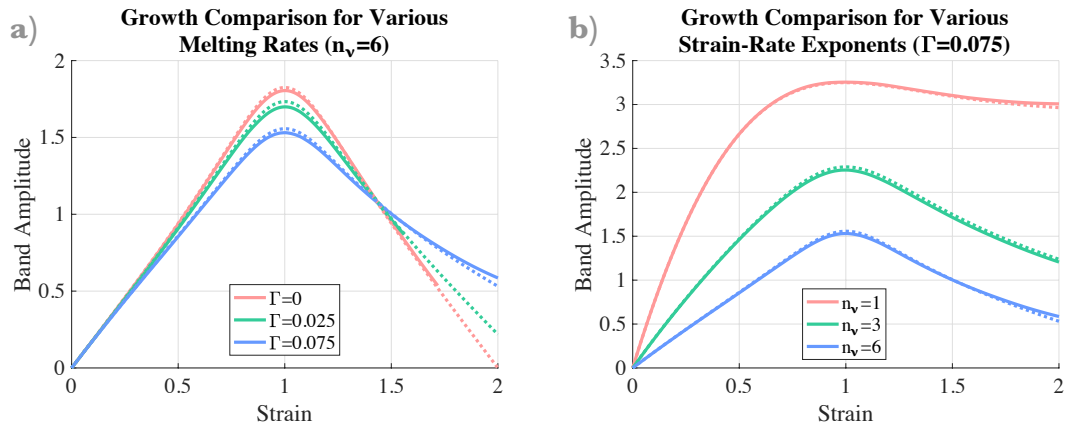


Fig. 5.4 Amplitude comparisons for models with a constant bulk viscosity, $\zeta = 5/3$, and density variation. a) Compares amplitudes for different values of melt rate. b) Compares amplitudes for different strain-rate exponents. The dotted lines are analytical results and solid lines are numerical results with a waveform initial porosity.

Without Applied Shear

Numerical and analytical results for isotropic expansion without applied shear for both variable and constant bulk viscosity are plotted in figure 5.5. The amplitude of the variable bulk viscosity case increases approximately linearly. The effect of isotropic expansion on the constant bulk viscosity case is negligible, which is in agreement with the difference seen between figure 5.1b and figure 5.1c.

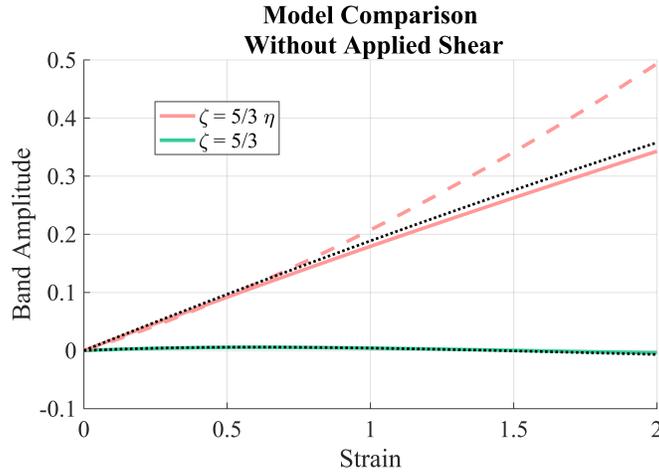


Fig. 5.5 Comparison of analytical and numerical results for isotropic expansion models with no applied shear and a melt rate of 0.075. The black dotted lines are analytical results and coloured lines are numerical results with the dashed line computed with a random initial porosity and solid lines with a waveform initial porosity.

A comparison of numerical and analytical results from the variable bulk viscosity case for a variety of input parameters are plotted in figure 5.5. The parameters excluded from the plot are k_x , k_y and β which do not have a significant effect on the growth rate. The models are in good agreement for all variations in parameters, which affirms the analytical solution as an accurate representation of the mathematical system.

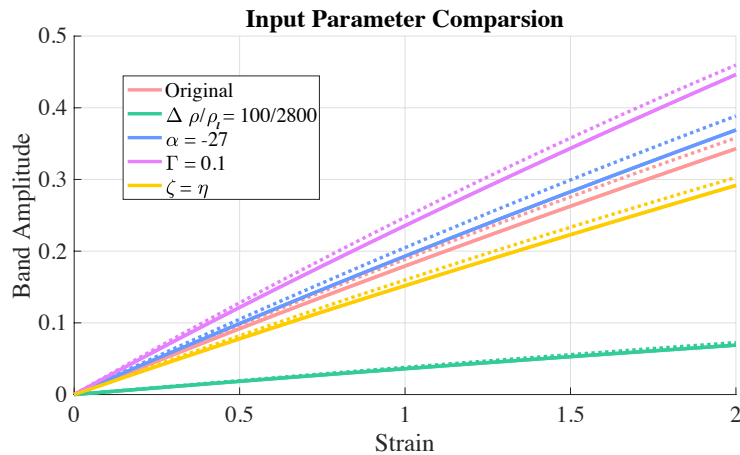


Fig. 5.6 Comparison of analytical and numerical results for the variable bulk viscosity model without applied shear for a variety of input parameters. Unless otherwise stated input parameters are the same as those outlined in Chapter 3 with a melting rate of 0.075.

5.3.2 Oscillation Frequency

Numerical and analytical results for porosity oscillations are plotted in figure 5.7. The difference between the porosity oscillations in the constant and variable bulk viscosity models is indistinguishable. The numerical and analytical results from both models are in excellent agreement.

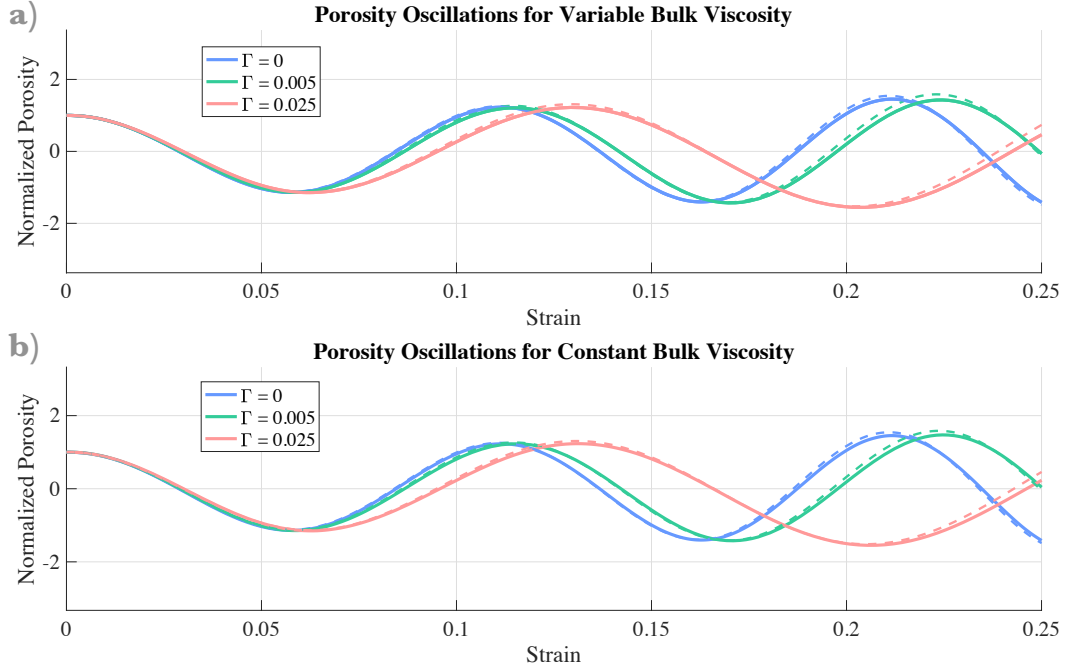


Fig. 5.7 Comparison of analytical and numerical solutions with density variation for a) variable bulk viscosity $\zeta = 5/3\eta$ and b) constant bulk viscosity $\zeta = 5/3$. The analytical porosity is plotted using dashed lines and normalized numerical porosity is plotted using solid lines. The numerical porosity is evaluated at the centre point of the model with waveform initial porosity. These models use various values of melt rate with $n_v = 6$, $w_0/U_0 = 10$ and $\phi_0 = 1\%$.

5.4 Discussion

The inclusion of density variation between solid and fluid does not have a major impact on the amplitude of the bands, except the strain-rate dependent viscosity, constant bulk viscosity model. For strain-rate independent viscosity, density variations are shown to decrease the maximum amplitude in the constant bulk viscosity model by 7.6% and increase the maximum amplitude in the porosity dependent bulk viscosity model by 5.8%. For strain-rate dependent

viscosity, the maximum amplitude for the constant bulk viscosity model is increased by 39.8% and by 9.5% for the porosity and strain-rate dependent bulk viscosity model. The large increase in maximum amplitude seen in the strain-rate dependent viscosity, constant bulk viscosity model decreases the effect of melting on the band amplitude from 40% to 15%. The model isolating isotropic expansion with a melting rate of 0.075 and porosity dependent bulk viscosity has an amplitude of about 0.36 at a strain of 2, which means this contributes to approximately 30% of the total effect of melting on the same model with applied shear, which deviates from the case with no melting by about 1.2 at a strain of 2. This amplitude also accounts for approximately 50% of the difference between models with and without density variations, the remainder of the difference is due to the background porosity's dependence on density variation. Although the density variation has a significant contribution to the effect of melting in the porosity dependent bulk viscosity case, this effect is only 3.1%. Whereas when the bulk viscosity is constant, internal melting can decrease the amplitude of the bands by up to 40%.

The previous chapter looked at internal melting as a possible explanation for the lack of bands in *Katz* (2010). Internal melting has a minor effect on the amplitude of the bands when bulk viscosity is dependent on porosity and strain-rate. For the density variation model the maximum amplitude is increased by 3.1% for the strain-rate independent case and by 6.5% for the strain-rate dependent case. For the model with no density variation the maximum amplitude is decrease by 2.9% in the strain-rate independent case and by 3.6% for the strain-rate dependent case. This means that internal melting does not explain the lack of bands in *Katz* (2010) as he included porosity dependent bulk viscosity.

5.5 Conclusions

The analytical solutions described in this chapter are reasonable approximations for the growth of the mathematical system since the analytical and numerical solutions are in excellent agreement. The addition of a density difference between solid and fluid had negligible effects, except on the strain-rate dependent viscosity and constant bulk viscosity model where the effect of density variation significantly decreases the overall effects of internal melting. The porosity and strain-rate dependent bulk viscosity model showed minimal effects of internal melting. Therefore, internal melting may not have as significant an impact on the melt bands as shown in the previous chapter.

Chapter 6

Computational Analysis of Two-Phase Corner-Flow

6.1 Model Setup

The experimental setup for the corner flow model is more complex than the idealized geometry, simple-shear model in the previous chapter. This section outlines the stress field, boundary conditions, initial conditions and geometry used for the corner flow model based on results from *Spiegelman and McKenzie (1987)*.

6.1.1 Background Velocity and Pressure

The background velocity and pressure (figure 6.1) are taken from *Spiegelman and McKenzie (1987)*. The velocity field is defined as

$$U_{bac} = \frac{\partial \psi_s}{\partial y}, \quad V_{bac} = -\frac{\partial \psi_s}{\partial x} \quad (6.1)$$

where x is horizontal, y is vertical and the solid streamline, ψ_s , is derived from the biharmonic equation with boundary conditions appropriate for a corner where both sides are pulling apart. The result is given by

$$\psi_s = r(A \sin \theta - B \theta \cos \theta) \quad (6.2)$$

where r is the radial distance, θ is the angle from vertical, A and B are constants relating to dip angle, γ (figure 6.1), and are defined as $A = 2/(\pi - 2\gamma - \sin(2\gamma))$ and $B = 2 \sin^2 \gamma / (\pi - 2\gamma - \sin(2\gamma))$. The background pressure is taken as the piezometric pressure

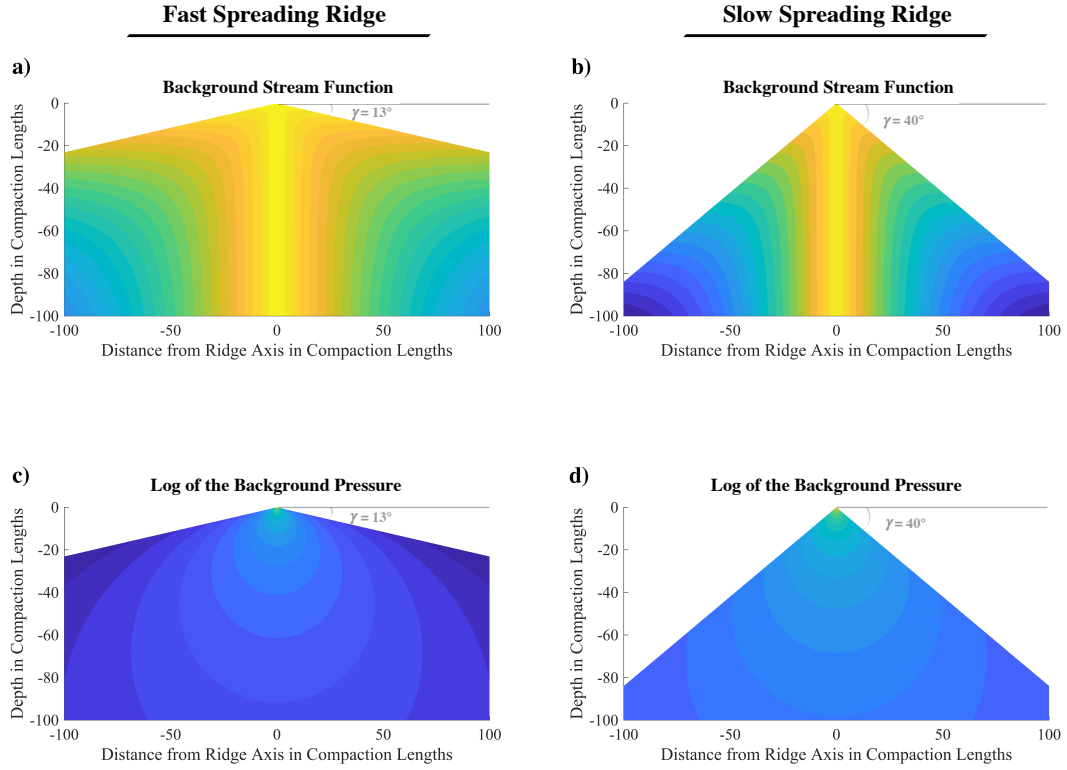


Fig. 6.1 Contour of background stream-function and pressure

from the background solid velocity, which is given by

$$p_{bac} = -2B \cos \theta / r. \quad (6.3)$$

6.1.2 Initial Conditions

The initial conditions for this model are similar to the previous chapter with U_1 , V_1 and p_1 set to zero meaning the velocity and pressure are equal to their background fields. For the porosity, only the random condition is used which has a maximum perturbation, $\Delta\phi$, from the initial porosity parameter, ϕ_0 .

6.1.3 Streamline Geometry

The geometry of the corner flow model has to be a bit more complex than the previous section since the pressure approaches infinity at the corner (when $r = 0$ in eq 6.3). To deal with this, the geometry is defined as being between two streamlines with the closer streamline a distance d from the ridge axis and enclosed by a circle which intercepts the closer streamline at one length scale L (figure 6.2).

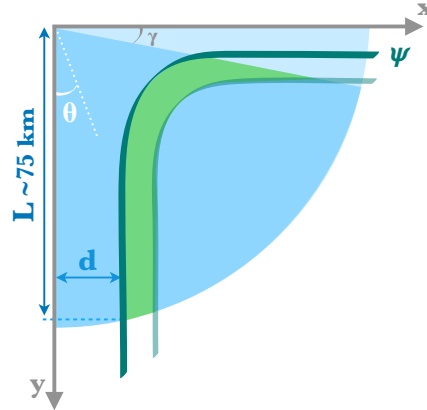


Fig. 6.2 Geometric setup of the corner flow model with the study area highlighted in green.

6.1.4 Boundary Conditions

Since the geometry is more complicated, the boundary conditions must be as well. Since all the boundaries are irregular, none of them can be periodic. Dirichlet boundaries are used on all sides for velocity and pressure where they are set to their background values. For porosity, a combination of Dirichlet for the inlet/outlet boundaries and zero flux ($[1 - \phi]\vec{U}_1 \cdot \hat{n} = 0$) for the streamline boundaries are used. The outlet boundary (the farthest off axis) is extended to twice the distance of the radius of the enclosing circle in order to decrease the boundary effects. These boundary conditions are illustrated in figure 6.3.

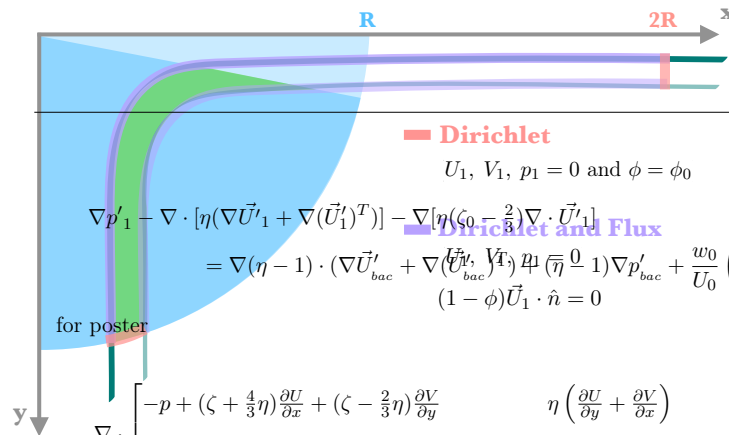


Fig. 6.3 Boundary conditions used for the corner flow model. The study area is shown in green. The inlet/outlet boundaries are highlighted in pink and the streamline boundaries are highlighted in purple.

6.2 Results

The resulting porosity distribution is shown in figure 6.4. Bands form mainly where the background velocity changes from vertical to horizontal. These bands are oriented approximately parallel to the corner of the streamline. The bands are mostly the same shape and orientation, except the radius of 25, without buoyancy force model which has no bands. This lack of bands is due to the large compaction length, which means the fluid flows easily, weakening the instability. The buoyancy models show bands further to the right (as seen in the radius 50 model) than the buoyancy free models. The change in radius changes the compaction length since the system is non-dimensionalized with the length scale being equal to the compaction length. This means, since the system has a maximum depth of 75 km, a radius of 25 has compaction length of 3 km, a radius of 50 has compaction length of 1.5 km, and a radius of 100 has compaction length of 750 m.

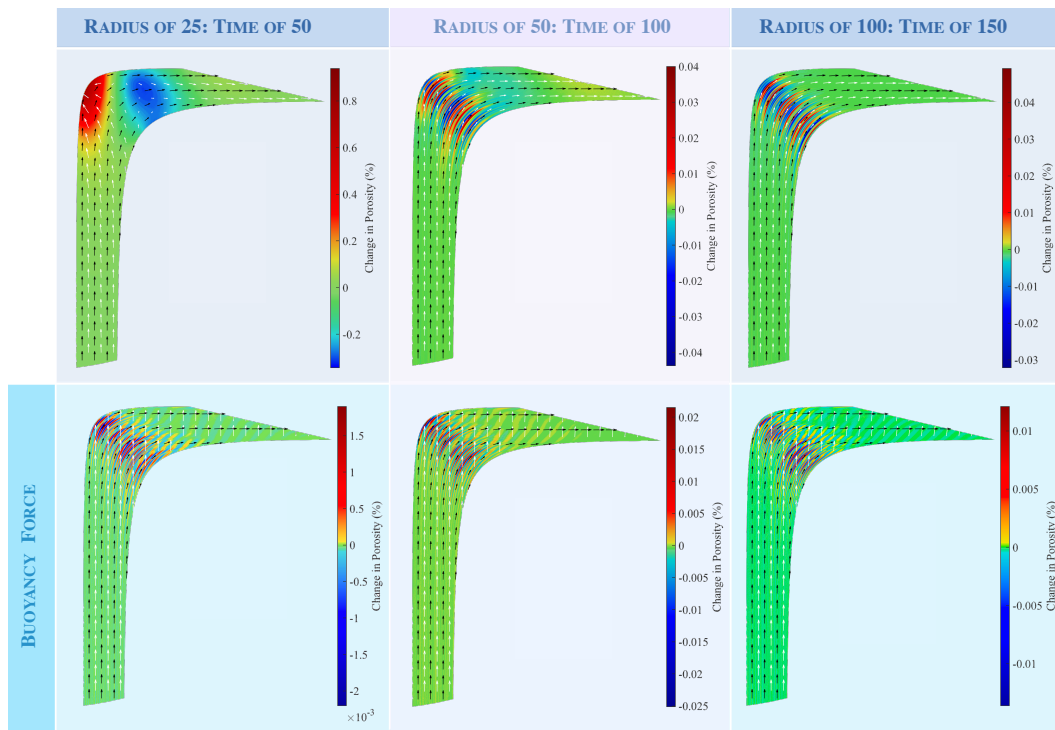


Fig. 6.4 Contours of change in porosity from initial porosity of 5% after strain applied by the background flow described above on a Mid-Ocean Ridge geometry with a ridge dip of 13 degrees and a grid mesh with 50,715 elements. Fluid velocity field lines in white, solid velocity field in black.

The model results can be compared to linear theory computing the amplitude at each time step then plotting the growth over time. This comparison is plotted in figure 6.5 where each numerical geometry is broken into five sections perpendicular to the lower streamline. The growth of each of these sections is found by integrating the amplitude of sections and then plotting this over time. These solutions are labelled MOR in the legend. These are plotted with analytical solutions for pure and simple shear as well as numerical results for a simple geometry. The addition of buoyancy forces does not change the growth-rate, but appears to reduce the fluctuations of the amplitude curve as seen by the smoothness contrast of the buoyant to non-buoyant solutions. The radius of the model does not strongly affect the growth-rate as seen by the grouping of the Mid-Ocean Ridge curves. The magnitude of the amplitude curve is strongly affected by the position along the model, with the largest amplitude at the corner of the model (the yellow region). The simple shear and Mid-Ocean Ridge growth are approximately parallel, meaning they have a comparable growth-rate.

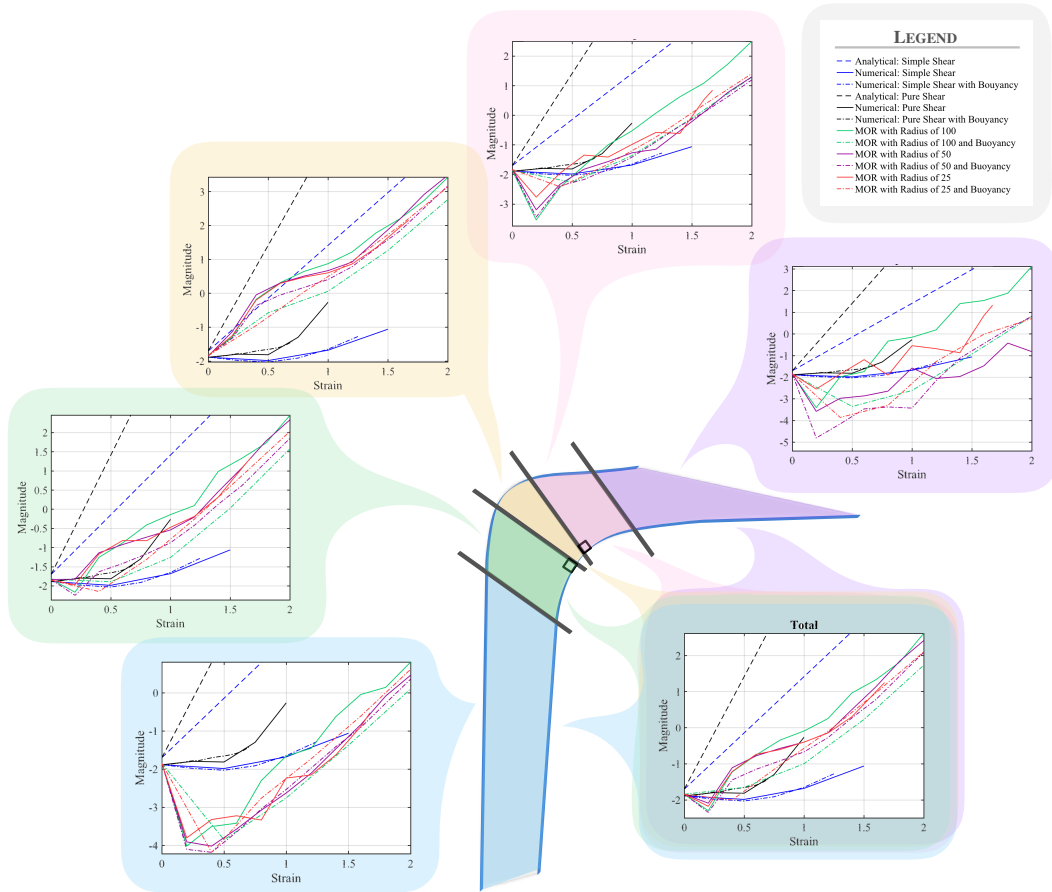


Fig. 6.5 Plots of the magnitude of band amplitude over time for different areas of the Mid-Ocean Ridge solutions (figure 6.4). These are plotted together with the analytical and numerical solutions for simple and pure shear.

6.3 Discussion

The growth rate of the bands in the Mid-Ocean Ridge model are found to be similar to the analytical solution for simple shear. This correlation is understandable since the material being moved is between two streamlines, this means that the velocity is largest on the side towards the ridge axis and gradually decreases away. This variation across the velocity field is applying a simple shear parallel to the imposing field, which is crucial as it justifies the use of the results from the previous chapter as an approximation to corner flow. The growth rate changes with position along the streamline since the magnitude of the shear changes. The

compaction length does not effect the growth rate of the bands, this is consistent with the analytical solution for simple shear.

The compaction length does not appear to have much effect on the formation of bands except for the solution with no buoyancy force and a compaction length of 3 km which has no bands forming and a fluid velocity field that corresponds to the solution found in *Spiegelman and McKenzie* (1987). This is due to the compaction length being comparable to the system size, which makes the background pressure drive fluid flow instead of compaction. This means the system is stable. If the compaction length is smaller, the solid deforms as well creating the instability.

6.4 Conclusions

The model in this chapter included a complex geometry encompassing the area between two streamlines underneath the Mid-Ocean Ridge as described by *Spiegelman and McKenzie* (1987). The resulting bands are oriented away from the ridge axis, which is not conducive to channeling melt. This result is in agreement with a previous analytical study by *Gebhardt and Butler* (2016). This orientation could concentrate melt toward a decompaction boundary layer described by *Sparks and Parmentier* (1991) at the base of the impermeable layer, which could then migrate to the ridge axis. These bands could still contribute to seismic (*Toomey et al.*, 1998) and electrical (*Evans et al.*, 1999) anisotropy observed at the Mid-Ocean Ridge. They may also reduce the effective viscosity, meaning the viscosity of the system as a whole is decreased by these planes of weakness, which would allow material to flow more easily toward the ridge axis.

Chapter 7

Conclusions

This study analysed an analytical solution and two numerical models: the first with simple geometry but more complex physics and the second with simplified physics but a more realistic Mid-Ocean Ridge geometry. The analytical solution approximated an expected outcome for band amplitude, orientation, and oscillation frequency for material in a simple-shear stress regime with internal melting, buoyancy, and strain-rate dependent viscosity. This solution was compared to numerical results from a simple geometry model under the same conditions. Then a second numerical model was made for a more complex geometry to determine orientation and amplitude of the bands at different positions between two streamlines under the Mid-Ocean Ridge.

The model with simple geometry discussed in Chapter 4 showed numerical and analytical results which are in agreement for growth, oscillation frequency, and orientation of the bands for various input parameters. This means that the analytical solutions for growth rate and oscillation frequency derived in Appendix A are sensible approximations of the mathematical system described in Chapter 3. There were important observations of the effects of internal melting, buoyancy and strain-rate exponent made in this chapter. The growth of the bands is decreased by both internal melting and viscosity's dependence on strain rate. The angle of maximum growth deviates symmetrically about 45° with increase in strain-rate exponent. Internal melting slightly increases this affect. The buoyancy force is found to have no effect on growth rate, but causes an oscillation frequency which was damped by internal melting.

The analytical and numerical solutions for the inclusion of density variation between solid and fluid for constant bulk viscosity, porosity and strain-rate dependent bulk viscosity, and without applied shear are in good agreement. This means the analytical solutions derived in Appendix D are reasonable approximations for the mathematical system described in Chapters 3 and 5. Density variation is shown to have little effect on the maximum amplitude

unless it is decreasing the effects of internal melting. Internal melting does not have a significant impact when bulk viscosity is dependent on porosity and strain-rate.

The Mid-Ocean Ridge geometry model in Chapter 5 showed that bands form oriented away from the ridge axis in a corner flow stress environment as described by *Spiegelman and McKenzie* (1987). This is not conducive to channeling melt toward the ridge axis. This orientation could support the theory by *Sparks and Parmentier* (1991) that melt could migrate to the ridge axis after forming a decompaction layer under the base of an impermeable layer. These bands have a growth rate approximate to the simple shear growth rate. This is important because it validates the use of the simple shear results as an analogy for the movement under the Mid-Ocean Ridge.

The Mid-Ocean Ridge model showed that bands form oriented away from the ridge axis. In a constant bulk viscosity case these bands might not have sufficient magnitude due to internal melting to channel melt. But in a porosity and strain-rate dependent viscosity case the effect of internal melting is minimal. This means melt bands may still be a viable explanation for the following: the localized volcanism at the axis, rapid transport with a broad area to accumulate melt, and significant seismic and electric anisotropy observed beneath the Mid-Ocean Ridge.

References

- Berman, R. G. (1988), Internally-consistent thermodynamic data for minerals in the system $Na_2O - K_2O - CaO - MgO - FeO - Fe_2O_3 - Al_2O_3 - SiO_2 - TiO_2 - H_2O - CO_2$, *Journal of Petrology*, 29(2), 445–522.
- Braun, M. G., and P. B. Kelemen (2002), Dunite distribution in the oman ophiolite: Implications for melt flux through porous dunite conduits, *Geochemistry, Geophysics, Geosystems*, 3(11), 1–21, doi:10.1029/2001GC000289.
- Butler, S. (2009), The effects of buoyancy on shear-induced melt bands in a compacting porous medium, *Physics of the Earth and Planetary Interiors*, 173(1), 51 – 59.
- Butler, S. (2010), Porosity localizing instability in a compacting porous layer in a pure shear flow and the evolution of porosity band wavelength, *Physics of the Earth and Planetary Interiors*, 182(1), 30 – 41.
- Butler, S. (2012), Numerical models of shear-induced melt band formation with anisotropic matrix viscosity, *Physics of the Earth and Planetary Interiors*, 200-201, 28 – 36.
- Butler, S. (2017), Shear-induced porosity bands in a compacting porous medium with damage rheology, *Physics of the Earth and Planetary Interiors*, 264, 7 – 17.
- Carman, P. C. (1939), Permeability of saturated sands, soils and clays, *The Journal of Agricultural Science*, 29(2), 262–273.
- Evans, R. L., P. Tarits, A. D. Chave, A. White, G. Heinson, J. H. Filloux, H. Toh, N. Seama, H. Utada, J. R. Booker, and M. J. Unsworth (1999), Asymmetric electrical structure in the mantle beneath the east pacific rise at 17°s, *Science*, 286(5440), 752–756.
- Forsyth, D. W., S. C. Webb, L. M. Dorman, and Y. Shen (1998), Phase velocities of rayleigh waves in the melt experiment on the east pacific rise, *Science*, 280(5367), 1235–1238, doi:10.1126/science.280.5367.1235.
- Gebhardt, D. J., and S. L. Butler (2016), Linear analysis of melt band formation in a mid-ocean ridge corner flow, *Geophysical Research Letters*, 43(8), 3700–3707.
- Gill, R. (2010), *Igneous Rocks and Processes*, 141-146 pp., Wiley-Blackwell, West Sussex, UK.
- Guillot, B., and N. Sator (2007), A computer simulation study of natural silicate melts. part i: Low pressure properties, *Geochimica et Cosmochimica Acta*, 71(5), 1249 – 1265.

- Hammond, W. C., and D. R. Toomey (2003), Seismic velocity anisotropy and heterogeneity beneath the mantle electromagnetic and tomography experiment (melt) region of the east pacific rise from analysis of p and s body waves, *Journal of Geophysical Research: Solid Earth*, 108(B4).
- Hess, H. H. (1964), Seismic anisotropy of the uppermost mantle under oceans, *Nature*, 203(4945), 629–631.
- Hirschmann, M. M., P. D. Asimow, M. S. Ghiorso, and E. M. Stolper (1999), Calculation of peridotite partial melting from thermodynamic models of minerals and melts. iii. controls on isobaric melt production and the effect of water on melt production, *Journal of Petrology*, 40(5), 831–851.
- Holtzman, B. K., and D. L. Kohlstedt (2007), Stress-driven Melt Segregation and Strain Partitioning in Partially Molten Rocks: Effects of Stress and Strain, *Journal of Petrology*, 48(12), 2379–2406.
- Holtzman, B. K., N. J. Groebner, M. E. Zimmerman, S. B. Ginsberg, and D. L. Kohlstedt (2003), Stress-driven melt segregation in partially molten rocks, *Geochemistry, Geophysics, Geosystems*, 4(5).
- Katsura, T., A. Yoneda, D. Yamazaki, T. Yoshino, and E. Ito (2010), Adiabatic temperature profile in the mantle, *Physics of the Earth and Planetary Interiors*, 183(1), 212 – 218, special Issue on Deep Slab and Mantle Dynamics.
- Katz, R. F. (2010), Porosity-driven convection and asymmetry beneath mid-ocean ridges, *Geochemistry, Geophysics, Geosystems*, 11(11).
- Katz, R. F., and Y. Takei (2013), Consequences of viscous anisotropy in a deforming, two-phase aggregate. part 2. numerical solutions of the full equations, *Journal of Fluid Mechanics*, 734, 456–485.
- Katz, R. F., M. Spiegelman, and B. Holtzman (2006), The dynamics of melt and shear localization in partially molten aggregates, *Nature*, 442, 676–679.
- Kearey, P., K. A. Klepeis, and F. J. Vine (2009), *Global Tectonics*, 3 ed., Wiley-Blackwell, The address.
- Kelemen, P. B., G. Hirth, N. Shimizu, M. Spiegelman, and H. J. B. Dick (1997), A review of melt migration processes in the adiabatically upwelling mantle beneath spreading ridge, *Philosophical Transactions of the Royal Society of London. Series A: Mathematical, Physical and Engineering Sciences*, 355, 283–318.
- Keller, T., R. F. Katz, and M. M. Hirschmann (2017), Volatiles beneath mid-ocean ridges: Deep melting, channelised transport, focusing, and metasomatism, *Earth and Planetary Science Letters*, 464, 55 – 68.
- Landau, L. D., and E. M. Lifshitz (1959), *Fluid Mechanics*, London: Pergamon Press.
- Lange, R. A., H. M. Frey, and J. Hector (2009), A thermodynamic model for the plagioclase-liquid hygrometer/thermometer, *American Mineralogist*, 94(4), 494–506.

- McKenzie, D. (1984), The Generation and Compaction of Partially Molten Rock, *Journal of Petrology*, 25(3), 713–765.
- Mei, S., W. Bai, T. Hiraga, and D. Kohlstedt (2002), Influence of melt on the creep behavior of olivine-basalt aggregates under hydrous conditions, *Earth and Planetary Science Letters*, 201(3), 491 – 507.
- Morgan, J. P. (1987), Melt migration beneath mid-ocean spreading centers, *Geophysical Research Letters*, 14(12), 1238–1241.
- Morgan, J. P. (2001), Thermodynamics of pressure release melting of a veined plum pudding mantle, *Geochemistry, Geophysics, Geosystems*, 2(4).
- Richardson, C. N. (1998), Melt flow in a variable viscosity matrix, *Geophysical Research Letters*, 25(7), 1099–1102.
- Richet, P., F. Leclerc, and L. Benoist (1993), Melting of forsterite and spinel, with implications for the glass transition of Mg_2SiO_4 liquid, *Geophysical Research Letters*, 20(16), 1675–1678.
- Scott, D. R., and D. J. Stevenson (1984), Magma solitons, *Geophysical Research Letters*, 11(11), 1161–1164.
- Sparks, D. W., and E. Parmentier (1991), Melt extraction from the mantle beneath spreading centers, *Earth and Planetary Science Letters*, 105(4), 368 – 377.
- Spiegelman, M. (2003), Linear analysis of melt band formation by simple shear, *Geochemistry, Geophysics, Geosystems*, 4(9).
- Spiegelman, M., and D. McKenzie (1987), Simple 2-d models for melt extraction at mid-ocean ridges and island arcs, *Earth and Planetary Science Letters*, 83(1), 137 – 152.
- Stevenson, D. J. (1989), Spontaneous small-scale melt segregation in partial melts undergoing deformation, *Geophysical Research Letters*, 16(9), 1067–1070.
- Toomey, D. R., W. S. D. Wilcock, S. C. Solomon, W. C. Hammond, and J. A. Orcutt (1998), Mantle seismic structure beneath the melt region of the east pacific rise from p and s wave tomography, *Science*, 280(5367), 1224–1227.
- Vera, E. E., J. C. Mutter, P. Buhl, J. A. Orcutt, A. J. Harding, M. E. Kappus, R. S. Detrick, and T. M. Brocher (1990), The structure of 0- to 0.2-m.y.-old oceanic crust at 9°n on the east pacific rise from expanded spread profiles, *Journal of Geophysical Research: Solid Earth*, 95(B10), 15,529–15,556.
- Wark, D. A., and E. Watson (1998), Grain-scale permeabilities of texturally equilibrated, monomineralic rocks, *Earth and Planetary Science Letters*, 164(3), 591 – 605.
- Wolfe, C. J., and P. G. Silver (1998), Seismic anisotropy of oceanic upper mantle: Shear wave splitting methodologies and observations, *Journal of Geophysical Research: Solid Earth*, 103(B1), 749–771.

Glossary

Dimensionless of Variables		
Symbol	Description	Value
Γ	Internal Melting Rate	$2 \cdot 10^{-5} - 0.075$
t	Strain	
ϕ	Porosity	
ϕ_{bac}	Background Porosity	
ϕ_0	Initial Porosity	1% – 5%
$\Delta\phi$	Initial Porosity Perturbation	$\phi_0 \cdot 10^{-3}$
\vec{u}	Fluid Velocity Field	
\vec{U}	Solid Velocity Field	
\vec{U}_{bac}	Background Solid Velocity Field	
p	Pressure	
p_{bac}	Background Pressure	
κ	Permeability	
κ_{bac}	Permeability For Background Conditions	
β	Permeability Exponent	3
μ	Fluid Viscosity	
η	Solid Shear Viscosity	
η_{bac}	Shear Viscosity For Background Conditions	
α	Viscosity Exponent	-25
n_v	Strain-Rate Exponent	1 – 6
ζ	Bulk Viscosity	
ζ_r	Bulk to Shear Viscosity Ratio	5/3
ψ_s	Solid Stream Function	
A	Stream Function Integration Constant	
B	Stream Function Integration Constant	
γ	Ridge Dip Angle	$13^\circ - 40^\circ$
k_x	Horizontal Wave-Number	
k_{x_0}	Initial Horizontal Wave-Number	4π
k_y	Vertical Wave-Number	
k_{y_0}	Initial Vertical Wave-Number	4π
k	Magnitude of the Wave-Numbers	
s	Porosity Amplitude	
ω	Porosity Oscillation Frequency	

Dimensional Variables		
Symbol	Description	Value
δ_c	Compaction Length	100m – 10km
L	Length Scale	75km
U_0	Characteristic Velocity	3mm/yr – 30mm/yr
w_0	Percolation Velocity	$1.6 \cdot 10^{-5}$ mm/yr – 158mm/yr
T	Temperature	1000K – 1550K
dF/dy	Melt Productivity	$2 \cdot 10^{-5}$ %/m – $7.5 \cdot 10^{-4}$ %/m
$(\partial T/\partial y)_a$	Adiabatic Temperature-Depth Gradient	-1.1K/km – -2K/km
$(\partial T/\partial y)_s$	Solidus Temperature-Depth Gradient	2.6K/km – 3.6K/km
$\partial F/\partial T$	Isobaric Melt Productivity	0.01%/K – 0.5%/K
ν	Thermal Expansion Coefficient	
C_p	Heat Capacity	320J/mol K – 345J/mol K
ΔS	Entropy of Fusion	44J/mol K – 65J/mol K
\vec{F}	Interactive Force (fluid on solid)	
m_{tot}	Total Mass	
m_f	Mass of the Fluid	
m_s	Mass of the Solid	
M	Rate that Solid Becomes Fluid	
ρ_f	Density of the Fluid	2800kg/m ²
ρ_s	Density of the Solid	3300kg/m ²
$\Delta\rho$	Density Difference (solid to fluid)	500kg/m ³
g	Acceleration Due to Gravity	9.8m/s ²

Coordinate System	
Symbol	Description
x	Horizontal Coordinate
y	Vertical Coordinate
r	Radial Coordinate
θ	Angle From Vertical
S	Surface Area
V	Volume

Appendix A

Derivations

This appendix outlines the derivation of the governing equations: conservation of mass and force balance for both fluid and solid.

A.1 Conservation of Mass

Consider an arbitrary porous volume (see Fig A.1) whose fluid density is denoted as ρ_f and solid density as ρ_s . The volume average density can be written as

$$\rho_{tot} = \rho_f \phi + \rho_s (1 - \phi) \quad (\text{A.1})$$

where ϕ is porosity. This weights the densities with the amount of solid and liquid that is present in the volume. Since the density is defined as weight per volume the mass can be written as

$$m_{tot} = V \rho_{tot} \quad (\text{A.2})$$

where m_{tot} is the total mass and V is the volume. Substituting equation A.1 into A.2 gives

$$m_{tot} = V(\rho_f \phi + \rho_s (1 - \phi)). \quad (\text{A.3})$$

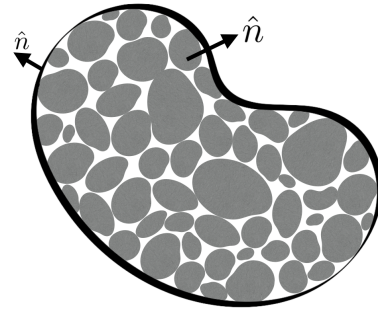


Fig. A.1 Porous volume with normal vectors \hat{n} , volume V , surface area S , and porosity ϕ

Since the volume can be re-written as the integral throughout the volume this can be re-written as

$$m_{tot} = \int (\rho_f \phi + \rho_s (1 - \phi)) dV. \quad (\text{A.4})$$

Now this can be separated and evaluated in two parts, solid and liquid contributions.

A.1.1 Fluid

The fluid contribution of the total mass (Eq A.4) is given by

$$m_f = \int \rho_f \phi dV. \quad (\text{A.5})$$

Since mass cannot be created or destroyed, the change in mass of the system over time must be equal to the amount of mass leaving the system. The change in mass of the fluid in the system can be written as the time derivative of the fluid mass equation (Eq A.5) which gives

$$\frac{\partial m_f}{\partial t} = \frac{\partial}{\partial t} \int \rho_f \phi dV \quad \text{which simplifies to} \quad (\text{A.6})$$

$$= \rho_f \int \frac{\partial \phi}{\partial t} dV. \quad (\text{A.7})$$

Now this is equated to a combinations of the amount of fluid material leaving the system and internal melting (i.e. the amount of solid becoming fluid). This can be written as

$$\frac{\partial m_f}{\partial t} = - \int \rho_f \phi \vec{u} \cdot \hat{n} dS + M \rho_f \quad (\text{A.8})$$

where \vec{u} is the fluid velocity, \hat{n} is the unit vector and S is the surface area and M is the rate at which solid is melting into fluid. Since the mass leaving the system and the change in mass must be equal, these equations can be combined. But first the divergence theorem must be used to make the integral in equation A.8 to be over the volume. So equation A.8 can be re-written as

$$\frac{\partial m_f}{\partial t} = - \int \nabla \cdot (\rho_f \phi \vec{u}) dV + M \quad \text{which simplifies to} \quad (\text{A.9})$$

$$= -\rho_f \int \nabla \cdot (\phi \vec{u}) dV + M. \quad (\text{A.10})$$

Now that the integrals are over the same spacial measurement, the equations for change of fluid mass in the system (Eq A.7) and the fluid mass leaving the system (Eq A.10) can be combined to obtain

$$\rho_f \int \frac{\partial \phi}{\partial t} dV = -\rho_f \int \nabla \cdot (\phi \vec{u}) dV + \frac{M}{\rho_f} \quad (\text{A.11})$$

the fluid densities cancel to obtain

$$\int \frac{\partial \phi}{\partial t} dV = - \int \nabla \cdot \phi \vec{u} dV + \frac{M}{\rho_f}. \quad (\text{A.12})$$

Now both sides of the equation can be combined and the arguments can be combined since they are integrated over the same variable. This process obtains

$$\int \left(\frac{\partial \phi}{\partial t} + \nabla \cdot (\phi \vec{u}) \right) dV = \frac{M}{\rho_f}. \quad (\text{A.13})$$

Taking the derivative yields the final conservation of mass equation for fluid equal,

$$\frac{\partial \phi}{\partial t} + \nabla \cdot (\phi \vec{u}) = \frac{1}{\rho_f} \frac{\partial M}{\partial V}, \quad (\text{A.14})$$

which is known as the conservation of mass equation for fluid where $\frac{\partial M}{\partial V}$ is the volume melting rate per unit volume per unit time.

A.1.2 Solid

The solid and remaining contribution of the total mass (Eq A.4) is given by

$$m_s = \int \rho_s (1 - \phi) dV. \quad (\text{A.15})$$

The conservation of solid mass can be found by simply repeating the analysis of the fluid mass. This starts with taking the time derivative

$$\frac{\partial m_s}{\partial t} = \frac{\partial}{\partial t} \int \rho_s (1 - \phi) dV \quad \text{which simplifies to} \quad (\text{A.16})$$

$$= -\rho_s \int \frac{\partial \phi}{\partial t} dV. \quad (\text{A.17})$$

Now the solid mass leaving the system can be written with relation to the velocity of solid \vec{U} and the rate at which the solid is melting (M) which yields the equation

$$\frac{\partial m_s}{\partial t} = - \int \rho_s (1 - \phi) \vec{U} \cdot \hat{n} dS - M. \quad (\text{A.18})$$

This can be related to volume using the divergence theorem to obtain

$$\frac{\partial m_s}{\partial t} = - \int \nabla \cdot [\rho_s (1 - \phi) \vec{U}] dV - M \quad (\text{A.19})$$

which simplifies to

$$= - \rho_s \int \nabla \cdot [(1 - \phi) \vec{U}] dV - M. \quad (\text{A.20})$$

Now the equation for change in solid mass of the system (Eq A.17) and the equation for solid mass leaving the system (Eq A.20) can be combined to obtain

$$\frac{\partial m_s}{\partial t} = - \rho_s \int \frac{\partial(\phi)}{\partial t} dV = - \rho_s \int \nabla \cdot [(1 - \phi) \vec{U}] dV - M. \quad (\text{A.21})$$

which simplifies to

$$\rho_s \int \frac{\partial(1 - \phi)}{\partial t} dV = - \rho_s \int \nabla \cdot [(1 - \phi) \vec{U}] dV - \frac{M}{\rho_s}. \quad (\text{A.22})$$

Now the integrals can be moved to one side and combined since they are over the same variable, the volume. This gives the equation

$$\int \left(\frac{\partial(1 - \phi)}{\partial t} + \nabla \cdot [(1 - \phi) \vec{U}] \right) dV = - \frac{M}{\rho_s}. \quad (\text{A.23})$$

Evaluating the derivative leaves the equation

$$- \frac{\partial \phi}{\partial t} + \nabla \cdot [(1 - \phi) \vec{U}] = - \frac{1}{\rho_s} \frac{\partial M}{\partial V} \quad (\text{A.24})$$

which simplifies to the the conservation of mass equation for solid

$$- \frac{\partial \phi}{\partial t} + \nabla \cdot [(1 - \phi) \vec{U}] = - \Gamma, \quad (\text{A.25})$$

where Γ is the volume melting rate per unit volume per unit time per solid density $\frac{1}{\rho_s} \frac{\partial M}{\partial V}$.

A.1.3 Total

Both conservation of mass equations for fluid and solid (Eq A.14 and A.25 respectively) can be added together to get

$$\frac{\partial \phi}{\partial t} + \nabla \cdot [\phi \vec{u}] - \frac{\partial \phi}{\partial t} + \nabla \cdot [(1 - \phi) \vec{U}] = \frac{\Gamma \rho_s}{\rho_l} - \Gamma. \quad (\text{A.26})$$

Now the time derivatives cancel and the equation

$$\nabla \cdot (\phi \vec{u} + (1 - \phi) \vec{U}) = \Gamma \frac{\Delta \rho}{\rho_l} \quad (\text{A.27})$$

is left. This is the conservation of mass equation for the system.

A.2 Force Balance

Momentum is defined as the product of the mass and velocity of an object. A net force is the total forces on a body which is equal to the rate of change in momentum. When there is no acceleration in the system the net force on the body is zero and therefore the momentum of the body is constant. This section is based on the derivation in *McKenzie* (1984). The rate of change of fluid momentum must to be equal to the forces acting on the fluids. There are three forces working on the fluid: gravity, the interactive force between the fluid and solid from Newton's third law, and the applied force from the background.

Fluid Momentum

The equation for rate of change of fluid momentum of the entire system can be written as

$$\frac{d}{dt} \int_V \rho \vec{u} dV = - \int_V \rho g \hat{j} dV - \int_V \vec{F} dV + \int_S \sigma_{ij}^f \cdot \hat{n} dS \quad (\text{A.28})$$

where g is acceleration due to gravity in the vertical direction, \vec{F} is the interaction force on the solid by the fluid, and σ_{ij}^f is the stress tensor acting on the fluid. Since there are two phases in this system this equation must be applied only to the fluid portion of the volume. This means dS must be replaced with ϕdS and $\rho = \rho_f \phi$. This makes the equation

$$\frac{d}{dt} \int_V \rho_f(\phi) \vec{u} dV = - \int_V \rho_f(\phi) g \hat{j} dV - \int_V \vec{F} dV + \int_S \sigma_{ij}^f \cdot \hat{n}(\phi) dS \quad (\text{A.29})$$

using divergence theorem this becomes

$$\frac{d}{dt} \int_V \rho_f(\phi) \vec{u} dV = - \int_V \rho_f(\phi) g \hat{j} dV - \int_V \vec{F} dV + \int_V \nabla \cdot (\sigma_{ij}^f \phi) dV \quad (\text{A.30})$$

The fluid is assumed to be sufficiently viscous such that the time scale on which things accelerate is much smaller than the time scale of interest. This means $\frac{d}{dt} \int_V \rho_f(\phi) \vec{u} dV = 0$. The equation can be rewritten as

$$0 = - \int_V \rho_f(\phi) g \hat{j} dV - \int_V \vec{F} dV + \int_V \nabla \cdot (\sigma_{ij}^f \phi) dV. \quad (\text{A.31})$$

Solid Momentum

Similarly the equation for rate of change of solid momentum of the entire system can be written as

$$\frac{d}{dt} \int_V \rho \vec{U} dV = - \int_V \rho g \hat{j} dV + \int_V \vec{F} dV + \int_S \sigma_{ij}^s \cdot \hat{n} dS \quad (\text{A.32})$$

where g is acceleration due to gravity in the vertical direction, \vec{F} is the interactive force, σ_{ij}^s is the stress tensor acting on the solid. Since the fluid force is defined as $-\vec{F}$, by Newton's third law the reaction force by the solid must be \vec{F} . Again since the system has two phases, the solid force is only acting on the surface of the solid, therefore dS must be replaced by $(1 - \phi) dS$ and $\rho = \rho_s(1 - \phi)$. This alters the above equation (Eq A.32) to obtain

$$\frac{d}{dt} \int_V \rho_s(1 - \phi) \vec{U} dV = - \int_V \rho_s(1 - \phi) g \hat{j} dV + \int_V \vec{F} dV + \int_S \sigma_{ij}^s \cdot \hat{n} (1 - \phi) dS \quad (\text{A.33})$$

then applying divergence theorem this becomes

$$\frac{d}{dt} \int_V \rho_s(1 - \phi) \vec{U} dV = - \int_V \rho_s(1 - \phi) g \hat{j} dV + \int_V \vec{F} dV + \int_V \nabla \cdot (\sigma_{ij}^s (1 - \phi)) dV. \quad (\text{A.34})$$

Assuming no acceleration ($\frac{d}{dt} \int_V \rho_s(1 - \phi) \vec{U} dV = 0$) obtains

$$0 = - \int_V \rho_s(1 - \phi) g \hat{j} dV + \int_V \vec{F} dV + \int_V \nabla \cdot (\sigma_{ij}^s (1 - \phi)) dV \quad (\text{A.35})$$

and finally the solid momentum equation is given by

$$0 = - \rho_s(1 - \phi) g \hat{j} + \vec{F} + \nabla \cdot (\sigma_{ij}^s (1 - \phi)). \quad (\text{A.36})$$

Putting it together

The inter-phase force must include a pressure term to account for the force created by the porosity gradient as well as a factor of the difference in velocity:

$$\vec{F} = C_1(\vec{u} - \vec{U}) - p\nabla\phi \quad (\text{A.37})$$

where C_1 , is a constant and p is the fluid pressure.

The stress tensor of an incompressible fluid is given by

$$\sigma_{ij}^f = -pI + \eta \left(\frac{\partial u_i}{\partial x_j} + \frac{\partial u_j}{\partial x_i} \right) \quad (\text{A.38})$$

(*Landau and Lifshitz*, 1959) where η is the dynamic viscosity and I is the identity matrix. By neglecting the second term in A.38 and subbing it into A.31 with A.37

$$-\rho_f\phi g\hat{j} - (C_1(\vec{u} - \vec{U}) - p\nabla\phi) + \nabla \cdot (-pI\phi) = 0. \quad (\text{A.39})$$

Expanding the term $\nabla \cdot (-pI\phi)$ obtains

$$\nabla \cdot (-pI\phi) = -\nabla \cdot \begin{bmatrix} p\phi & 0 \\ 0 & p\phi \end{bmatrix}. \quad (\text{A.40})$$

This simplifies to

$$= - \begin{bmatrix} \frac{\partial}{\partial x} p\phi \\ \frac{\partial}{\partial y} p\phi \end{bmatrix}. \quad (\text{A.41})$$

By applying the product rule : $\frac{\partial}{\partial x} f(x,y)g(x,y) = \frac{\partial f}{\partial x}g + \frac{\partial g}{\partial x}f$ this becomes

$$= - \begin{bmatrix} \phi \frac{\partial}{\partial x} p + p \frac{\partial}{\partial x} \phi \\ \phi \frac{\partial}{\partial y} p + p \frac{\partial}{\partial y} \phi \end{bmatrix} \quad (\text{A.42})$$

which can be rewritten as

$$= -(\phi\nabla p + p\nabla\phi). \quad (\text{A.43})$$

Now this can be substituted back into equation A.39

$$(\vec{u} - \vec{U}) = \frac{1}{C_1} (-\rho_f\phi g\hat{j} + p\nabla\phi - (\phi\nabla p + p\nabla\phi)). \quad (\text{A.44})$$

To obtain C_1 this equation needs to be in the same form as D'Arcy's Law (rearrange to the form $\vec{u} = -c \nabla(p + \rho_f g y)$). Rearranging the equation above and substituting in $\rho_f g \hat{j} = \nabla \rho_f g y$ this becomes

$$(\vec{u} - \vec{U}) = -\frac{\phi}{C_1} \nabla(p + \rho_f g y). \quad (\text{A.45})$$

When $U = 0$ this corresponds to D'Arcy's law:

$$\vec{u} = -\frac{\phi}{C_1} \nabla(p + \rho_f g y). \quad (\text{A.46})$$

D'Arcy's law is given by

$$\vec{u} = -\frac{\kappa_\phi}{\phi \eta} \nabla(p + \rho_f g y) \quad (\text{A.47})$$

where κ_ϕ and η is the viscosity of the fluid. Equation A.46 must satisfy D'Arcy's law equation A.47 therefore

$$C_1 = \frac{\eta \phi^2}{\kappa_\phi}. \quad (\text{A.48})$$

A.2.1 Fluid Force Balance

The fluid force balance is given by the interactive force derived above:

$$\phi(\vec{u} - \vec{U}) = -\frac{-\kappa}{\mu} \nabla(p + \rho_f g y). \quad (\text{A.49})$$

To simplify the computation, conservation of mass (Eq A.27) will be used to cancel the fluid velocity term. The conservation of mass is written as

$$\nabla \cdot (\phi \vec{u} + (1 - \phi) \vec{U}) = \Gamma \frac{\Delta \rho}{\rho_l} \quad (\text{A.50})$$

which can be rearranged to

$$\nabla \cdot (\phi(\vec{u} - \vec{U})) = -\nabla \cdot \vec{U} + \Gamma \frac{\Delta \rho}{\rho_l} \quad (\text{A.51})$$

By substituting Darcy's Law in, the equation

$$\nabla \cdot \left(\frac{-\kappa}{\mu} \nabla(p_{fluid} + \rho_f g y) \right) = -\nabla \cdot \vec{U} + \Gamma \frac{\Delta \rho}{\rho_l} \quad (\text{A.52})$$

is obtained, which takes the divergence of Darcy's Law. This simplifies to

$$\nabla \cdot \left(\vec{U} - \frac{\kappa}{\mu} \nabla(p_{fluid} + \rho_f g y) \right) = \Gamma \frac{\Delta \rho}{\rho_l}. \quad (\text{A.53})$$

In order to relate the buoyancy term to the difference in density instead of the respective densities, the pressure is transformed to : $p = p_{fluid} + ((1 - \phi_{bac})\rho_s + \phi_{bac}\rho_f)gy$. This is substituted into the equation to obtain

$$\nabla \cdot \left(\vec{U} - \frac{\kappa}{\mu} \nabla (p - ((1 - \phi_{bac})\rho_s + \phi_{bac}\rho_f)gy + \rho_f gy) \right) = \Gamma \frac{\Delta\rho}{\rho_l} \quad \text{which simplifies to} \quad (\text{A.54})$$

$$\nabla \cdot \left(\vec{U} - \frac{\kappa}{\mu} \nabla (p - ((1 - \phi_{bac})\rho_s + \phi_{bac}\rho_f - \rho_f)gy) \right) = \Gamma \frac{\Delta\rho}{\rho_l}. \quad (\text{A.55})$$

By isolating the density terms and substituting in $\Delta\rho = \rho_s - \rho_f$ this further simplifies to the final form of the dimensional fluid force balance equation:

$$\nabla \cdot \left(\vec{U} - \frac{\kappa}{\mu} \nabla (p - (1 - \phi_{bac})\Delta\rho gy) \right) = \Gamma \frac{\Delta\rho}{\rho_l}. \quad (\text{A.56})$$

A.2.2 Solid Force Balance

For solids the stresses are more complicated. Ignoring gravity for now, the solid stress tensor can be given by

$$\sigma_{ij}^s = -p_{fluid}I + \sigma'_{ij}. \quad (\text{A.57})$$

If stress is small, the shear will behave linearly, meaning this can be rewritten as

$$\sigma'_{ij} = \zeta I \nabla \cdot \vec{U} + \eta \left(\frac{\partial U_i}{\partial x_j} + \frac{\partial U_j}{\partial x_i} - \frac{2}{3} I \nabla \cdot \vec{U} \right) \quad (\text{A.58})$$

where ζ is the bulk viscosity and η the solid shear viscosity, both of which can depend on ϕ . This is the simplest equation for σ'_{ij} which will be valid at low stresses. Now this equation can be substituted into equation A.57 to obtain

$$\sigma_{ij}^s = -p_{fluid}I + \zeta I \nabla \cdot \vec{U} + \eta \left(\frac{\partial U_i}{\partial x_j} + \frac{\partial U_j}{\partial x_i} - \frac{2}{3} I \nabla \cdot \vec{U} \right) \quad (\text{A.59})$$

which is then substituted into equation A.36 which gives

$$-\rho_s(1 - \phi)g\hat{j} + \vec{F} + \nabla \cdot \left(-p_{fluid}I + \zeta I \nabla \cdot \vec{U} + \eta \left(\frac{\partial U_i}{\partial x_j} + \frac{\partial U_j}{\partial x_i} - \frac{2}{3} I \nabla \cdot \vec{U} \right) \right) (1 - \phi) = 0. \quad (\text{A.60})$$

This simplifies to

$$-\rho_s(1-\phi)g\hat{j} + \vec{F} + \nabla \cdot (-(1-\phi)p_{fluid}I + (1-\phi)\sigma'_{ij}) = 0 \quad (\text{A.61})$$

which can be expanded to

$$-\rho_s(1-\phi)g\hat{j} + \vec{F} + \nabla \cdot (-p_{fluid}I + p_{fluid}I\phi + (1-\phi)\sigma'_{ij}) = 0. \quad (\text{A.62})$$

Recall $\nabla \cdot p_{fluid}I\phi = (\phi\nabla p_{fluid} + p_{fluid}\nabla\phi)$, subbing this in, the equation above becomes

$$-\rho_s(1-\phi)g\hat{j} + \vec{F} + (\phi\nabla p_{fluid} + p_{fluid}\nabla\phi) + \nabla \cdot (-p_{fluid}I + (1-\phi)\sigma'_{ij}) = 0 \quad (\text{A.63})$$

Interactive force is known from the previous part A.37 and A.48 which is given by $\vec{F} = \frac{\eta\phi^2}{\kappa_\phi}(\vec{u} - \vec{U}) - p_{fluid}\nabla\phi$ this is also substituted to yield

$$-\rho_s(1-\phi)g\hat{j} + \frac{\eta\phi^2}{\kappa_\phi}(\vec{u} - \vec{U}) - p_{fluid}\nabla\phi + (\phi\nabla p_{fluid} + p_{fluid}\nabla\phi) + \nabla \cdot (-p_{fluid}I + (1-\phi)\sigma'_{ij}) = 0. \quad (\text{A.64})$$

Cancelling terms and substituting in equation A.46 this becomes

$$-\rho_s(1-\phi)g\hat{j} - \phi\nabla(p_{fluid} + \rho_f g y) + \phi\nabla p_{fluid} + \nabla \cdot (-p_{fluid}I + (1-\phi)\sigma'_{ij}) = 0. \quad (\text{A.65})$$

Since ρ_f is constant $\nabla\rho_f g y = \rho_f g\hat{j}$ which simplifies the above equation to

$$-(1-\phi)\rho_s g\hat{j} - \phi\rho_f g\hat{j} - \cancel{\phi\nabla p_{fluid}} + \cancel{\phi\nabla p_{fluid}} + \nabla \cdot (-p_{fluid}I + (1-\phi)\sigma'_{ij}) = 0. \quad (\text{A.66})$$

Now σ'_{ij} can be substituted back in to rewrite the equation as

$$-(1-\phi)\rho_s g\hat{j} - \phi\rho_f g\hat{j} + \nabla \cdot \left(-p_{fluid}I + (1-\phi) \left(\zeta I\nabla \cdot \vec{U} + \eta \left(\frac{\partial U_i}{\partial x_j} + \frac{\partial U_j}{\partial x_i} - \frac{2}{3} I\nabla \cdot \vec{U} \right) \right) \right) = 0 \quad (\text{A.67})$$

which can be rearranged to obtain

$$\nabla \cdot \left(-p_{fluid}I + (1-\phi) \left(\zeta I\nabla \cdot \vec{U} + \eta \left(\frac{\partial U_i}{\partial x_j} + \frac{\partial U_j}{\partial x_i} - \frac{2}{3} I\nabla \cdot \vec{U} \right) \right) \right) = \begin{bmatrix} 0 \\ (1-\phi)\rho_s g + \phi\rho_f g \end{bmatrix}. \quad (\text{A.68})$$

Putting this equation in matrix form gives the expression

$$\begin{aligned} \nabla \cdot \left(- \begin{bmatrix} p_{fluid} & 0 \\ 0 & p_{fluid} \end{bmatrix} + (1-\phi) \begin{bmatrix} \zeta \left(\frac{\partial U_1}{\partial x_1} + \frac{\partial U_2}{\partial x_2} \right) & 0 \\ 0 & \zeta \left(\frac{\partial U_1}{\partial x_1} + \frac{\partial U_2}{\partial x_2} \right) \end{bmatrix} \right. \\ \left. + (1-\phi)\eta \begin{bmatrix} \left(\frac{\partial U_1}{\partial x_1} + \frac{\partial U_1}{\partial x_1} - \frac{2}{3} \left(\frac{\partial U_1}{\partial x_1} + \frac{\partial U_2}{\partial x_2} \right) \right) & \left(\frac{\partial U_1}{\partial x_2} + \frac{\partial U_2}{\partial x_1} \right) \\ \left(\frac{\partial U_2}{\partial x_1} + \frac{\partial U_1}{\partial x_2} \right) & \left(\frac{\partial U_2}{\partial x_2} + \frac{\partial U_2}{\partial x_2} - \frac{2}{3} \left(\frac{\partial U_1}{\partial x_1} + \frac{\partial U_2}{\partial x_2} \right) \right) \end{bmatrix} \right) \\ = \begin{bmatrix} 0 \\ (1-\phi)\rho_s g + \phi\rho_f g \end{bmatrix} \end{aligned} \quad (\text{A.69})$$

By adding the matrices and if $(1-\phi)$ is assumed to be part of the porosity dependence of viscosity, and therefore negated when multiplied by ζ or η (also approximately equal to 1) this becomes

$$\begin{aligned} \nabla \cdot \begin{bmatrix} -p_{fluid} + \left(\zeta \left(\frac{\partial U_1}{\partial x_1} + \frac{\partial U_2}{\partial x_2} \right) + \eta \left(\frac{\partial U_1}{\partial x_1} + \frac{\partial U_1}{\partial x_1} - \frac{2}{3} \left(\frac{\partial U_1}{\partial x_1} + \frac{\partial U_2}{\partial x_2} \right) \right) \right) & \eta \left(\frac{\partial U_1}{\partial x_2} + \frac{\partial U_2}{\partial x_1} \right) \\ \eta \left(\frac{\partial U_2}{\partial x_1} + \frac{\partial U_1}{\partial x_2} \right) & -p_{fluid} + \left(\zeta \left(\frac{\partial U_1}{\partial x_1} + \frac{\partial U_2}{\partial x_2} \right) + \eta \left(\frac{\partial U_2}{\partial x_2} + \frac{\partial U_2}{\partial x_2} - \frac{2}{3} \left(\frac{\partial U_1}{\partial x_1} + \frac{\partial U_2}{\partial x_2} \right) \right) \right) \end{bmatrix} \\ = \begin{bmatrix} 0 \\ (1-\phi)\rho_s g + \phi\rho_f g \end{bmatrix} \end{aligned} \quad (\text{A.70})$$

which simplifies to

$$\nabla \cdot \begin{bmatrix} -p_{fluid} + \left(\zeta + \frac{4}{3}\eta \right) \frac{\partial U_1}{\partial x_1} + \left(\zeta - \frac{2}{3}\eta \right) \frac{\partial U_2}{\partial x_2} & \eta \left(\frac{\partial U_2}{\partial x_1} + \frac{\partial U_1}{\partial x_2} \right) \\ \eta \left(\frac{\partial U_2}{\partial x_1} + \frac{\partial U_1}{\partial x_2} \right) & -p_{fluid} + \left(\zeta - \frac{2}{3}\eta \right) \frac{\partial U_1}{\partial x_1} + \left(\zeta + \frac{4}{3}\eta \right) \frac{\partial U_2}{\partial x_2} \end{bmatrix} = \begin{bmatrix} 0 \\ (1-\phi)\rho_s g + \phi\rho_f g \end{bmatrix}. \quad (\text{A.71})$$

By applying a transformation ($p = p_{fluid} + ((1-\phi_0)\rho_s + \phi_0\rho_f)gy$) to the pressure field this becomes

$$\begin{aligned} \nabla \cdot \begin{bmatrix} -\left(p - ((1-\phi_0)\rho_s + \phi_0\rho_f)gy \right) + \left(\zeta + \frac{4}{3}\eta \right) \frac{\partial U_1}{\partial x_1} + \left(\zeta - \frac{2}{3}\eta \right) \frac{\partial U_2}{\partial x_2} & \eta \left(\frac{\partial U_2}{\partial x_1} + \frac{\partial U_1}{\partial x_2} \right) \\ \eta \left(\frac{\partial U_2}{\partial x_1} + \frac{\partial U_1}{\partial x_2} \right) & -\left(p - ((1-\phi_0)\rho_s + \phi_0\rho_f)gy \right) + \left(\zeta - \frac{2}{3}\eta \right) \frac{\partial U_1}{\partial x_1} + \left(\zeta + \frac{4}{3}\eta \right) \frac{\partial U_2}{\partial x_2} \end{bmatrix} \\ = \begin{bmatrix} 0 \\ (1-\phi)\rho_s g + \phi\rho_f g \end{bmatrix} \end{aligned} \quad (\text{A.72})$$

which can be rewritten as

$$\nabla \cdot \begin{bmatrix} -p + (\zeta + \frac{4}{3}\eta)\frac{\partial U_1}{\partial x_1} + (\zeta - \frac{2}{3}\eta)\frac{\partial U_2}{\partial x_2} & \eta \left(\frac{\partial U_2}{\partial x_1} + \frac{\partial U_1}{\partial x_2} \right) \\ \eta \left(\frac{\partial U_2}{\partial x_1} + \frac{\partial U_1}{\partial x_2} \right) & -p + (\zeta - \frac{2}{3}\eta)\frac{\partial U_1}{\partial x_1} + (\zeta + \frac{4}{3}\eta)\frac{\partial U_2}{\partial x_2} \end{bmatrix} + \begin{bmatrix} 0 \\ (1 - \phi_0)\rho_s + \phi_0\rho_f \end{bmatrix} g = \begin{bmatrix} 0 \\ (1 - \phi)\rho_s g + \phi\rho_f g \end{bmatrix}. \quad (\text{A.73})$$

This equation can be rearranged to obtain

$$\nabla \cdot \begin{bmatrix} -p + (\zeta + \frac{4}{3}\eta)\frac{\partial U_1}{\partial x_1} + (\zeta - \frac{2}{3}\eta)\frac{\partial U_2}{\partial x_2} & \eta \left(\frac{\partial U_2}{\partial x_1} + \frac{\partial U_1}{\partial x_2} \right) \\ \eta \left(\frac{\partial U_2}{\partial x_1} + \frac{\partial U_1}{\partial x_2} \right) & -p + (\zeta - \frac{2}{3}\eta)\frac{\partial U_1}{\partial x_1} + (\zeta + \frac{4}{3}\eta)\frac{\partial U_2}{\partial x_2} \end{bmatrix} = \begin{bmatrix} 0 \\ (1 - \phi)\rho_s g + \phi\rho_f g \end{bmatrix} - \begin{bmatrix} 0 \\ (1 - \phi_{bac})\rho_s + \phi_{bac}\rho_f \end{bmatrix} g$$

which simplifies to

$$= \begin{bmatrix} 0 \\ (\chi - \phi - \chi + \phi_{bac})\rho_s g - (\phi_{bac} - \phi)\rho_f g \end{bmatrix}. \quad (\text{A.74})$$

Further simplification gives the final form of the dimensional solid force balance equation:

$$\nabla \cdot \begin{bmatrix} -p + (\zeta + \frac{4}{3}\eta)\frac{\partial U_1}{\partial x_1} + (\zeta - \frac{2}{3}\eta)\frac{\partial U_2}{\partial x_2} & \eta \left(\frac{\partial U_2}{\partial x_1} + \frac{\partial U_1}{\partial x_2} \right) \\ \eta \left(\frac{\partial U_2}{\partial x_1} + \frac{\partial U_1}{\partial x_2} \right) & -p + (\zeta - \frac{2}{3}\eta)\frac{\partial U_1}{\partial x_1} + (\zeta + \frac{4}{3}\eta)\frac{\partial U_2}{\partial x_2} \end{bmatrix} = \begin{bmatrix} 0 \\ (\phi_{bac} - \phi)\Delta\rho g \end{bmatrix}$$

(A.75)

Appendix B

Non-Dimensionalization

To simplify the system, it is non-dimensionalized using a length scale equal to the compaction length which is defined as $\delta_c = \sqrt{\eta_0 \kappa_0 / \mu}$. The dimensionless variables are defined as $\vec{U}' = \vec{U} / \vec{U}_0$ and $p' = \delta_c p / (U_0 \eta_0)$.

B.1 Conservation of Mass of Solid

Recall the conservation of solid mass equation (Eq A.25),

$$-\frac{\partial \phi}{\partial t} + \nabla \cdot (1 - \phi) \vec{U} = -\Gamma \quad (\text{B.1})$$

which can be rewritten as

$$-\frac{\partial \phi}{\partial t} + \nabla \cdot \vec{U} - \nabla \cdot \phi \vec{U} = -\Gamma \quad (\text{B.2})$$

this can be expanded to obtain

$$-\frac{\partial \phi}{\partial t} + \nabla \cdot \vec{U} - (\phi \nabla \cdot \vec{U} + \vec{U} \cdot \nabla \phi) = -\Gamma. \quad (\text{B.3})$$

This can be rearranged to

$$\frac{\partial \phi}{\partial t} + \vec{U} \cdot \nabla \phi = (1 - \phi) \nabla \cdot \vec{U} + \Gamma \quad (\text{B.4})$$

by applying the non-dimensionalization this becomes

$$\frac{U_0}{\delta_c} \frac{\partial \phi}{\partial t'} + \frac{U_0}{\delta_c} \vec{U}' \cdot \nabla' \phi = \frac{U_0}{\delta_c} (1 - \phi) \nabla' \cdot \vec{U}' + \frac{U_0}{\delta_c} \Gamma'. \quad (\text{B.5})$$

This can be re-written as the final form of the dimensionless conservation of solid mass equation:

$$\frac{\partial \phi}{\partial t} + \vec{U} \cdot \nabla \phi = (1 - \phi) \nabla \cdot \vec{U} + \Gamma \quad (\text{B.6})$$

where the variables are redefined as dimensionless, meaning the primes are left out.

B.2 Fluid Force Balance with Conservation of Total Mass

The dimensional fluid force balance equation (Eq A.56) is given by

$$\nabla \cdot \left(\vec{U} - \frac{\kappa}{\mu} \nabla (p - (1 - \phi_{bac}) \Delta \rho g y) \right) = \Gamma \frac{\Delta \rho}{\rho_l}. \quad (\text{B.7})$$

By applying the non-dimensionalization including $\kappa' = \delta_c \kappa / \kappa_0$ this becomes

$$\frac{U_0}{\delta_c} \nabla \cdot (\vec{U}') = \nabla' \cdot \left(\frac{\kappa_0 \kappa'}{\delta_c \mu} \nabla' \frac{U_0 \eta_0}{\delta_c^2} (p') - (1 - \phi_{bac}) \Delta \rho g \hat{j} \right) + \frac{U_0}{\delta_c} \Gamma \frac{\Delta \rho}{\rho_l} \quad (\text{B.8})$$

which can be rearranged to

$$\nabla \cdot (\vec{U}') = \frac{\kappa_0 \eta_0}{\delta_c^2 \mu} \nabla \cdot \kappa' \left(\nabla (p') - \frac{\delta_c^2 \Delta \rho g}{U_0 \eta_0} (1 - \phi_{bac}) \hat{j} \right) + \Gamma \frac{\Delta \rho}{\rho_l} \quad (\text{B.9})$$

by substituting in the compaction length and a new parameter, the percolation velocity $w_0 = \frac{g \Delta \rho \delta_c^2}{\eta_0}$, this becomes

$$\nabla' \cdot (\vec{U}') = \frac{\kappa_0 \eta_0}{(\frac{\eta_0 \kappa_0}{\mu}) \mu} \nabla' \cdot \left(\kappa' \left(\nabla' (p') - \frac{w_0}{U_0} (1 - \phi_{bac}) \hat{j} \right) \right) + \Gamma \frac{\Delta \rho}{\rho_l}. \quad (\text{B.10})$$

The final dimensionless equation for the fluid force mass equation combined with conservation of total mass is given by:

$$\nabla \cdot [\vec{U} - \kappa \nabla p] = - \frac{w_0}{U_0} (1 - \phi_{bac}) \hat{j} \nabla \cdot \kappa + \Gamma \frac{\Delta \rho}{\rho_l}. \quad (\text{B.11})$$

B.3 Solid Force Balance

Recall the dimensional solid force balance equation (Eq A.75) is given by

$$\nabla p = \nabla \cdot [\eta (\nabla \vec{U} + \nabla \vec{U}^T)] + \nabla (\zeta - \frac{2}{3} \eta) \nabla \cdot \vec{U} + (\phi - \phi_{bac}) \Delta \rho g \hat{j}. \quad (\text{B.12})$$

By applying the non-dimensionalization this becomes

$$\frac{\eta_0 U_0}{\delta_c^2} \nabla' p' = \frac{\eta_0 U_0}{\delta_c^2} \nabla' \cdot [\eta' (\nabla' \vec{U}' + \nabla' \vec{U}'^T)] + \frac{\eta_0 U_0}{\delta_c^2} \nabla' (\zeta' - \frac{2}{3} \eta') \nabla' \cdot \vec{U}' + (\phi - \phi_{bac}) \Delta \rho g \hat{j} \quad (\text{B.13})$$

which can be rearranged to

$$\nabla p' = \nabla' \cdot [\eta'(\nabla' \vec{U}' + \nabla' \vec{U}'^T)] + \nabla'(\zeta' - \frac{2}{3}\eta')\nabla' \cdot \vec{U}' + \frac{\delta_c^2 \Delta \rho g}{\eta_0 U_0}(\phi - \phi_{bac})\hat{j}. \quad (\text{B.14})$$

By substituting in the percolation velocity this simplifies to the final form of the dimensionless solid force balance equation:

$$\nabla p = \nabla \cdot [\eta(\nabla \vec{U} + (\nabla \vec{U})^T)] + \nabla(\zeta - \frac{2}{3}\eta)\nabla \cdot \vec{U} + \frac{w_0}{U_0}(\phi - \phi_{bac})\hat{j}. \quad (\text{B.15})$$

Appendix C

Analytical Solution : Excluding Density Variation in Non-Buoyancy Terms

The expected outcome of a set of PDEs under specific conditions found using mathematical methods are known as analytical solutions. These solutions are important for validating certain aspects of numerical models as analytical solutions can only be found in certain cases.

In this study linear theory is used to derive an equation for the growth-rate of the porosity bands. an essential way to test accuracy of the model for input parameters. The viscosity is defined in equation 3.5 as

$$\eta = e^{\frac{\alpha(\phi-\phi_0)}{n\nu}} \left(\sqrt{2} \left(\left(\frac{\partial U}{\partial x} \right)^2 + \left(\frac{\partial V}{\partial y} \right)^2 + \frac{1}{2} \left(\frac{\partial U}{\partial y} + \frac{\partial V}{\partial x} \right)^2 \right)^{\frac{1}{2}} \right)^{\frac{(1-n\nu)}{n\nu}} \quad (\text{C.1})$$

and the permeability is defined in equation 3.7 as $\kappa = \left(\frac{\phi}{\phi_0} \right)^\beta$. The governing equations derived in the previous appendix are expressed as:

$$\frac{\partial \phi}{\partial t} - (1 - \phi) \nabla \cdot \vec{U} + \vec{U} \cdot \nabla \phi = \Gamma, \quad (\text{C.2})$$

since $\Delta \rho = 0$ for non-gravity terms, the fluid force balance equation simplifies to

$$\nabla \cdot [\vec{U} - \kappa \nabla p] = -\nabla \cdot \kappa \left(\frac{w_0}{U_0} (1 - \phi_{bac}) \hat{j} \right), \text{ and} \quad (\text{C.3})$$

$$\nabla p - \nabla \cdot [\eta (\nabla \vec{U} + (\nabla \vec{U})^T)] - \nabla \cdot \left[\left(\zeta - \frac{2}{3} \eta \right) \nabla \cdot \vec{U} \right] = \frac{w_0}{U_0} (\phi - \phi_{bac}) \hat{j}. \quad (\text{C.4})$$

The solid force balance equation (Eq C.4) can be dealt with in two components, the first equation can be written as

$$\frac{\partial p}{\partial x} - \frac{\partial}{\partial x} \left(2\eta \frac{\partial U}{\partial x} + (\zeta - \frac{2}{3}\eta) \left(\frac{\partial U}{\partial x} + \frac{\partial V}{\partial y} \right) \right) - \frac{\partial}{\partial y} \eta \left(\frac{\partial U}{\partial y} + \frac{\partial V}{\partial x} \right) = 0 \quad (\text{C.5})$$

which simplifies to

$$\frac{\partial p}{\partial x} - \frac{\partial}{\partial x} \left((\zeta + \frac{4}{3}\eta) \frac{\partial U}{\partial x} + (\zeta - \frac{2}{3}\eta) \frac{\partial V}{\partial y} \right) - \frac{\partial}{\partial y} \eta \left(\frac{\partial U}{\partial y} + \frac{\partial V}{\partial x} \right) = 0 \quad (\text{C.6})$$

and the second component is given by

$$\frac{\partial p}{\partial y} - \frac{\partial}{\partial x} \eta \left(\frac{\partial U}{\partial y} + \frac{\partial V}{\partial x} \right) - \frac{\partial}{\partial y} \left((\zeta - \frac{2}{3}\eta) \left(\frac{\partial U}{\partial x} + \frac{\partial V}{\partial y} \right) + 2\eta \frac{\partial V}{\partial y} \right) = \frac{w_0}{U_0} (\phi - \phi_{bac}) \quad (\text{C.7})$$

which simplifies to

$$\frac{\partial p}{\partial y} - \frac{\partial}{\partial x} \eta \left(\frac{\partial U}{\partial y} + \frac{\partial V}{\partial x} \right) - \frac{\partial}{\partial y} \left((\zeta - \frac{2}{3}\eta) \frac{\partial U}{\partial x} + (\zeta + \frac{4}{3}\eta) \frac{\partial V}{\partial y} \right) = \frac{w_0}{U_0} (\phi - \phi_{bac}). \quad (\text{C.8})$$

C.1 Zeroth Order

The zeroth order of the variables are defined by the initial conditions which are

$$\phi = \phi_{bac}, \quad p = p_{bac} = 0, \quad U = U_{bac} = y, \quad \text{and} \quad V = V_{bac} = 0. \quad (\text{C.9})$$

The background quantities specify the zeroth order. The internal melting causes the zeroth order approximation to change with time. This is due to the non-constant background porosity outlined below.

C.1.1 Background Porosity

Zeroth order of conservation of mass are derived by substituting these zeroth order variables and parameters into said equations. The zeroth order porosity and solid velocity are subbed into the equation for conservation of mass of the solid derived above (Eq A.25)

$$\frac{\partial \phi}{\partial t} - (1 - \phi) \nabla \cdot \vec{U} + \vec{U} \cdot \nabla \phi = \Gamma \quad (\text{C.10})$$

sub in values

$$\frac{\partial \phi_{bac}}{\partial t} - (1 - \phi_{bac}) \left(\frac{\partial y}{\partial x} + \frac{\partial \theta}{\partial y} \right) + \vec{U} \cdot \nabla \phi_{bac} = \Gamma \quad (\text{C.11})$$

Since ϕ_{bac} does not vary spatially this simplifies to

$$\frac{\partial \phi_{bac}}{\partial t} = \Gamma \quad (\text{C.12})$$

by integration this becomes:

$$\phi_{bac} = \Gamma t + C \quad (\text{C.13})$$

at $t = 0$, $\phi_{bac} = \phi_0$ therefore

$$\phi_{bac} = \Gamma t + \phi_0. \quad (\text{C.14})$$

C.1.2 Zeroth Order Viscosity and Permeability

The zeroth order viscosity and permeability are derived by substituting in these variables. The zeroth order of permeability, κ_0 , is obtained by subbing in the zeroth order of porosity, ϕ_{bac} , into the equation for porosity dependent permeability (Eq 3.7) to obtain

$$\kappa_0 = \left(\frac{\phi_{bac}}{\phi_0} \right)^\beta \quad (\text{C.15})$$

substituting in ϕ_{bac} (Eq C.14) this becomes

$$= \left(\frac{\Gamma t + \phi_0}{\phi_0} \right)^\beta \quad (\text{C.16})$$

which simplifies to

$$\kappa_0 = \left(\frac{\Gamma t}{\phi_0} + 1 \right)^\beta. \quad (\text{C.17})$$

Similarly zeroth order viscosity, η_0 , is found by substituting the zeroth order of porosity, ϕ_0 , into the equation for porosity dependent, shear strain independent viscosity (Eq 3.6) which gives

$$\eta_0 = e^{\frac{\alpha(\phi_{bac} - \phi_0)}{nv}} \quad (\text{C.18})$$

substituting in zeroth order porosity (Eq C.14) this becomes

$$= e^{\frac{\alpha(\Gamma t + \phi_0 - \phi_0)}{nv}} \quad (\text{C.19})$$

which simplifies to

$$\eta_0 = e^{\frac{\alpha \Gamma t}{nv}} \quad (\text{C.20})$$

These equations will be useful in the first order portion of this perturbation approximation.

C.1.3 Zeroth Order Governing Equations

The zeroth order viscosity, permeability, pressure and solid velocity are subbed into the equation for force balance of fluid equation related to solid velocity (Eq A.56). This gives the equation

$$\nabla \cdot [\vec{U} - \kappa \nabla p] = -\nabla \cdot \kappa \left(\frac{w_0}{U_0} (1 - \phi_0) \hat{j} \right) \quad (\text{C.21})$$

by substituting in the zeroth order variables (Eq C.9) and zeroth order viscosity (Eq C.20) and permeability (Eq C.17) this becomes

$$\nabla \cdot \left[\begin{bmatrix} y \\ 0 \end{bmatrix} - \left(\frac{\Gamma t}{\phi_0} + 1 \right) \nabla \theta \right] = -\nabla \cdot \left(\frac{\Gamma t}{\phi_0} + 1 \right) \left(\frac{w_0}{U_0} (1 - \phi_{bac}) \hat{j} \right) \quad (\text{C.22})$$

which simplifies to

$$\left(\frac{\partial y}{\partial x} + \frac{\partial \theta}{\partial y} \right) = 0 \quad (\text{C.23})$$

which further simplifies to

$$0 = 0. \quad \checkmark \text{ TRUE} \quad (\text{C.24})$$

The zeroth order of the solid force balance (Eq A.75) is obtained by substituting the zeroth order of viscosity, permeability, pressure and solid velocity into this equation. As the solid force balance is actually two equations, it will be analysed in two components. The first component is given by

$$\frac{\partial p}{\partial x} - \frac{\partial}{\partial x} \left(\left(\zeta + \frac{4}{3} \eta \right) \frac{\partial U}{\partial x} + \left(\zeta - \frac{2}{3} \eta \right) \frac{\partial V}{\partial y} \right) - \frac{\partial}{\partial y} \eta \left(\frac{\partial U}{\partial y} + \frac{\partial V}{\partial x} \right) = 0 \quad (\text{C.25})$$

by substituting in zeroth order values this becomes

$$\frac{\partial \theta}{\partial x} - \frac{\partial}{\partial x} \left(\left(\zeta + \frac{4}{3} e^{\frac{\alpha \Gamma t}{n_v}} \right) \frac{\partial y}{\partial x} + \left(\zeta - \frac{2}{3} e^{\frac{\alpha \Gamma t}{n_v}} \right) \frac{\partial \theta}{\partial y} \right) - \frac{\partial}{\partial y} e^{\frac{\alpha \Gamma t}{n_v}} \left(\frac{\partial y}{\partial y} + \frac{\partial \theta}{\partial x} \right) = 0 \quad (\text{C.26})$$

which simplifies to

$$-\frac{\partial \theta}{\partial y} = 0 \quad (\text{C.27})$$

which further simplifies to obtain

$$0 = 0. \quad \checkmark \text{ TRUE} \quad (\text{C.28})$$

The second component of the solid force balance equation is given by

$$\frac{\partial p}{\partial y} - \frac{\partial}{\partial x} \eta \left(\frac{\partial U}{\partial y} + \frac{\partial V}{\partial x} \right) - \frac{\partial}{\partial y} \left(\left(\zeta - \frac{2}{3} \eta \right) \frac{\partial U}{\partial x} + \left(\zeta + \frac{4}{3} \eta \right) \frac{\partial V}{\partial y} \right) = \frac{w_0}{U_0} (\phi - \phi_{bac}) \quad (\text{C.29})$$

again substituting in zeroth order values, this becomes

$$\frac{\partial \theta}{\partial y} - \frac{\partial}{\partial x} e^{\frac{\alpha \Gamma t}{n v}} \left(\frac{\partial y}{\partial y} + \frac{\partial \theta}{\partial x} \right) - \frac{\partial}{\partial y} \left(\left(\zeta - \frac{2}{3} e^{\frac{\alpha \Gamma t}{n v}} \right) \frac{\partial y}{\partial x} + \left(\zeta + \frac{4}{3} e^{\frac{\alpha \Gamma t}{n v}} \right) \frac{\partial \theta}{\partial y} \right) = \frac{w_0}{U_0} (\phi_{bac} - \phi_{bac}) \quad (\text{C.30})$$

which simplifies to

$$\frac{\partial \theta}{\partial x} = 0 \quad (\text{C.31})$$

which further simplifies to

$$0 = 0. \quad \checkmark \text{ TRUE} \quad (\text{C.32})$$

C.2 First Order

The first order of the linear approximation is defined as the zeroth order plus a perturbation, which is denoted with subscript 1. The first order of the variables are defined as

$$\phi = \phi_{bac} + \phi_1, \quad p = p_{bac} + p_1, \quad U = U_{bac} + U_1, \quad \text{and} \quad V = V_{bac} + V_1. \quad (\text{C.33})$$

In order to use the properties of Fourier transforms and derivatives the perturbation of porosity is defined as a constant $\Delta\phi$ multiplied by the exponential term of the inverse Fourier transform in k_x , where k_x is the wavenumber in x , also multiplied by the exponential term of the inverse Fourier transform in k_y , where k_y is the wavenumber in y , as well as the Laplace transform in s , which is the growth-rate. This is expressed as

$$\phi_1 = \Delta\phi e^{i(k_x(t)x + k_y(t)y - \Omega(t)) + s(t)} \quad (\text{C.34})$$

The first order porosity is given by

$$\phi = \phi_{bac} + \phi_1 \quad \text{by substituting in } \phi_1 \quad (\text{C.35})$$

$$\phi = \phi_{bac} + \Delta\phi e^{i(k_x(t)x + k_y(t)y - \Omega(t)) + s(t)} \quad (\text{C.36})$$

$$\phi = \phi_0 + \Gamma t + \Delta\phi e^{i(k_x(t)x + k_y(t)y - \Omega(t)) + s(t)}. \quad (\text{C.37})$$

C.2.1 Linearizing First Order Viscosity and Permeability

The first order parameters are found by taking the first order Taylor Series approximation ($f(x) = f(a) + f'(a)(x - a)$) of said parameter about ϕ_0 . The permeability is given by

$$\kappa(\phi) = \kappa_0 + \kappa_1. \quad (\text{C.38})$$

By substituting the first order Taylor series approximation of κ_1 about ϕ_0 this equation becomes

$$= \kappa_0 + \left. \frac{\partial \kappa}{\partial \phi} \right|_{\phi=\phi_{bac}} (\phi - \phi_{bac}). \quad (\text{C.39})$$

By substituting the equation for permeability (Eq 3.7), this becomes

$$= \kappa_0 + \left. \frac{\beta}{\phi_0} \left(\frac{\phi}{\phi_0} \right)^{\beta-1} \right|_{\phi=\phi_{bac}} (\phi - \Gamma t - \phi_0). \quad (\text{C.40})$$

The initial porosity and the equation for porosity are substituted to obtain

$$= \left(\frac{\Gamma t}{\phi_0} + 1 \right)^\beta + \frac{\beta}{\phi_0} \left(\frac{\Gamma t + \phi_0}{\phi_0} \right)^{\beta-1} (\phi_0 + \mathcal{V}t + \phi_1 - \mathcal{V}t - \phi_0) \quad (\text{C.41})$$

which simplifies to

$$\kappa(\phi) = \left(\frac{\Gamma t}{\phi_0} + 1 \right)^\beta + \frac{\beta}{\phi_0} \left(\frac{\Gamma t}{\phi_0} + 1 \right)^{\beta-1} \phi_1. \quad (\text{C.42})$$

The viscosity is evaluated the same way. The equation for viscosity is given by

$$\eta = e^{\frac{\alpha(\phi-\phi_0)}{n\nu}} \left(\sqrt{2} \left(\left(\frac{\partial U}{\partial x} \right)^2 + \left(\frac{\partial V}{\partial y} \right)^2 + \frac{1}{2} \left(\frac{\partial U}{\partial y} + \frac{\partial V}{\partial x} \right)^2 \right)^{\frac{1}{2}} \right)^{\frac{(1-n\nu)}{n\nu}} \quad (\text{C.43})$$

In order to find the first order linearization, both porosity and velocity dependent terms must be linearized. The first is linearized using the Taylor Series about ϕ_{bac} :

$$e^{\frac{\alpha(\phi-\phi_0)}{n\nu}} \approx \eta_0 + \left. \frac{\partial}{\partial \phi} \left[e^{\frac{\alpha(\phi-\phi_0)}{n\nu}} \right] \right|_{\phi=\phi_{bac}} (\phi - \phi_{bac}) \quad (\text{C.44})$$

by evaluating the derivative and substituting in first order porosity and background porosity this becomes

$$\approx \eta_0 + \frac{\alpha}{n\nu} e^{\frac{\alpha(\phi_0+\Gamma t-\phi_0)}{n\nu}} (\phi_0 + \mathcal{V}t + \phi_1 - \phi_0 - \mathcal{V}t) \quad (\text{C.45})$$

which simplifies to

$$e^{\frac{\alpha(\phi-\phi_0)}{n\nu}} \approx \eta_0 + \frac{\alpha}{n\nu} e^{\frac{\alpha\Gamma t}{n\nu}} \phi_1. \quad (\text{C.46})$$

$$(\text{C.47})$$

The second term is linearized using Binomial approximation $(1+x)^\alpha \approx 1+\alpha x$:

$$\begin{aligned} & \left(\sqrt{2} \left(\left(\frac{\partial U}{\partial x} \right)^2 + \left(\frac{\partial V}{\partial y} \right)^2 + \frac{1}{2} \left(\frac{\partial U}{\partial y} + \frac{\partial V}{\partial x} \right)^2 \right)^{\frac{1}{2}} \right)^{\frac{(1-n_v)}{n_v}} \\ & = \left(\sqrt{2} \left(\left(\frac{\partial U_0 + U_1}{\partial x} \right)^2 + \left(\frac{\partial V_0 + V_1}{\partial y} \right)^2 + \frac{1}{2} \left(\frac{\partial U_0 + U_1}{\partial y} + \frac{\partial V_0 + V_1}{\partial x} \right)^2 \right)^{\frac{1}{2}} \right)^{\frac{(1-n_v)}{n_v}} \end{aligned} \quad (\text{C.48})$$

by substituting in values this becomes

$$= \left(\sqrt{2} \left(\left(\frac{\partial(y+U_1)}{\partial x} \right)^2 + \left(\frac{\partial(0+V_1)}{\partial y} \right)^2 + \frac{1}{2} \left(\frac{\partial(y+U_1)}{\partial y} + \frac{\partial(0+V_1)}{\partial x} \right)^2 \right)^{\frac{1}{2}} \right)^{\frac{(1-n_v)}{n_v}} \quad (\text{C.49})$$

which simplifies to

$$= \left(\sqrt{2} \left(\left(\frac{\partial U_1}{\partial x} \right)^2 + \left(\frac{\partial V_1}{\partial y} \right)^2 + \frac{1}{2} \left(\frac{\partial U_1}{\partial y} + \frac{\partial V_1}{\partial x} + 1 \right)^2 \right)^{\frac{1}{2}} \right)^{\frac{(1-n_v)}{n_v}}. \quad (\text{C.50})$$

This can then be expanded to yield

$$= \left(2 \overset{\text{second order}}{\cancel{\left(\frac{\partial U_1}{\partial x} \right)^2}} + 2 \overset{\text{second order}}{\cancel{\left(\frac{\partial V_1}{\partial y} \right)^2}} + \left(\overset{\text{second order}}{\cancel{\left(\frac{\partial U_1}{\partial y} \right)^2}} + \overset{\text{second order}}{\cancel{\left(\frac{\partial V_1}{\partial x} \right)^2}} + 2 \overset{\text{second order}}{\cancel{\frac{\partial U_1}{\partial y} \frac{\partial V_1}{\partial x}}} + 2 \frac{\partial U_1}{\partial y} + 2 \frac{\partial V_1}{\partial x} + 1 \right)^{\frac{1}{2}} \right)^{\frac{(1-n_v)}{n_v}} \quad (\text{C.51})$$

by neglecting second order terms this becomes

$$= \left(2 \frac{\partial U_1}{\partial y} + 2 \frac{\partial V_1}{\partial x} + 1 \right)^{\frac{(1-n_v)}{2n_v}}. \quad (\text{C.52})$$

Now using the Binomial approximation this becomes

$$\approx 1 + \frac{(1-n_v)}{2n_v} \left(2 \frac{\partial U_1}{\partial y} + 2 \frac{\partial V_1}{\partial x} \right). \quad (\text{C.53})$$

By combining these terms the first order approximation of viscosity can be expressed as

$$\eta \approx \eta_0 + e^{\frac{\alpha \Gamma}{n_v}} \frac{\alpha}{n_v} \phi_1 \left(1 + \frac{(1-n_v)}{2n_v} \left(2 \frac{\partial U_1}{\partial y} + 2 \frac{\partial V_1}{\partial x} \right) \right) \quad (\text{C.54})$$

which simplifies to

$$\eta \approx e^{\frac{\alpha \Gamma}{n_v}} + e^{\frac{\alpha \Gamma}{n_v}} \frac{\alpha}{n_v} \phi_1 \left(1 + \frac{(1-n_v)}{n_v} \left(\frac{\partial U_1}{\partial y} + \frac{\partial V_1}{\partial x} \right) \right). \quad (\text{C.55})$$

C.2.2 First Order Governing Equations

Now that the first order viscosity and permeability have been linearized, the first order governing equations can be evaluated.

Conservation of Solid Mass

The equation for conservation of solid mass (Eq A.25) is given by

$$\frac{\partial \phi}{\partial t} - (1 - \phi) \nabla \cdot \vec{U} + \vec{U} \cdot \nabla \phi = \Gamma \quad (\text{C.56})$$

by substituting in first order variables (Eq C.33) this becomes

$$\frac{\partial (\phi_{bac} + \phi_1)}{\partial t} - (1 - (\phi_{bac} + \phi_1)) \nabla \cdot (\vec{U}_{bac} + \vec{U}_1) + (\vec{U}_{bac} + \vec{U}_1) \cdot \nabla (\phi_{bac} + \phi_1) = \Gamma \quad (\text{C.57})$$

which simplifies to

$$\frac{\partial \phi_{bac}}{\partial t} + \frac{\partial \phi_1}{\partial t} - (1 - (\phi_{bac} + \phi_1)) \nabla \cdot (\vec{U}_1) + (\vec{U}_{bac} + \vec{U}_1) \cdot \nabla \phi_1 = \Gamma \quad (\text{C.58})$$

by neglecting second order terms this becomes

$$\frac{\partial \phi_{bac}}{\partial t} + \frac{\partial \phi_1}{\partial t} - (1 - \phi_{bac}) \nabla \cdot \vec{U}_1 + y \frac{\partial \phi_1}{\partial x} = \Gamma. \quad (\text{C.59})$$

Recall $\frac{\partial \phi_{bac}}{\partial t} = \Gamma$ (Eq C.12), by substitution this becomes

$$\Gamma + \frac{\partial \phi_1}{\partial t} - (1 - \phi_{bac}) \nabla \cdot \vec{U}_1 + y \frac{\partial \phi_1}{\partial x} = \Gamma \quad (\text{C.60})$$

which simplifies to

$$\frac{\partial \phi_1}{\partial t} - (1 - \phi_0 - \Gamma t) \nabla \cdot \vec{U}_1 + y \frac{\partial \phi_1}{\partial x} = 0. \quad (\text{C.61})$$

Recall the equation for ϕ_1 (Eq C.34). In order to evaluate the above equation, expressions for $\frac{\partial \phi_1}{\partial t}$ and $\frac{\partial \phi_1}{\partial x}$ are required. By taking the time derivative of the definition of ϕ_1 the equation

$$\frac{\partial \phi_1}{\partial t} = \Delta \phi e^{i(k_x(t)x + k_y(t)y - \Omega(t)) + s(t)} \left(i \left(\frac{\partial k_x}{\partial t} x + \frac{\partial k_y}{\partial t} y - \frac{\partial \Omega}{\partial t} \right) + \frac{\partial s}{\partial t} \right) \quad \text{is obtained.} \quad (\text{C.62})$$

This can be simplified to

$$\frac{\partial \phi_1}{\partial t} = \phi_1 \left(i \left(\frac{\partial k_x}{\partial t} x + \frac{\partial k_y}{\partial t} y - \frac{\partial \Omega}{\partial t} \right) + \frac{\partial s}{\partial t} \right). \quad (\text{C.63})$$

The spatial derivative in x is taken of ϕ_1 to obtain

$$\frac{\partial \phi_1}{\partial x} = \Delta \phi e^{i(k_x(t)x + k_y(t)y - \Omega(t)) + s(t)} (ik_x) \quad (\text{C.64})$$

which simplifies to

$$\frac{\partial \phi_1}{\partial x} = ik_x \phi_1. \quad (\text{C.65})$$

The expressions for $\frac{\partial \phi_1}{\partial t}$ and $\frac{\partial \phi_1}{\partial t}$ can be substituted into equation C.61 to obtain

$$\phi_1 \left(i \left(\frac{\partial k_x}{\partial t} x + \frac{\partial k_y}{\partial t} y - \frac{\partial \Omega}{\partial t} \right) + \frac{\partial s}{\partial t} \right) - (1 - \phi_0 - \Gamma t) \nabla \cdot \vec{U}_1 + y(ik_x \phi_1) = 0 \quad (\text{C.66})$$

The property of Fourier Transforms of derivatives is given by $\frac{\partial f(t)}{\partial t} = i\lambda \tilde{f}$. Applying this to the remaining derivatives in the equation, this becomes

$$\phi_1 \left(i \left(\frac{\partial k_x}{\partial t} x + \frac{\partial k_y}{\partial t} y - \frac{\partial \Omega}{\partial t} \right) + \frac{\partial s}{\partial t} \right) - (1 - \phi_0 - \Gamma t) (\tilde{U}_1 ik_x + \tilde{V}_1 ik_y) + ik_x \phi_1 y = 0. \quad (\text{C.67})$$

The goal of this derivation is the growth-rate $\frac{\partial s}{\partial t}$, so this equation is rearranged to give

$$\frac{\partial s}{\partial t} - i \frac{\partial \Omega}{\partial t} = \frac{(1 - \phi_0 - \Gamma t)}{\phi_1} (ik_x \tilde{U}_1 + ik_y \tilde{V}_1) + i \left(x \frac{\partial k_x}{\partial t} + y \left(\frac{\partial k_y}{\partial t} - k_x \right) \right). \quad (\text{C.68})$$

Since $\frac{\partial s}{\partial t}$ is not spatially dependent, $\frac{\partial k_x}{\partial t}$ must be equal to zero and $\frac{\partial k_y}{\partial t}$ must be equal to k_x .

This simplifies the equation to

$$\frac{\partial s}{\partial t} - i \frac{\partial \Omega}{\partial t} = \frac{(1 - \phi_0 - \Gamma t)}{\phi_1} (ik_x \tilde{U}_1 + ik_y \tilde{V}_1). \quad (\text{C.69})$$

Fluid Force Balance

The equation for fluid force balance (Eq A.56) is given by

$$\nabla \cdot [\vec{U} - \kappa \nabla p] = -\nabla \cdot \kappa \left(\frac{w_0}{U_0} (1 - \phi_{bac}) \hat{j} \right). \quad (\text{C.70})$$

By substituting in first order variable (Eq C.33) this becomes

$$\nabla \cdot [(\vec{U}_0 + \vec{U}_1) - (\kappa_0 + \kappa_1) \nabla (p_0 + p_1)] = -\nabla \cdot (\kappa_0 + \kappa_1) \left(\frac{w_0}{U_0} (1 - \phi_{bac}) \hat{j} \right) \quad (\text{C.71})$$

which simplifies to

$$\nabla \cdot [\vec{U}_1 - (\kappa_0 + \overset{\text{second order}}{\cancel{\kappa_1}}) \nabla p_1] = -\nabla \cdot (\kappa_0 + \kappa_1) \left(\frac{w_0}{U_0} (1 - \phi_{bac}) \hat{j} \right). \quad (\text{C.72})$$

Substituting in first order viscosity (Eq C.55) and permeability (Eq C.42) this becomes

$$\nabla \cdot [\vec{U}_1 - \left(\frac{\Gamma t}{\phi_0} + 1 \right)^\beta \nabla p_1] = -\nabla \cdot \frac{\beta}{\phi_0} \left(\frac{\Gamma t}{\phi_0} + 1 \right)^{\beta-1} \phi_1 \left(\frac{w_0}{U_0} (1 - \phi_{bac}) \hat{j} \right) \quad (\text{C.73})$$

which can be expanded to become

$$\frac{\partial U_1}{\partial x} + \frac{\partial V_1}{\partial y} - \left(\frac{\Gamma t}{\phi_0} + 1 \right)^\beta \left(\frac{\partial^2 p_1}{\partial x^2} + \frac{\partial^2 p_1}{\partial y^2} \right) = -\frac{\beta}{\phi_0} \left(\frac{\Gamma t}{\phi_0} + 1 \right)^{\beta-1} \frac{w_0}{U_0} (1 - \phi_{bac}) \frac{\partial \phi_1}{\partial y} \quad (\text{C.74})$$

The goal is to obtain a series of linear equations such that $\frac{\partial s}{\partial t}$ can be found. The Fourier Transform of the above equation is taken to give

$$i\tilde{U}_1 k_x + i\tilde{V}_1 k_y - \left(\frac{\Gamma t}{\phi_0} + 1 \right)^\beta \left(i^2 \tilde{p}_1 k_x^2 + i^2 \tilde{p}_1 k_y^2 \right) = -(1 - \phi_{bac}) \frac{\beta}{\phi_0} \left(\frac{\Gamma t}{\phi_0} + 1 \right)^{\beta-1} \frac{w_0}{U_0} i\tilde{\phi}_1 k_y \quad (\text{C.75})$$

which simplifies to the final form of the linearized fluid force balance equation:

$$k_x i\tilde{U}_1 + k_y i\tilde{V}_1 + \left(\frac{\Gamma t}{\phi_0} + 1 \right)^\beta (k_x^2 + k_y^2) \tilde{p}_1 = -(1 - \phi_{bac}) \left(\frac{\Gamma t}{\phi_0} + 1 \right)^{\beta-1} \frac{\beta}{\phi_0} \frac{w_0}{U_0} k_y i\tilde{\phi}_1. \quad (\text{C.76})$$

Solid Force Balance

Recall the equation for solid force balance (Eq A.75), since this equation is actually two equations they will be evaluated separately. The first component of the solid force balance equation is given by

$$\frac{\partial p}{\partial x} - \frac{\partial}{\partial x} \left(\left(\zeta + \frac{4}{3}\eta \right) \frac{\partial U}{\partial x} + \left(\zeta - \frac{2}{3}\eta \right) \frac{\partial V}{\partial y} \right) - \frac{\partial}{\partial y} \eta \left(\frac{\partial U}{\partial y} + \frac{\partial V}{\partial x} \right) = 0 \quad (\text{C.77})$$

By substituting in the equations for first order viscosity (Eq C.55), pressure (Eq C.33), and solid velocity (Eq C.33), this becomes

$$\begin{aligned} \frac{\partial(p_0 + p_1)}{\partial x} - \frac{\partial}{\partial x} \left((\zeta + \frac{4}{3}(\eta_0 + \eta_1)) \frac{\partial(U_0 + U_1)}{\partial x} + (\zeta - \frac{2}{3}(\eta_0 + \eta_1)) \frac{\partial(V_0 + V_1)}{\partial y} \right) \\ - \frac{\partial}{\partial y} (\eta_0 + \eta_1) \left(\frac{\partial(U_0 + U_1)}{\partial y} + \frac{\partial(V_0 + V_1)}{\partial x} \right) = 0 \end{aligned} \quad (\text{C.78})$$

sub in values for U_0 and V_0

$$\begin{aligned} \frac{\partial(p_0^0 + p_1)}{\partial x} - \frac{\partial}{\partial x} \left((\zeta + \frac{4}{3}(\eta_0 + \eta_1)) \frac{\partial(y^0 + U_1)}{\partial x} + (\zeta - \frac{2}{3}(\eta_0 + \eta_1)) \frac{\partial(0 + V_1)}{\partial y} \right) \\ - \frac{\partial}{\partial y} (\eta_0 + \eta_1) \left(\frac{\partial(y + U_1)}{\partial y} + \frac{\partial(0 + V_1)}{\partial x} \right) = 0 \end{aligned} \quad (\text{C.79})$$

By further expansion this became

$$\begin{aligned} \frac{\partial p_1}{\partial x} - \frac{\partial}{\partial x} \left((\zeta + \frac{4}{3}(\eta_0 + \eta_1)) \frac{\overset{\text{second order}}{\partial U_1}}{\partial x} + (\zeta - \frac{2}{3}(\eta_0 + \eta_1)) \frac{\overset{\text{second order}}{\partial V_1}}{\partial y} \right) \\ - \frac{\partial}{\partial y} \eta_0 \left(1 + \frac{\partial U_1}{\partial y} + \frac{\partial V_1}{\partial x} \right) + \eta_1 + \eta_1 \left(\frac{\partial U_1}{\partial y} + \frac{\partial V_1}{\partial x} \right) \overset{\text{second order}}{=} 0 \end{aligned} \quad (\text{C.80})$$

$$\frac{\partial p_1}{\partial x} - \frac{\partial}{\partial x} \left((\zeta + \frac{4}{3}\eta_0) \frac{\partial U_1}{\partial x} + (\zeta - \frac{2}{3}\eta_0) \frac{\partial V_1}{\partial y} \right) - \frac{\partial}{\partial y} \left[\eta_0 \left(1 + \frac{\partial U_1}{\partial y} + \frac{\partial V_1}{\partial x} \right) + \eta_1 \right] = 0 \quad (\text{C.81})$$

sub in values for η_0 and η_1

$$\begin{aligned} \frac{\partial p_1}{\partial x} - \frac{\partial}{\partial x} \left[(\zeta + \frac{4}{3}e^{\frac{\alpha\Gamma_r}{n_v}}) \frac{\partial U_1}{\partial x} + (\zeta - \frac{2}{3}e^{\frac{\alpha\Gamma_r}{n_v}}) \frac{\partial V_1}{\partial y} \right] \\ - \frac{\partial}{\partial y} \left[e^{\frac{\alpha\Gamma_r}{n_v}} \left(1 + \left(\frac{\partial U_1}{\partial y} \right) + \frac{\partial V_1}{\partial x} \right) + \frac{\alpha}{n_v} e^{\frac{\alpha\Gamma_r}{n_v}} \phi_1 + e^{\frac{\alpha\Gamma_r}{n_v} \frac{(1-n_v)}{n_v}} \left(\frac{\partial U_1}{\partial y} + \frac{\partial V_1}{\partial x} \right) \right] = 0 \end{aligned} \quad (\text{C.82})$$

$$\begin{aligned} \frac{\partial p_1}{\partial x} - (\zeta + \frac{4}{3}e^{\frac{\alpha\Gamma_r}{n_v}}) \frac{\partial^2 U_1}{\partial x^2} - (\zeta - \frac{2}{3}e^{\frac{\alpha\Gamma_r}{n_v}}) \frac{\partial^2 V_1}{\partial x \partial y} - e^{\frac{\alpha\Gamma_r}{n_v}} \left(\frac{\partial^2 U_1}{\partial y^2} + \frac{\partial^2 V_1}{\partial x \partial y} \right) \\ - \frac{\alpha}{n_v} e^{\frac{\alpha\Gamma_r}{n_v}} \frac{\partial \phi_1}{\partial y} - e^{\frac{\alpha\Gamma_r}{n_v} \frac{(1-n_v)}{n_v}} \left(\frac{\partial^2 U_1}{\partial y^2} + \frac{\partial^2 V_1}{\partial x \partial y} \right) = 0 \end{aligned} \quad (\text{C.83})$$

Taking the Fourier Transform of this equation yields

$$\begin{aligned} \tilde{p}_1 i k_x - \left(\zeta + \frac{4}{3} e^{\frac{\alpha \Gamma}{n\nu}} \right) i^2 \tilde{U}_1 k_x^2 - \left(\zeta - \frac{2}{3} e^{\frac{\alpha \Gamma}{n\nu}} \right) i^2 \tilde{V}_1 k_x k_y \\ - e^{\frac{\alpha \Gamma}{n\nu}} (i^2 U_1 k_y^2 + i^2 V_1 k_x k_y) - e^{\frac{\alpha \Gamma}{n\nu}} \frac{(1-n\nu)}{n\nu} (i^2 U_1 k_y^2 + i^2 V_1 k_x k_y) = \frac{\alpha}{n\nu} e^{\frac{\alpha \Gamma}{n\nu}} i \phi_1 k_y \end{aligned} \quad (\text{C.84})$$

which simplifies to the final form of the first component of the linearized solid force balance equation:

$$\tilde{p}_1 i k_x - \left(\left(\zeta + \frac{4}{3} e^{\frac{\alpha \Gamma}{n\nu}} \right) k_x^2 + e^{\frac{\alpha \Gamma}{n\nu}} \left(1 + \frac{(1-n\nu)}{n\nu} \right) k_y^2 \right) i^2 \tilde{U}_1 - \left(\zeta + e^{\frac{\alpha \Gamma}{n\nu}} \left(\frac{1}{3} + \frac{(1-n\nu)}{n\nu} \right) \right) i^2 \tilde{V}_1 k_x k_y = \frac{\alpha}{n\nu} e^{\frac{\alpha \Gamma}{n\nu}} i \phi_1 k_y. \quad (\text{C.85})$$

The second component of the solid force balance equation is given by

$$\frac{\partial p}{\partial y} - \frac{\partial}{\partial x} \eta \left(\frac{\partial U}{\partial y} + \frac{\partial V}{\partial x} \right) - \frac{\partial}{\partial y} \left(\left(\zeta - \frac{2}{3} \eta \right) \frac{\partial U}{\partial x} + \left(\zeta + \frac{4}{3} \eta \right) \frac{\partial V}{\partial y} \right) = \frac{w_0}{U_0} (\phi - \phi_{bac}) \quad (\text{C.86})$$

By substituting in the equations for first order viscosity (Eq C.55), pressure (Eq C.33), and solid velocity (Eq C.33), this becomes

$$\begin{aligned} \frac{\partial (p_0^0 + p_1)}{\partial y} - \frac{\partial}{\partial x} (\eta_0 + \eta_1) \left(\frac{\partial (U_0 + U_1)}{\partial y} + \frac{\partial (V_0 + V_1)}{\partial x} \right) \\ - \frac{\partial}{\partial y} \left(\left(\zeta - \frac{2}{3} (\eta_0 + \eta_1) \right) \frac{\partial (U_0 + U_1)}{\partial x} + \left(\zeta + \frac{4}{3} (\eta_0 + \eta_1) \right) \frac{\partial (V_0 + V_1)}{\partial y} \right) \\ = \frac{w_0}{U_0} ((\phi_0 + \mathcal{P}\mathcal{I} + \phi_1) - \phi_0 - \mathcal{P}\mathcal{I}) \end{aligned} \quad (\text{C.87})$$

by substituting in initial values this becomes

$$\begin{aligned} \frac{\partial p_1}{\partial y} - \frac{\partial}{\partial x} (\eta_0 + \eta_1) \left(\frac{\partial U_1}{\partial y} + \frac{\partial (0 + V_1)}{\partial x} \right) \\ - \frac{\partial}{\partial y} \left(\left(\zeta - \frac{2}{3} (\eta_0 + \eta_1) \right) \left(\frac{\partial U_1}{\partial x} + \frac{\partial U_1}{\partial x} \right) + \left(\zeta + \frac{4}{3} (\eta_0 + \eta_1) \right) \frac{\partial (0 + V_1)}{\partial y} \right) = \frac{w_0}{U_0} \phi_1 \end{aligned} \quad (\text{C.88})$$

which simplifies to

$$\begin{aligned} \frac{\partial p_1}{\partial y} - \frac{\partial}{\partial x} \left((\eta_0 + \eta_1) + (\eta_0 + \eta_1) \overset{\text{second order}}{\left(\frac{\partial U_1}{\partial y} + \frac{\partial V_1}{\partial x} \right)} \right) \\ - \frac{\partial}{\partial y} \left(\left(\zeta - \frac{2}{3}(\eta_0 + \eta_1) \right) \overset{\text{second order}}{\frac{\partial U_1}{\partial x}} + \left(\zeta + \frac{4}{3}(\eta_0 + \eta_1) \right) \overset{\text{second order}}{\frac{\partial V_1}{\partial y}} \right) = \frac{w_0}{U_0} \phi_1. \end{aligned} \quad (\text{C.89})$$

By neglecting all the second order terms and subbing in zeroth and first order viscosity (η_0 and η_1) this becomes

$$\begin{aligned} \frac{\partial p_1}{\partial y} - \frac{\partial}{\partial x} \left(\left(e^{\frac{\alpha \Gamma_1}{n\nu}} + \frac{\alpha}{n\nu} e^{\frac{\alpha \Gamma_1}{n\nu}} \phi_1 + e^{\frac{\alpha \Gamma_1}{n\nu}} \frac{(1-n\nu)}{n\nu} \left(\frac{\partial U_1}{\partial y} + \frac{\partial V_1}{\partial x} \right) \right) + \left(e^{\frac{\alpha \Gamma_1}{n\nu}} \left(\frac{\partial U_1}{\partial y} + \frac{\partial V_1}{\partial x} \right) \right) \right) \\ - \frac{\partial}{\partial y} \left(\left(\zeta - \frac{2}{3} e^{\frac{\alpha \Gamma_1}{n\nu}} \right) \frac{\partial U_1}{\partial x} + \left(\zeta + \frac{4}{3} e^{\frac{\alpha \Gamma_1}{n\nu}} \right) \frac{\partial V_1}{\partial y} \right) = \frac{w_0}{U_0} \phi_1 \end{aligned} \quad (\text{C.90})$$

which can be rewritten as

$$\begin{aligned} \frac{\partial p_1}{\partial y} - \frac{\partial}{\partial x} \left(\frac{\alpha}{n\nu} e^{\frac{\alpha \Gamma_1}{n\nu}} \phi_1 + e^{\frac{\alpha \Gamma_1}{n\nu}} \left(1 + \frac{(1-n\nu)}{n\nu} \right) \left(\frac{\partial U_1}{\partial y} + \frac{\partial V_1}{\partial x} \right) \right) \\ - \frac{\partial}{\partial y} \left(\left(\zeta - \frac{2}{3} e^{\frac{\alpha \Gamma_1}{n\nu}} \right) \frac{\partial U_1}{\partial x} + \left(\zeta + \frac{4}{3} e^{\frac{\alpha \Gamma_1}{n\nu}} \right) \frac{\partial V_1}{\partial y} \right) = \frac{w_0}{U_0} \phi_1. \end{aligned} \quad (\text{C.91})$$

By expansion this equations becomes

$$\begin{aligned} \frac{\partial p_1}{\partial y} - \left(\zeta - \frac{2}{3} e^{\frac{\alpha \Gamma_1}{n\nu}} \right) \frac{\partial^2 U_1}{\partial x y} - e^{\frac{\alpha \Gamma_1}{n\nu}} \left(1 + \frac{(1-n\nu)}{n\nu} \right) \frac{\partial^2 U_1}{\partial x y} \\ - e^{\frac{\alpha \Gamma_1}{n\nu}} \left(1 + \frac{(1-n\nu)}{n\nu} \right) \frac{\partial^2 V_1}{\partial x^2} - \left(\zeta + \frac{4}{3} e^{\frac{\alpha \Gamma_1}{n\nu}} \right) \frac{\partial^2 V_1}{\partial y^2} = \frac{w_0}{U_0} \phi_1 + \frac{\alpha}{n\nu} e^{\frac{\alpha \Gamma_1}{n\nu}} \frac{\partial \phi_1}{\partial x}. \end{aligned} \quad (\text{C.92})$$

The Fourier transform of this equation is taken to yield

$$\begin{aligned} i\tilde{p}_1 k_y - \left(\zeta + e^{\frac{\alpha \Gamma_1}{n\nu}} \left(\frac{1}{3} + \frac{(1-n\nu)}{n\nu} \right) \right) i^2 \tilde{U}_1 k_x k_y \\ - e^{\frac{\alpha \Gamma_1}{n\nu}} \left(1 + \frac{(1-n\nu)}{n\nu} \right) i^2 \tilde{V}_1 k_x^2 - \left(\zeta + \frac{4}{3} e^{\frac{\alpha \Gamma_1}{n\nu}} \right) i^2 \tilde{V}_1 k_y^2 = \frac{w_0}{U_0} \tilde{\phi}_1 + \frac{\alpha}{n\nu} e^{\frac{\alpha \Gamma_1}{n\nu}} i \tilde{\phi}_1 k_x \end{aligned} \quad (\text{C.93})$$

which simplifies to the final form of the second component of the linearized solid force balance equation:

$$-\tilde{p}_1 k_y + \left(\zeta + e^{\frac{\alpha \Gamma_1}{n\nu}} \left(\frac{1}{3} + \frac{(1-n\nu)}{n\nu} \right) \right) i k_x k_y \tilde{U}_1 + \left(e^{\frac{\alpha \Gamma_1}{n\nu}} \left(1 + \frac{(1-n\nu)}{n\nu} \right) k_x^2 + \left(\zeta + \frac{4}{3} e^{\frac{\alpha \Gamma_1}{n\nu}} \right) k_y^2 \right) i \tilde{V}_1 = \frac{w_0}{U_0} i \tilde{\phi}_1 - \frac{\alpha}{n\nu} e^{\frac{\alpha \Gamma_1}{n\nu}} \tilde{\phi}_1 k_x. \quad (\text{C.94})$$

C.2.3 Bringing It All Together

Now that the equation for growth-rate and frequency is found from the solid force mass balance equation (Eq C.69) and each of the other governing equations are linearized and in Fourier space (Eq C.76, C.85, C.94), which can be written as a matrix in order to find the unknowns and evaluate the growth-rate and frequency. The unknowns are evaluated in matrix form ($M\vec{p} = \vec{q}$) where M is the coefficient matrix, \vec{p} is the parameter vector and \vec{q} is coefficient vector for $\tilde{\phi}_1$. The matrix form is given by

$$\begin{bmatrix} k_x & k_y & (\frac{\Gamma t}{\phi_0} + 1)^\beta (k_x^2 + k_y^2) \\ k_x^2 (\zeta + \frac{4}{3} e^{\frac{\alpha \Gamma t}{n\nu}}) + (1 + \frac{(1-n\nu)}{n\nu}) e^{\frac{\alpha \Gamma t}{n\nu}} k_y^2 & (\zeta + (\frac{1}{3} + \frac{(1-n\nu)}{n\nu}) e^{\frac{\alpha \Gamma t}{n\nu}}) k_x k_y & -k_x \\ (\zeta + (\frac{1}{3} + \frac{(1-n\nu)}{n\nu}) e^{\frac{\alpha \Gamma t}{n\nu}}) k_x k_y & (1 + \frac{(1-n\nu)}{n\nu}) e^{\frac{\alpha \Gamma t}{n\nu}} k_x^2 + (\zeta + \frac{4}{3} e^{\frac{\alpha \Gamma t}{n\nu}}) k_y^2 & -k_y \end{bmatrix} \begin{bmatrix} i\tilde{U}_1 \\ i\tilde{V}_1 \\ \tilde{p}_1 \end{bmatrix} = \begin{bmatrix} -(1 - \phi_0 - \Gamma t) \left(\frac{\Gamma t}{\phi_0} + 1 \right)^{\beta-1} \frac{\beta}{\phi_0} \frac{w_0}{U_0} k_y i \\ -\frac{\alpha}{n\nu} e^{\frac{\alpha \Gamma t}{n\nu}} k_y \\ w_0/U_0 i - \frac{\alpha}{n\nu} e^{\frac{\alpha \Gamma t}{n\nu}} k_x \end{bmatrix} \tilde{\phi}_1. \quad (\text{C.95})$$

This equation can be rearranged to find the parameter vector ($\vec{p} = M^{-1}\vec{q}$). Mathematica is used to find the inverse of the M matrix. The growth-rate and oscillatory frequency are found by inputting the variables found in Mathematica into the equation found from the conservation of solid mass equation $\frac{\partial s}{\partial t} - i\frac{\partial \Omega}{\partial t} = \frac{(1-\phi_0-\Gamma t)}{\tilde{\phi}_1} (ik_x \tilde{U}_1 + ik_y \tilde{V}_1)$ (Eq C.69).

Growth-Rate

The growth-rate is given by the real part of (Eq C.69) and is found to be

$$\frac{\partial s}{\partial t} = \frac{-6(1 - \phi_0 - \Gamma t) \alpha e^{\frac{\alpha \Gamma t}{n\nu}} \kappa_0 k_x k_y k^4}{n\nu (3\psi + \kappa_0 (k_x^2 + k_y^2)) (4e^{\frac{\alpha \Gamma t}{n\nu}} ((k_x^4 + k_y^4)(1 + \sigma) + k_x^2 k_y^2 (2 + \sigma)) + 3\psi \zeta)}$$

(C.96)

where $\kappa_0 = \left(\frac{\Gamma t}{\phi_0} + 1\right)^\beta$, $k = (k_x^2 + k_y^2)^{1/2}$, $\sigma = \frac{(1-n_v)}{n_v}$, and $\psi = k^4 + (k_x^2 - k_y^2)^2 \sigma$. The growth-rate for the strain-rate independent viscosity case ($n_v = 1$) can be expressed as

$$\frac{\partial s}{\partial t} = \frac{-6k_x k_y \kappa_0 (1 - \phi_0 - \Gamma t) \alpha e^{\frac{\alpha \Gamma t}{n_v}}}{3 + \kappa_0 k^2 (4e^{\frac{\alpha \Gamma t}{n_v}} + 3\zeta)}. \quad (\text{C.97})$$

Oscillatory Frequency

The oscillatory frequency is given by the imaginary part of (Eq C.69) and is given by

$$i \frac{\partial \Omega}{\partial t} = 3k_y (1 - \phi_0 - \Gamma t) \frac{w_0}{U_0} \frac{\kappa_0 (k^4 + (k_y^4 - k_x^4) \sigma) - \kappa_1 \psi (1 - \phi_0 - \Gamma t)}{3\psi + \kappa_0 k^2 (4e^{\frac{\alpha \Gamma t}{n_v}} ((k_x^4 + k_y^4)(1 + \sigma) + k_x^2 k_y^2 (2 + \sigma)) + 3\psi \zeta)} \quad (\text{C.98})$$

where $\kappa_1 = \left(\frac{\Gamma t}{\phi_0} + 1\right)^{\beta-1} \frac{\beta}{\phi_0}$. The frequency for the strain-rate independent viscosity case ($n_v = 1$) can be expressed as

$$i \frac{\partial \Omega}{\partial t} = 3k_y (1 - \phi_0 - \Gamma t) \frac{w_0}{U_0} \frac{\kappa_0 - \kappa_1 (1 - \phi_0 - \Gamma t)}{3 + \kappa_0 k^2 (4e^{\frac{\alpha \Gamma t}{n_v}} + 3\zeta)}. \quad (\text{C.99})$$

Appendix D

Analytical Solution : Isotropic Expansion

The method in Appendix C is repeated including density variation in non-buoyancy terms for strain-rate dependent solid viscosity and linearly dependent bulk viscosity. This means the governing equations used for this derivation are:

$$\frac{\partial \phi}{\partial t} - (1 - \phi) \nabla \cdot \vec{U} + \vec{U} \cdot \nabla \phi = \Gamma, \quad (\text{D.1})$$

$$\nabla \cdot [\vec{U} - \kappa \nabla p] = -\frac{w_0}{U_0} (1 - \phi_{bac}) \nabla \cdot \kappa \hat{j} + \Gamma \frac{\Delta \rho}{\rho_l}, \text{ and} \quad (\text{D.2})$$

$$\nabla p - \nabla \cdot [\eta (\nabla \vec{U} + (\nabla \vec{U})^T)] - \nabla [(\zeta - \frac{2}{3} \eta) \nabla \cdot \vec{U}] = \frac{w_0}{U_0} (\phi - \phi_{bac}) \hat{j}. \quad (\text{D.3})$$

The permeability used is defined in equation 3.7 as $\left(\frac{\phi}{\phi_0}\right)^\beta$. The strain-rate dependent solid viscosity is defined in equation 3.5 as

$$\eta = e^{\frac{\alpha(\phi - \phi_0)}{nv}} \left(\sqrt{2} \left(\left(\frac{\partial U}{\partial x} \right)^2 + \left(\frac{\partial V}{\partial y} \right)^2 + \frac{1}{2} \left(\frac{\partial U}{\partial y} + \frac{\partial V}{\partial x} \right)^2 \right)^{\frac{1}{2}} \right)^{\frac{(1-nv)}{nv}}. \quad (\text{D.4})$$

The bulk viscosity is defined as $\zeta = \zeta_r \eta$, where ζ_r is the ratio between ζ and η . This is based on *Katz and Takei (2013)* who suggested that the bulk viscosity is linearly dependent on the solid viscosity.

D.1 Zeroth Order

The zeroth order variables are defined as

$$\phi = \phi_{bac}, \quad p = p_{bac}, \quad U = U_{bac} = U_{melt} + U_{ext}, \quad \text{and} \quad V = V_{bac} = V_{melt} + V_{ext}$$

where U_{melt} and V_{melt} is the velocity field due to melting and U_{ext} and V_{ext} is the velocity field which is applying shear. For the vertical shear case $U_{ext} = 0$ and $V_{ext} = x$.

D.1.1 Fluid Force Balance

The fluid force balance equation is used to find \vec{U}_{melt} and p_{bac} . Since buoyancy force is a first order term, the zeroth order fluid force balance equation is given by

$$\nabla \cdot [\vec{U}_{bac} - \kappa \nabla p_{bac}] = \Gamma \frac{\Delta \rho}{\rho_l} \quad (\text{D.5})$$

and since $\nabla \cdot \vec{U}_{ext} = 0$ this equation simplifies to

$$\nabla \cdot [\vec{U}_{melt} - \kappa \nabla p_{bac}] = \Gamma \frac{\Delta \rho}{\rho_l}. \quad (\text{D.6})$$

This equation can be satisfied by setting $\nabla \cdot \vec{U}_{melt}$ to $\Gamma \frac{\Delta \rho}{\rho_l}$ with p_{bac} being spatially independent. $\nabla \cdot \vec{U}_{melt} = \Gamma \frac{\Delta \rho}{\rho_l}$ has many solutions. The one chosen for this study corresponds to isotropic expansion which is expressed as: $\vec{U}_{melt} = \Gamma \frac{\Delta \rho}{2\rho_l} x \hat{i} + \Gamma \frac{\Delta \rho}{2\rho_l} y \hat{j}$.

D.1.2 Conservation of Solid Mass

Now the conservation of solid mass equation combined with \vec{U}_{melt} and p_{bac} from the section above are used to find ϕ_{bac} . The zeroth order conservation of solid mass equation is expressed as

$$\frac{\partial \phi_{bac}}{\partial t} - (1 - \phi_{bac}) \nabla \cdot \vec{U}_{bac} + \vec{U}_{bac} \cdot \nabla \phi_{bac} = \Gamma \quad (\text{D.7})$$

since $\nabla \cdot \vec{U}_{bac} = \Gamma \frac{\Delta \rho}{\rho_l}$ and assuming ϕ_{bac} is not spatially dependent this equation can be rewritten as

$$\frac{\partial \phi_{bac}}{\partial t} + \phi_{bac} \Gamma \frac{\Delta \rho}{\rho_l} = \Gamma + \Gamma \frac{\Delta \rho}{\rho_l}. \quad (\text{D.8})$$

In order to isolate the derivative of ϕ_{bac} both sides are multiplied by $\exp(\Gamma t \Delta \rho / \rho_l)$ which yields

$$e^{\Gamma t \Delta \rho / \rho_l} \left(\frac{\partial \phi_{bac}}{\partial t} + \phi_{bac} \Gamma \frac{\Delta \rho}{\rho_l} \right) = (\Gamma + \Gamma \frac{\Delta \rho}{\rho_l}) e^{\Gamma t \Delta \rho / \rho_l}. \quad (\text{D.9})$$

This simplifies to

$$\frac{\partial}{\partial t} \phi_{bac} e^{\Gamma t \Delta \rho / \rho_l} = (\Gamma + \Gamma \frac{\Delta \rho}{\rho_l}) e^{\Gamma t \Delta \rho / \rho_l}. \quad (D.10)$$

By integration with respect to time this becomes

$$\phi_{bac} e^{\Gamma t \Delta \rho / \rho_l} = (\Gamma + \Gamma \frac{\Delta \rho}{\rho_l}) \frac{\rho_l}{\Gamma \Delta \rho} e^{\Gamma t \Delta \rho / \rho_l} + C. \quad (D.11)$$

In order to isolate ϕ_{bac} this equation can be divided by $e^{\Gamma t \Delta \rho / \rho_l}$ which give the expression

$$\phi_{bac} = (\frac{\rho_l}{\Delta \rho} + 1) + C e^{-\Gamma t \Delta \rho / \rho_l}. \quad (D.12)$$

Since $\Gamma t \Delta \rho / \rho_l$ is much less than one, a linear approximation $e^{-\Gamma t \Delta \rho / \rho_l} \approx (1 - \Gamma t \Delta \rho / \rho_l)$ can be used. Substituting this approximation yields

$$\phi_{bac} \approx (\frac{\rho_l}{\Delta \rho} + 1) + C(1 - \Gamma t \Delta \rho / \rho_l). \quad (D.13)$$

The initial condition $\phi_{bac}(t = 0) = \phi_0$ is used to find the constant C . The initial condition yields the equation

$$\phi_{bac}(t = 0) = \phi_0 = (\frac{\rho_l}{\Delta \rho} + 1) + C \quad (D.14)$$

which can be rearrange to find

$$C = \phi_0 - (\frac{\rho_l}{\Delta \rho} + 1). \quad (D.15)$$

Substituting this equation back into Eq D.13 obtains

$$\phi_{bac} = (\frac{\rho_l}{\Delta \rho} + 1) + (\phi_0 - \frac{\rho_l}{\Delta \rho} + 1)(1 - \Gamma t \Delta \rho / \rho_l) \quad (D.16)$$

which can be expanded to

$$\phi_{bac} = \frac{\rho_l}{\Delta \rho} + \chi + \phi_0 - \phi_0 \Gamma t \frac{\Delta \rho}{\rho_l} - \frac{\rho_l}{\Delta \rho} + \frac{\rho_l}{\Delta \rho} \Gamma t \frac{\Delta \rho}{\rho_l} + \chi - \Gamma t \frac{\Delta \rho}{\rho_l}. \quad (D.17)$$

This simplifies to

$$\phi_{bac} = \phi_0 - \phi_0 \Gamma t \frac{\Delta \rho}{\rho_l} + \Gamma t - \Gamma t \frac{\Delta \rho}{\rho_l} \quad (D.18)$$

which can be rewritten as the final form of the background porosity:

$$\phi_{bac} = \phi_0 + \Gamma t \left[\frac{\Delta \rho}{\rho_l} (1 - \phi_0) + 1 \right]. \quad (D.19)$$

D.1.3 Viscosity and Permeability

Now that all the zeroth order variables are known, zeroth order viscosity and permeability can be found. Zeroth order strain-rate dependent viscosity is given by

$$\eta_{bac} = e^{\frac{\alpha(\phi_{bac} - \phi_0)}{n_v}} \left(\sqrt{2} \left(\left(\frac{\partial U_{bac}}{\partial x} \right)^2 + \left(\frac{\partial V_{bac}}{\partial y} \right)^2 + \frac{1}{2} \left(\frac{\partial U_{bac}}{\partial y} + \frac{\partial V_{bac}}{\partial x} \right)^2 \right)^{\frac{1}{2}} \right)^{\frac{(1-n_v)}{n_v}}. \quad (D.20)$$

By substituting in \vec{U}_{bac} found in the previous section this becomes

$$= e^{\frac{\alpha}{nv}(\phi_{bac} - \phi_0)} \left(\sqrt{2} \left(\left(\frac{\partial}{\partial x} \Gamma \frac{\Delta \rho}{2\rho_l} x \right)^2 + \left(\frac{\partial}{\partial y} [\Gamma \frac{\Delta \rho}{2\rho_l} y + x] \right)^2 + \frac{1}{2} \left(\frac{\partial}{\partial y} \Gamma \frac{\Delta \rho}{2\rho_l} x + \frac{\partial}{\partial x} [\Gamma \frac{\Delta \rho}{2\rho_l} y + x] \right)^2 \right)^{\frac{1}{2}} \right)^{\frac{(1-nv)}{nv}} \quad (\text{D.21})$$

by evaluating the derivatives this becomes

$$= e^{\frac{\alpha}{nv}(\phi_{bac} - \phi_0)} \left(\sqrt{2} \left(\left(\Gamma \frac{\Delta \rho}{2\rho_l} \right)^2 + \left(\Gamma \frac{\Delta \rho}{2\rho_l} \right)^2 + \frac{1}{2} (1)^2 \right)^{\frac{1}{2}} \right)^{\frac{(1-nv)}{nv}}. \quad (\text{D.22})$$

This can be rewritten as

$$= e^{\frac{\alpha}{nv}(\phi_{bac} - \phi_0)} \left(4 \left(\Gamma \frac{\Delta \rho}{2\rho_l} \right)^2 + 1 \right)^{\frac{(1-nv)}{2nv}}. \quad (\text{D.23})$$

The final form of the zeroth order viscosity is given by

$$\eta_{bac} = e^{\frac{\alpha}{nv}(\phi_{bac} - \phi_0)} \left(\left(\Gamma \frac{\Delta \rho}{\rho_l} \right)^2 + 1 \right)^{\frac{(1-nv)}{2nv}}. \quad (\text{D.24})$$

Similarly, the zeroth order permeability is given by

$$\kappa_{bac} = \left(\frac{\phi_{bac}}{\phi_0} \right)^{\beta}. \quad (\text{D.25})$$

D.1.4 Solid Force Balance

The solid force balance equations are checked for the variables above to see if they are satisfied. The zeroth order of the first component of the solid force balance equation is given by

$$\frac{\partial p_{bac}}{\partial x} - \frac{\partial}{\partial x} \left(\left(\zeta_r + \frac{4}{3} \eta_{bac} \right) \frac{\partial U_{bac}}{\partial x} + \left(\zeta_r - \frac{2}{3} \eta_{bac} \right) \frac{\partial V_{bac}}{\partial y} \right) - \frac{\partial}{\partial y} \eta_{bac} \left(\frac{\partial U_{bac}}{\partial y} + \frac{\partial V_{bac}}{\partial x} \right) = 0 \quad (\text{D.26})$$

by substituting in zeroth order velocity and pressure this becomes

$$\frac{\partial \phi}{\partial x} - \frac{\partial}{\partial x} \left(\left(\zeta_r + \frac{4}{3} \right) \eta_{bac} \frac{\partial}{\partial x} \Gamma \frac{\Delta \rho}{2\rho_l} x + \left(\zeta_r - \frac{2}{3} \right) \eta_{bac} \frac{\partial}{\partial y} [\Gamma \frac{\Delta \rho}{2\rho_l} y + x] \right) - \frac{\partial}{\partial y} \eta_{bac} \left(\frac{\partial}{\partial y} \Gamma \frac{\Delta \rho}{2\rho_l} x + \frac{\partial}{\partial x} [\Gamma \frac{\Delta \rho}{2\rho_l} y + x] \right) = 0 \quad (\text{D.27})$$

which simplifies to

$$-\frac{\partial}{\partial x} \left(\zeta_r + \frac{4}{3} \right) \eta_{bac} \Gamma \frac{\Delta \rho}{2\rho_l} - \frac{\partial}{\partial x} \left(\zeta_r - \frac{2}{3} \right) \eta_{bac} \Gamma \frac{\Delta \rho}{2\rho_l} - \eta_{bac} \frac{\partial}{\partial y} (1) = 0 \quad (\text{D.28})$$

since $\eta_{bac} \Gamma \frac{\Delta \rho}{2\rho_l}$ and ζ_r do not vary spatially this simplifies to

$$0 = 0. \quad \checkmark \text{ TRUE} \quad (\text{D.29})$$

Similarly, the zeroth order of the second component of the solid force balance equation is expressed as

$$\frac{\partial p_{bac}}{\partial y} - \frac{\partial}{\partial x} \eta \left(\frac{\partial U_{bac}}{\partial y} + \frac{\partial V_{bac}}{\partial x} \right) - \frac{\partial}{\partial y} \left(\left(\zeta_r - \frac{2}{3} \right) \eta \frac{\partial U_{bac}}{\partial x} + \left(\zeta_r + \frac{4}{3} \right) \eta \frac{\partial V_{bac}}{\partial y} \right) = \frac{w_0}{U_0} (\phi_{bac} - \phi_{bac}). \quad (\text{D.30})$$

Substituting in zeroth order velocity and pressure yields

$$\frac{\partial \phi}{\partial y} - \frac{\partial}{\partial x} \eta_{bac} \left(\frac{\partial}{\partial y} \Gamma \frac{\Delta \rho}{2\rho_l} x + \frac{\partial}{\partial x} [\Gamma \frac{\Delta \rho}{2\rho_l} y + x] \right) - \frac{\partial}{\partial y} \left(\left(\zeta_r - \frac{2}{3} \right) \eta_{bac} \frac{\partial}{\partial x} \Gamma \frac{\Delta \rho}{2\rho_l} x + \left(\zeta_r + \frac{4}{3} \right) \eta_{bac} \frac{\partial}{\partial y} [\Gamma \frac{\Delta \rho}{2\rho_l} y + x] \right) = 0 \quad (\text{D.31})$$

which simplifies to

$$-\eta_{bac} \frac{\partial}{\partial x} (1) - \frac{\partial}{\partial y} \left(\zeta_r - \frac{2}{3} \right) \eta_{bac} \Gamma \frac{\Delta \rho}{2\rho_l} - \frac{\partial}{\partial y} \left(\zeta_r + \frac{4}{3} \right) \eta_{bac} \Gamma \frac{\Delta \rho}{2\rho_l} = 0. \quad (\text{D.32})$$

Since $\eta_{bac} \Gamma \frac{\Delta \rho}{2\rho_l}$ and ζ_r do not vary spatially this simplifies to

$$0 = 0. \quad \checkmark \text{ TRUE} \quad (\text{D.33})$$

This means both components of the solid force balance equation are satisfied by the zeroth order variables found in this section.

D.2 First Order

The first order variables are defined as

$$\phi = \phi_{bac} + \phi_1, \quad p = p_{bac} + p_1, \quad U = U_{bac} + U_1, \quad \text{and} \quad V = V_{bac} + V_1.$$

D.2.1 Viscosity and Permeability

The first order viscosity and permeability are found using the same method as Appendix C. Viscosity is linearized in two parts: porosity dependent and velocity dependent. The first, porosity dependent, term is linearized using a Taylor series expansion about ϕ_{bac} . This can be written as

$$e^{\frac{\alpha(\phi - \phi_0)}{nv}} \approx \eta_{bac} + \frac{\partial}{\partial \phi} e^{\frac{\alpha(\phi - \phi_0)}{nv}} \Bigg|_{\phi = \phi_{bac}} (\phi_1 + \phi_{bac} - \phi_{bac}). \quad (\text{D.34})$$

By evaluating the derivative this becomes

$$= \eta_{bac} + \frac{\alpha}{n_V} e^{\frac{\alpha(\phi-\phi_0)}{n_V}} \Big|_{\phi=\phi_{bac}} \phi_1. \quad (\text{D.35})$$

Substituting in $\phi = \phi_{bac}$ yields the final linearized form of this term:

$$e^{\frac{\alpha(\phi-\phi_0)}{n_V}} = \eta_{bac} + \frac{\alpha}{n_V} e^{\frac{\alpha}{n_V}(\phi_{bac}-\phi_0)} \phi_1. \quad (\text{D.36})$$

The second, velocity dependent, term is linearized using a binomial expansion $(1+x)^\alpha \approx 1 + \alpha x$. Before this approximation can be made, this term must be put in the form $(1+x)^\alpha$. This is done by substituting in first order variables and evaluating the derivatives. The first order of the velocity dependent term is given by

$$\left(\sqrt{2} \left(\left(\frac{\partial}{\partial x} (U_{bac} + U_1) \right)^2 + \left(\frac{\partial}{\partial y} (V_{bac} + V_1) \right)^2 + \frac{1}{2} \left(\frac{\partial}{\partial y} (U_{bac} + U_1) + \frac{\partial}{\partial x} (V_{bac} + V_1) \right)^2 \right)^{\frac{1}{2}} \right)^{\frac{(1-n_V)}{n_V}}. \quad (\text{D.37})$$

By expansion this becomes

$$\left(\sqrt{2} \left(\left(\frac{\partial U_{bac}}{\partial x} \right)^2 + 2 \frac{\partial U_1}{\partial x} \frac{\partial U_{bac}}{\partial x} + \left(\frac{\partial U_1}{\partial x} \right)^2 + \left(\frac{\partial V_{bac}}{\partial y} \right)^2 + 2 \frac{\partial V_1}{\partial y} \frac{\partial V_{bac}}{\partial y} + \left(\frac{\partial V_1}{\partial y} \right)^2 + \frac{1}{2} \left(\frac{\partial}{\partial y} (U_{bac} + U_1) + \frac{\partial}{\partial x} (V_{bac} + V_1) \right)^2 \right)^{\frac{1}{2}} \right)^{\frac{(1-n_V)}{n_V}}, \quad (\text{D.38})$$

neglecting second order terms yields

$$\left(\sqrt{2} \left(\left(\frac{\partial U_{bac}}{\partial x} \right)^2 + 2 \frac{\partial U_1}{\partial x} \frac{\partial U_{bac}}{\partial x} + \left(\frac{\partial V_{bac}}{\partial y} \right)^2 + 2 \frac{\partial V_1}{\partial y} \frac{\partial V_{bac}}{\partial y} + \frac{1}{2} \left(\frac{\partial U_{bac}}{\partial y} + \frac{\partial U_1}{\partial y} + \frac{\partial V_{bac}}{\partial x} + \frac{\partial V_1}{\partial x} \right)^2 \right)^{\frac{1}{2}} \right)^{\frac{(1-n_V)}{n_V}}. \quad (\text{D.39})$$

For simplicity, the last term is expanded separately. This is given by

$$\left(\frac{\partial U_{bac}}{\partial y} + \frac{\partial U_1}{\partial y} + \frac{\partial V_{bac}}{\partial x} + \frac{\partial V_1}{\partial x} \right)^2 = \left(\frac{\partial U_1}{\partial y} + \frac{\partial V_1}{\partial x} + 1 \right) \left(\frac{\partial U_1}{\partial y} + \frac{\partial V_1}{\partial x} + 1 \right) \quad (\text{D.40})$$

which expands to

$$= \left(\frac{\partial U_1}{\partial y} \right)^2 + 2 \frac{\partial U_1}{\partial y} \frac{\partial V_1}{\partial x} + 2 \frac{\partial U_1}{\partial y} + \left(\frac{\partial V_1}{\partial x} \right)^2 + 2 \frac{\partial V_1}{\partial x} + 1 \quad (\text{D.41})$$

by neglecting second order terms this simplifies to

$$= 2 \frac{\partial U_1}{\partial y} + 2 \frac{\partial V_1}{\partial x} + 1. \quad (\text{D.42})$$

By substituting this equation back into equation D.39 gives the expression

$$\left(\sqrt{2} \left(\left(\frac{\partial U_{bac}}{\partial x} \right)^2 + 2 \frac{\partial U_1}{\partial x} \frac{\partial U_{bac}}{\partial x} + \left(\frac{\partial V_{bac}}{\partial y} \right)^2 + 2 \frac{\partial V_1}{\partial y} \frac{\partial V_{bac}}{\partial y} + \frac{1}{2} \left(2 \frac{\partial U_1}{\partial y} + 2 \frac{\partial V_1}{\partial x} + 1 \right) \right)^{\frac{1}{2}} \right)^{\frac{(1-n_v)}{n_v}} \quad (\text{D.43})$$

by evaluating the derivatives this becomes

$$\left(\sqrt{2} \left(\left(\Gamma \frac{\Delta \rho}{2 \rho_l} \right)^2 + 2 \Gamma \frac{\Delta \rho}{2 \rho_l} \frac{\partial U_1}{\partial x} + \left(\Gamma \frac{\Delta \rho}{2 \rho_l} \right)^2 + 2 \Gamma \frac{\Delta \rho}{2 \rho_l} \frac{\partial V_1}{\partial y} + \frac{1}{2} \left(2 \frac{\partial U_1}{\partial y} + 2 \frac{\partial V_1}{\partial x} + 1 \right) \right)^{\frac{1}{2}} \right)^{\frac{(1-n_v)}{n_v}} . \quad (\text{D.44})$$

This can be rewritten as

$$\left(2 \left(\Gamma \frac{\Delta \rho}{2 \rho_l} \right)^2 + 2 \Gamma \frac{\Delta \rho}{\rho_l} \frac{\partial U_1}{\partial x} + 2 \left(\Gamma \frac{\Delta \rho}{2 \rho_l} \right)^2 + 2 \Gamma \frac{\Delta \rho}{\rho_l} \frac{\partial V_1}{\partial y} + 2 \frac{\partial U_1}{\partial y} + 2 \frac{\partial V_1}{\partial x} + 1 \right)^{\frac{(1-n_v)}{2 n_v}} \quad (\text{D.45})$$

which simplifies to

$$\left(\left(\Gamma \frac{\Delta \rho}{\rho_l} \right)^2 + 2 \left(\Gamma \frac{\Delta \rho}{\rho_l} \frac{\partial U_1}{\partial x} + \frac{\partial U_1}{\partial y} \right) + 2 \left(\Gamma \frac{\Delta \rho}{\rho_l} \frac{\partial V_1}{\partial y} + \frac{\partial V_1}{\partial x} \right) + 1 \right)^{\frac{(1-n_v)}{2 n_v}} . \quad (\text{D.46})$$

This is now in required form for the binomial approximation. Applying the approximation yields the linearized form of the velocity dependent term:

$$1 + \frac{(1-n_v)}{2 n_v} \left(\left(\Gamma \frac{\Delta \rho}{\rho_l} \right)^2 + 2 \left(\Gamma \frac{\Delta \rho}{\rho_l} \frac{\partial U_1}{\partial x} + \frac{\partial U_1}{\partial y} \right) + 2 \left(\Gamma \frac{\Delta \rho}{\rho_l} \frac{\partial V_1}{\partial y} + \frac{\partial V_1}{\partial x} \right) \right) . \quad (\text{D.47})$$

Now that both porosity and velocity dependent terms are linearized, they can be put back together to obtain the expression for viscosity. This is done by multiplying these terms together which yields

$$\eta \approx \left(\eta_{bac} + \frac{\alpha}{n_v} e^{\frac{\alpha}{n_v} (\phi_{bac} - \phi_0)} \phi_1 \right) \left(1 + \frac{(1-n_v)}{2 n_v} \left(\left(\Gamma \frac{\Delta \rho}{\rho_l} \right)^2 + 2 \left(\Gamma \frac{\Delta \rho}{\rho_l} \frac{\partial U_1}{\partial x} + \frac{\partial U_1}{\partial y} \right) + 2 \left(\Gamma \frac{\Delta \rho}{\rho_l} \frac{\partial V_1}{\partial y} + \frac{\partial V_1}{\partial x} \right) \right) \right) . \quad (\text{D.48})$$

By expansion this becomes

$$\begin{aligned} &= \eta_{bac} + \eta_{bac} \left(\frac{(1-n_v)}{2 n_v} \left(\left(\Gamma \frac{\Delta \rho}{\rho_l} \right)^2 + 2 \left(\Gamma \frac{\Delta \rho}{\rho_l} \frac{\partial U_1}{\partial x} + \frac{\partial U_1}{\partial y} \right) + 2 \left(\Gamma \frac{\Delta \rho}{\rho_l} \frac{\partial V_1}{\partial y} + \frac{\partial V_1}{\partial x} \right) \right) \right) + \frac{\alpha}{n_v} e^{\frac{\alpha}{n_v} (\phi_{bac} - \phi_0)} \phi_1 \\ &\quad + \frac{\alpha}{n_v} e^{\frac{\alpha}{n_v} (\phi_{bac} - \phi_0)} \phi_1 \left(\frac{(1-n_v)}{2 n_v} \left(\left(\Gamma \frac{\Delta \rho}{\rho_l} \right)^2 + 2 \left(\Gamma \frac{\Delta \rho}{\rho_l} \frac{\partial U_1}{\partial x} + \frac{\partial U_1}{\partial y} \right) + 2 \left(\Gamma \frac{\Delta \rho}{\rho_l} \frac{\partial V_1}{\partial y} + \frac{\partial V_1}{\partial x} \right) \right) \right) . \end{aligned} \quad (\text{D.49})$$

Neglecting second order terms obtains

$$\begin{aligned}
&= \eta_{bac} + \eta_{bac} \left(\frac{(1-n_v)}{2n_v} \left((\Gamma \frac{\Delta \rho}{\rho_l})^2 + 2(\Gamma \frac{\Delta \rho}{\rho_l} \frac{\partial U_1}{\partial x} + \frac{\partial U_1}{\partial y}) + 2(\Gamma \frac{\Delta \rho}{\rho_l} \frac{\partial V_1}{\partial y} + \frac{\partial V_1}{\partial x}) \right) \right) \\
&\quad + \frac{\alpha}{n_v} e^{\frac{\alpha}{n_v}(\phi_{bac}-\phi_0)} \phi_1 + \frac{\alpha}{n_v} e^{\frac{\alpha}{n_v}(\phi_{bac}-\phi_0)} \phi_1 \left(\frac{(1-n_v)}{2n_v} \left(\Gamma \frac{\Delta \rho}{\rho_l} \right)^2 \right)
\end{aligned} \tag{D.50}$$

which can be rewritten as

$$\begin{aligned}
&= \eta_{bac} + \eta_{bac} \left(\frac{(1-n_v)}{2n_v} \left((\Gamma \frac{\Delta \rho}{\rho_l})^2 + 2(\Gamma \frac{\Delta \rho}{\rho_l} \frac{\partial U_1}{\partial x} + \frac{\partial U_1}{\partial y}) + 2(\Gamma \frac{\Delta \rho}{\rho_l} \frac{\partial V_1}{\partial y} + \frac{\partial V_1}{\partial x}) \right) \right) \\
&\quad + \frac{\alpha}{n_v} e^{\frac{\alpha}{n_v}(\phi_{bac}-\phi_0)} \phi_1 \left(\frac{(1-n_v)}{2n_v} \left(\Gamma \frac{\Delta \rho}{\rho_l} \right)^2 + 1 \right).
\end{aligned} \tag{D.51}$$

The objective is to find first order viscosity, since $\eta = \eta_{bac} + \eta_1$, this must be given by

$$\eta_1 = \eta_{bac} \left(\frac{(1-n_v)}{2n_v} \left((\Gamma \frac{\Delta \rho}{\rho_l})^2 + 2(\Gamma \frac{\Delta \rho}{\rho_l} \frac{\partial U_1}{\partial x} + \frac{\partial U_1}{\partial y}) + 2(\Gamma \frac{\Delta \rho}{\rho_l} \frac{\partial V_1}{\partial y} + \frac{\partial V_1}{\partial x}) \right) \right) + \frac{\alpha}{n_v} \eta_{bac} \phi_1. \tag{D.52}$$

Since the permeability is only dependent on porosity, it can be linearized only using the Taylor series expansion about $\phi = \phi_{bac}$. This expansion can be written as

$$\kappa \approx \kappa_{bac} + \frac{\partial}{\partial \phi} \left(\frac{\phi}{\phi_0} \right)^\beta \Big|_{\phi_1=\phi_{bac}} (\phi - \phi_{bac}). \tag{D.53}$$

By evaluating the derivative this becomes

$$= \kappa_{bac} + \frac{\beta}{\phi_0} \left(\frac{\phi}{\phi_0} \right)^{\beta-1} \Big|_{\phi=\phi_{bac}} (\phi_1 + \phi_{bac} - \phi_{bac}) \tag{D.54}$$

which when substituting in $\phi = \phi_{bac}$ this becomes

$$\kappa = \kappa_{bac} + \frac{\beta}{\phi_0} \left(\frac{\phi_{bac}}{\phi_0} \right)^{\beta-1} (\phi_1) \tag{D.55}$$

$$\tag{D.56}$$

Again the objective is the first order term, since $\kappa = \kappa_{bac} + \kappa_1$ the first order permeability can be expressed as

$$\kappa_1 = \frac{\beta}{\phi_0} \left(\frac{\phi_{bac}}{\phi_0} \right)^{\beta-1} (\phi_1). \tag{D.57}$$

D.2.2 Conservation of Solid Mass

The first order conservation of solid mass equation is used to find the expression for growth rate and frequency which will be used with the other first order governing equations to find

the final analytical solution. The first order conservation of solid mass equation is given by

$$\frac{\partial}{\partial t}(\phi_{bac} + \phi_1) - (1 - (\phi_{bac} + \phi_1))\nabla \cdot (\vec{U}_{bac} + \vec{U}_1) + (\vec{U}_{bac} + \vec{U}_1) \cdot \nabla(\phi_{bac} + \phi_1) = \Gamma \quad (\text{D.58})$$

since ϕ_{bac} does not vary spatially, $\frac{\partial \phi_{bac}}{\partial t} = \Gamma \left[\frac{\Delta \rho}{\rho_l} (1 - \phi_0) + 1 \right]$ and $\nabla \cdot \vec{U}_{bac} = \Gamma \frac{\Delta \rho}{\rho_l}$ this can be rewritten as

$$\Gamma \left[\frac{\Delta \rho}{\rho_l} (1 - \phi_0) + 1 \right] + \frac{\partial \phi_1}{\partial t} - (1 - \phi_{bac} - \phi_1) \Gamma \frac{\Delta \rho}{\rho_l} + (1 - \phi_{bac} - \phi_1) \overset{\text{second order}}{\nabla} \cdot \vec{U}_1 + (\vec{U}_{bac} + \vec{U}_1) \overset{\text{second order}}{\cdot} \nabla \phi_1 = \Gamma. \quad (\text{D.59})$$

By neglecting second order terms this becomes

$$\Gamma \left[\frac{\Delta \rho}{\rho_l} (1 - \phi_0) + 1 \right] + \frac{\partial \phi_1}{\partial t} - (1 - \phi_{bac} - \phi_1) \Gamma \frac{\Delta \rho}{\rho_l} + (1 - \phi_{bac}) \nabla \cdot \vec{U}_1 + \vec{U}_{bac} \cdot \nabla \phi_1 = \Gamma. \quad (\text{D.60})$$

Recall the expression for first order porosity described in Appendix C (Eq C.34).

$$\phi_1 = \Delta \phi e^{i(k_x(t)x + k_y(t)y - \Omega(t)) + s(t)} \quad (\text{D.61})$$

The time derivative of the first order porosity can be expressed as

$$\frac{\partial \phi_1}{\partial t} = \phi_1 \left(i \left(\frac{\partial k_x}{\partial t} x + \frac{\partial k_y}{\partial t} y - \frac{\partial \Omega}{\partial t} \right) + \frac{\partial s}{\partial t} \right). \quad (\text{D.62})$$

The gradient of the first order porosity is given by

$$\nabla \phi_1 = \phi_1 \begin{bmatrix} ik_x \\ ik_y \end{bmatrix}. \quad (\text{D.63})$$

Substituting Eq D.62 and D.63 into Eq D.60 yields the expression

$$\begin{aligned} & \Gamma \left[\frac{\Delta \rho}{\rho_l} (1 - \phi_0) + 1 \right] + \tilde{\phi}_1 \left(i \left(\frac{\partial k_x}{\partial t} x + \frac{\partial k_y}{\partial t} y - \frac{\partial \Omega}{\partial t} \right) + \frac{\partial s}{\partial t} \right) \\ & + \tilde{\phi}_1 \Gamma \frac{\Delta \rho}{\rho_l} + (1 - \phi_{bac}) \nabla \cdot \vec{U}_1 + \vec{U}_{bac} \cdot \phi_1 \begin{bmatrix} ik_x \\ ik_y \end{bmatrix} = \Gamma. \end{aligned} \quad (\text{D.64})$$

The Fourier transform of this equation is taken to obtain

$$\begin{aligned} \tilde{\phi}_1 \left(i \left(\frac{\partial k_x}{\partial t} x + \frac{\partial k_y}{\partial t} y - \frac{\partial \Omega}{\partial t} \right) + \frac{\partial s}{\partial t} \right) + \tilde{\phi}_1 \Gamma \frac{\Delta \rho}{\rho_l} \\ + (1 - \phi_{bac})(\tilde{U}_1 k_x i + \tilde{V}_1 k_y i) + ik_x \phi_1 \Gamma \frac{\Delta \rho}{2\rho_l} x + ik_y \phi_1 \left(\Gamma \frac{\Delta \rho}{2\rho_l} y + x \right) = 0. \end{aligned} \quad (\text{D.65})$$

This can be rearranged to obtain

$$\begin{aligned} \tilde{\phi}_1 \left(i \left(\frac{\partial k_x}{\partial t} x + \frac{\partial k_y}{\partial t} y - \frac{\partial \Omega}{\partial t} \right) + \frac{\partial s}{\partial t} \right) = -\tilde{\phi}_1 \Gamma \frac{\Delta \rho}{\rho_l} \\ - (1 - \phi_{bac})(\tilde{U}_1 k_x i + \tilde{V}_1 k_y i) - ik_x \tilde{\phi}_1 \Gamma \frac{\Delta \rho}{2\rho_l} x - ik_y \tilde{\phi}_1 \left(\Gamma \frac{\Delta \rho}{2\rho_l} y + x \right). \end{aligned} \quad (\text{D.66})$$

The goal is to obtain the growth rate and frequency, isolating these terms obtains

$$\begin{aligned} \frac{\partial s}{\partial t} - \frac{\partial \Omega}{\partial t} i = -\frac{(1 - \phi_{bac})}{\tilde{\phi}_1} (1 - \phi_{bac})(\tilde{U}_1 k_x i + \tilde{V}_1 k_y i) - \Gamma \frac{\Delta \rho}{\rho_l} \\ - ik_x \Gamma \frac{\Delta \rho}{2\rho_l} x - ik_y \left(\Gamma \frac{\Delta \rho}{2\rho_l} y + x \right) - i \frac{\partial k_x}{\partial t} x - i \frac{\partial k_y}{\partial t} y. \end{aligned} \quad (\text{D.67})$$

Since the growth rate and frequency do not vary spatially this can be rewritten as

$$\frac{\partial s}{\partial t} - \frac{\partial \Omega}{\partial t} i = -\frac{(1 - \phi_{bac})}{\tilde{\phi}_1} (\tilde{U}_1 k_x i + \tilde{V}_1 k_y i) - \Gamma \frac{\Delta \rho}{\rho_l}. \quad (\text{D.68})$$

In order for the growth rate and frequency to be spatially dependent the following equation must be satisfied

$$x \left(\frac{\partial k_x}{\partial t} + k_x \Gamma \frac{\Delta \rho}{2\rho_l} + k_y \right) + y \left(\frac{\partial k_y}{\partial t} + k_y \Gamma \frac{\Delta \rho}{2\rho_l} \right) = 0. \quad (\text{D.69})$$

Both the vertical and horizontal components of this equation must be zero. The vertical term is given by

$$\frac{\partial k_y}{\partial t} + k_y \Gamma \frac{\Delta \rho}{2\rho_l} = 0 \quad (\text{D.70})$$

which has the solution $k_y = k_{y0} e^{-\Gamma \frac{\Delta \rho}{2\rho_l} t}$. The horizontal component is given by

$$\frac{\partial k_x}{\partial t} + k_x \Gamma \frac{\Delta \rho}{2\rho_l} + k_y = 0 \quad (\text{D.71})$$

by substituting in the solution for k_y this becomes

$$\frac{\partial k_x}{\partial t} + k_x \Gamma \frac{\Delta \rho}{2\rho_l} + k_{y_0} e^{-\Gamma \frac{\Delta \rho}{2\rho_l} t} = 0 \quad (\text{D.72})$$

which has the solution $k_x = e^{-\Gamma \frac{\Delta \rho}{2\rho_l} t} (k_{x_0} + k_{y_0} t)$.

D.2.3 Fluid Force Balance

The first order fluid force balance equation is expressed as

$$\nabla \cdot \vec{U}_{bac} + \nabla \cdot \vec{U}_1 - \nabla \cdot [(\kappa_{bac} + \kappa_1) \nabla (p_{bac} + p_1)] = -\frac{w_0}{U_0} (1 - \phi_{bac}) \nabla \cdot (\kappa_{bac} + \kappa_1) \hat{j} + \Gamma \frac{\Delta \rho}{\rho_l}. \quad (\text{D.73})$$

By substituting in $\nabla \cdot \vec{U}_{bac} = \Gamma \frac{\Delta \rho}{\rho_l}$ and $p_{bac} = 0$ this becomes

$$\cancel{\Gamma \frac{\Delta \rho}{\rho_l}} + \nabla \cdot \vec{U}_1 - \nabla \cdot [(\kappa_{bac} + \kappa_1) \nabla p_1] = -\frac{w_0}{U_0} (1 - \phi_{bac}) \nabla \cdot (\kappa_{bac} + \kappa_1) \hat{j} + \cancel{\Gamma \frac{\Delta \rho}{\rho_l}} \quad (\text{D.74})$$

This simplifies to

$$\nabla \cdot \vec{U}_1 - \nabla \cdot [\kappa_{bac} \nabla p_1 + \kappa_1 \nabla p_1] = -\frac{w_0}{U_0} (1 - \phi_{bac}) (\nabla \cdot \kappa_{bac} \hat{j} + \nabla \cdot \kappa_1 \hat{j}) \quad (\text{D.75})$$

which, by neglecting second order terms and substituting in first order permeability (Eq D.57), further simplifies to

$$\nabla \cdot \vec{U}_1 - \kappa_{bac} \nabla^2 p_1 = -\frac{w_0}{U_0} (1 - \phi_{bac}) \frac{\beta}{\phi_0} \left(\frac{\phi_{bac}}{\phi_0} \right)^{\beta-1} \frac{\partial \phi_1}{\partial y}. \quad (\text{D.76})$$

Taking the Fourier transform of this equation yields

$$\tilde{U}_1 k_x i + \tilde{V}_1 k_y i - \kappa_{bac} \tilde{p}_1 (k_x^2 + k_y^2) i^2 = -\frac{w_0}{U_0} (1 - \phi_{bac}) \frac{\beta}{\phi_0} \left(\frac{\phi_{bac}}{\phi_0} \right)^{\beta-1} \tilde{\phi}_1 k_y i \quad (\text{D.77})$$

which can be rewritten as

$$\tilde{U}_1 k_x i + \tilde{V}_1 k_y i + \tilde{p}_1 \kappa_{bac} (k_x^2 + k_y^2) = -\tilde{\phi}_1 \frac{w_0}{U_0} (1 - \phi_{bac}) \frac{\beta}{\phi_0} \left(\frac{\phi_{bac}}{\phi_0} \right)^{\beta-1} k_y i. \quad (\text{D.78})$$

D.2.4 Solid Force Balance

The first component of the first order solid force balance equation is given by

$$\begin{aligned} \frac{\partial}{\partial x}(p_{bac} + p_1) - \frac{\partial}{\partial x} \left((\zeta_r + \frac{4}{3})\eta \frac{\partial}{\partial x}(U_{bac} + U_1) + (\zeta_r - \frac{2}{3})\eta \frac{\partial}{\partial y}(V_{bac} + V_1) \right) \\ - \frac{\partial}{\partial y} \eta \left(\frac{\partial}{\partial y}(U_{bac} + U_1) + \frac{\partial}{\partial x}(V_{bac} + V_1) \right) = 0. \end{aligned} \quad (D.79)$$

By substituting in first order variables this becomes

$$\begin{aligned} \frac{\partial p_1}{\partial x} - \frac{\partial}{\partial x} \left((\zeta_r + \frac{4}{3})(\eta_{bac} + \eta_1) \left(\frac{\partial U_1}{\partial x} + \Gamma \frac{\Delta \rho}{2\rho_l} \right) + (\zeta_r - \frac{2}{3})(\eta_{bac} + \eta_1) \left(\frac{\partial V_1}{\partial y} + \Gamma \frac{\Delta \rho}{2\rho_l} \right) \right) \\ - \frac{\partial}{\partial y} (\eta_{bac} + \eta_1) \left(\frac{\partial U_1}{\partial y} + \frac{\partial V_1}{\partial x} + 1 \right) = 0. \end{aligned} \quad (D.80)$$

Neglecting second order terms and since η_{bac} does not vary spatially this simplifies to

$$\begin{aligned} -\frac{\partial p_1}{\partial x} + (\zeta_r + \frac{4}{3})\eta_{bac} \frac{\partial^2 U_1}{\partial x^2} + (\zeta_r + \frac{4}{3})\Gamma \frac{\Delta \rho}{2\rho_l} \frac{\partial \eta_1}{\partial x} + (\zeta_r - \frac{2}{3})\eta_{bac} \frac{\partial^2 V_1}{\partial x \partial y} \\ + (\zeta_r - \frac{2}{3})\Gamma \frac{\Delta \rho}{2\rho_l} \frac{\partial \eta_1}{\partial x} + \eta_{bac} \frac{\partial^2 U_1}{\partial y^2} + \eta_{bac} \frac{\partial^2 V_1}{\partial x \partial y} + \frac{\partial \eta_1}{\partial y} = 0 \end{aligned} \quad (D.81)$$

which can be further simplified to

$$\begin{aligned} -\frac{\partial p_1}{\partial x} + (\zeta_r + \frac{4}{3})\eta_{bac} \frac{\partial^2 U_1}{\partial x^2} + (\zeta_r + \frac{1}{3})\Gamma \frac{\Delta \rho}{\rho_l} \frac{\partial \eta_1}{\partial x} + (\zeta_r - \frac{2}{3})\eta_{bac} \frac{\partial^2 V_1}{\partial x \partial y} \\ + \eta_{bac} \frac{\partial^2 U_1}{\partial y^2} + \eta_{bac} \frac{\partial^2 V_1}{\partial x \partial y} + \frac{\partial \eta_1}{\partial y} = 0. \end{aligned} \quad (D.82)$$

The spatial derivatives of η_1 are given by

$$\frac{\partial \eta_1}{\partial x} = \eta_{bac} \frac{\partial}{\partial x} \left(\frac{(1-n_v)}{2n_v} \left((\Gamma \frac{\Delta \rho}{\rho_l})^2 + 2(\Gamma \frac{\Delta \rho}{\rho_l} \frac{\partial U_1}{\partial x} + \frac{\partial U_1}{\partial y}) + 2(\Gamma \frac{\Delta \rho}{\rho_l} \frac{\partial V_1}{\partial y} + \frac{\partial V_1}{\partial x}) \right) \right) + \frac{\alpha}{n_v} \eta_{bac} \frac{\partial \phi_1}{\partial x} \quad (D.83)$$

which simplifies to

$$\frac{\partial \eta_1}{\partial x} = \eta_{bac} \frac{(1-n_v)}{n_v} \left(\Gamma \frac{\Delta \rho}{\rho_l} \frac{\partial^2 U_1}{\partial x^2} + \frac{\partial^2 U_1}{\partial x \partial y} + \Gamma \frac{\Delta \rho}{\rho_l} \frac{\partial^2 V_1}{\partial x \partial y} + \frac{\partial^2 V_1}{\partial x^2} \right) + \frac{\alpha}{n_v} \eta_{bac} \frac{\partial \phi_1}{\partial x} \quad (D.84)$$

and

$$\frac{\partial \eta_1}{\partial y} = \eta_{bac} \frac{\partial}{\partial y} \left(\frac{(1-n_v)}{2n_v} \left((\Gamma \frac{\Delta \rho}{\rho_l})^2 + 2(\Gamma \frac{\Delta \rho}{\rho_l} \frac{\partial U_1}{\partial x} + \frac{\partial U_1}{\partial y}) + 2(\Gamma \frac{\Delta \rho}{\rho_l} \frac{\partial V_1}{\partial y} + \frac{\partial V_1}{\partial x}) \right) \right) + \frac{\alpha}{n_v} \eta_{bac} \frac{\partial \phi_1}{\partial y} \quad (D.85)$$

which simplifies to

$$\frac{\partial \eta_1}{\partial y} = \eta_{bac} \frac{(1-n_v)}{n_v} \left(\Gamma \frac{\Delta \rho}{\rho_l} \frac{\partial^2 U_1}{\partial x \partial y} + \frac{\partial^2 U_1}{\partial y^2} + \Gamma \frac{\Delta \rho}{\rho_l} \frac{\partial^2 V_1}{\partial y^2} + \frac{\partial^2 V_1}{\partial x \partial y} \right) + \frac{\alpha}{n_v} \eta_{bac} \frac{\partial \phi_1}{\partial y}. \quad (D.86)$$

Substituting Eq D.86 and D.86 into Eq D.82 yields the expression

$$\begin{aligned}
& -\frac{\partial p_1}{\partial x} + (\zeta_r + \frac{4}{3})\eta_{bac} \frac{\partial^2 U_1}{\partial x^2} + (\zeta_r + \frac{1}{3})\Gamma \frac{\Delta \rho}{\rho_l} \left(\eta_{bac} \frac{(1-n_v)}{n_v} \left(\Gamma \frac{\Delta \rho}{\rho_l} \frac{\partial^2 U_1}{\partial x^2} + \frac{\partial^2 U_1}{\partial x \partial y} \right. \right. \\
& \quad \left. \left. + \Gamma \frac{\Delta \rho}{\rho_l} \frac{\partial^2 V_1}{\partial x \partial y} + \frac{\partial^2 V_1}{\partial x^2} \right) + \frac{\alpha}{n_v} \eta_{bac} \frac{\partial \phi_1}{\partial x} \right) + (\zeta_r - \frac{2}{3})\eta_{bac} \frac{\partial^2 V_1}{\partial x \partial y} + \eta_{bac} \frac{\partial^2 U_1}{\partial y^2} + \eta_{bac} \frac{\partial^2 V_1}{\partial x \partial y} \\
& \quad + \eta_{bac} \frac{(1-n_v)}{n_v} \left(\Gamma \frac{\Delta \rho}{\rho_l} \frac{\partial^2 U_1}{\partial x \partial y} + \frac{\partial^2 U_1}{\partial y^2} + \Gamma \frac{\Delta \rho}{\rho_l} \frac{\partial^2 V_1}{\partial y^2} + \frac{\partial^2 V_1}{\partial x \partial y} \right) + \frac{\alpha}{n_v} \eta_{bac} \frac{\partial \phi_1}{\partial y} = 0.
\end{aligned} \tag{D.87}$$

Taking the Fourier transform of this equation gives

$$\begin{aligned}
& -i\tilde{p}_1 k_x + (\zeta_r + \frac{4}{3})\eta_{bac} i^2 \tilde{U}_1 k_x^2 + (\zeta_r + \frac{1}{3})\Gamma \frac{\Delta \rho}{\rho_l} \left(\eta_{bac} \frac{(1-n_v)}{n_v} \left(\Gamma \frac{\Delta \rho}{\rho_l} i^2 \tilde{U}_1 k_x^2 + i^2 \tilde{U}_1 k_x k_y \right. \right. \\
& \quad \left. \left. + \Gamma \frac{\Delta \rho}{\rho_l} i^2 \tilde{V}_1 k_x k_y + i^2 \tilde{V}_1 k_x^2 \right) + \frac{\alpha}{n_v} \eta_{bac} i \phi_1 k_x \right) + (\zeta_r - \frac{2}{3})\eta_{bac} i^2 \tilde{V}_1 k_x k_y + \eta_{bac} i^2 \tilde{U}_1 k_y^2 + \eta_{bac} i^2 \tilde{V}_1 k_x k_y \\
& \quad + \eta_{bac} \frac{(1-n_v)}{n_v} \left(\Gamma \frac{\Delta \rho}{\rho_l} i^2 \tilde{U}_1 k_x k_y + i^2 \tilde{U}_1 k_y^2 + \Gamma \frac{\Delta \rho}{\rho_l} i^2 \tilde{V}_1 k_y^2 + i^2 \tilde{V}_1 k_x k_y \right) + \frac{\alpha}{n_v} \eta_{bac} i \tilde{\phi}_1 k_y = 0.
\end{aligned} \tag{D.88}$$

which can be rewritten as

$$\begin{aligned}
& -\tilde{p}_1 k_x \\
& + \tilde{U}_1 i \left[(\zeta_r + \frac{4}{3})\eta_{bac} k_x^2 + \eta_{bac} k_y^2 + (\zeta_r + \frac{1}{3})\Gamma \frac{\Delta \rho}{\rho_l} \eta_{bac} \frac{(1-n_v)}{n_v} (\Gamma \frac{\Delta \rho}{\rho_l} k_x^2 + k_x k_y) + \eta_{bac} \frac{(1-n_v)}{n_v} (\Gamma \frac{\Delta \rho}{\rho_l} k_x k_y + k_y^2) \right] \\
& + \tilde{V}_1 i \left[(\zeta_r + \frac{1}{3})\eta_{bac} k_x k_y + (\zeta_r + \frac{1}{3})\Gamma \frac{\Delta \rho}{\rho_l} \eta_{bac} \frac{(1-n_v)}{n_v} (\Gamma \frac{\Delta \rho}{\rho_l} k_x k_y + k_x^2) + \eta_{bac} \frac{(1-n_v)}{n_v} (\Gamma \frac{\Delta \rho}{\rho_l} k_y^2 + k_x k_y) \right] \\
& = -\tilde{\phi} \left[(\zeta_r + \frac{1}{3})\Gamma \frac{\Delta \rho}{\rho_l} \frac{\alpha}{n_v} \eta_{bac} k_x + \frac{\alpha}{n_v} \eta_{bac} k_y \right].
\end{aligned} \tag{D.89}$$

The first order of the second component of the solid force balance equation is given by

$$\begin{aligned}
& \frac{\partial}{\partial y} (\cancel{p_{bac}} + p_1) - \frac{\partial}{\partial x} \left((\eta_{bac} + \eta_1) \left(\frac{\partial}{\partial y} (U_{bac} + U_1) + \frac{\partial}{\partial x} (V_{bac} + V_1) \right) \right) \\
& \quad - \frac{\partial}{\partial y} \left((\zeta_r - \frac{2}{3})(\eta_{bac} + \eta_1) \frac{\partial}{\partial x} (U_{bac} + U_1) + (\zeta_r + \frac{4}{3})(\eta_{bac} + \eta_1) \frac{\partial}{\partial y} (V_{bac} + V_1) \right) \\
& \quad = \frac{w_0}{U_0} ((\cancel{\phi_{bac}} + \phi_1) - \cancel{\phi_{bac}}).
\end{aligned} \tag{D.90}$$

Substituting in first order variables yields the equation

$$\begin{aligned}
& \frac{\partial p_1}{\partial y} - \frac{\partial}{\partial x} \left((\eta_{bac} + \eta_1) \left(\frac{\partial U_1}{\partial y} + \frac{\partial V_1}{\partial x} + 1 \right) \right) - \frac{\partial}{\partial y} \left((\zeta_r - \frac{2}{3})(\eta_{bac} + \eta_1) \left(\frac{\partial U_1}{\partial x} + \Gamma \frac{\Delta \rho}{2\rho_l} \right) \right. \\
& \quad \left. + (\zeta_r + \frac{4}{3})(\eta_{bac} + \eta_1) \left(\frac{\partial V_1}{\partial y} + \Gamma \frac{\Delta \rho}{2\rho_l} \right) \right) = \frac{w_0}{U_0} \phi_1
\end{aligned} \tag{D.91}$$

Neglecting second order terms and since η_{bac} does not vary spatially this simplifies to

$$-\frac{\partial p_1}{\partial y} + \eta_0 \frac{\partial^2 U_1}{\partial x \partial y} + \eta_0 \frac{\partial^2 V_1}{\partial x^2} + \frac{\partial \eta_1}{\partial x} + (\zeta_r - \frac{1}{3}) \frac{\partial \eta_1}{\partial y} \Gamma \frac{\Delta \rho}{\rho_l} + (\zeta_r - \frac{2}{3}) \eta_{bac} \frac{\partial^2 U_1}{\partial x \partial y} + (\zeta_r + \frac{2}{3}) \frac{\partial \eta_1}{\partial y} \Gamma \frac{\Delta \rho}{\rho_l} + (\zeta_r + \frac{4}{3}) \eta_{bac} \frac{\partial^2 V_1}{\partial y^2} = -\frac{w_0}{U_0} \phi_1 \quad (\text{D.92})$$

which can be rewritten as

$$-\frac{\partial p_1}{\partial y} + \eta_0 \frac{\partial^2 U_1}{\partial x \partial y} + \eta_0 \frac{\partial^2 V_1}{\partial x^2} + \frac{\partial \eta_1}{\partial x} + (\zeta_r - \frac{2}{3}) \eta_{bac} \frac{\partial^2 U_1}{\partial x \partial y} + (\zeta_r + \frac{1}{3}) \frac{\partial \eta_1}{\partial y} \Gamma \frac{\Delta \rho}{\rho_l} + (\zeta_r + \frac{4}{3}) \eta_{bac} \frac{\partial^2 V_1}{\partial y^2} = -\frac{w_0}{U_0} \phi_1. \quad (\text{D.93})$$

By substituting in the spatial derivatives of η_1 (Eq D.86 and D.86) this becomes

$$-\frac{\partial p_1}{\partial y} + \eta_0 \frac{\partial^2 U_1}{\partial x \partial y} + \eta_0 \frac{\partial^2 V_1}{\partial x^2} + \eta_{bac} \frac{(1-n_v)}{n_v} \left(\Gamma \frac{\Delta \rho}{\rho_l} \frac{\partial^2 U_1}{\partial x^2} + \frac{\partial^2 U_1}{\partial x \partial y} + \Gamma \frac{\Delta \rho}{\rho_l} \frac{\partial^2 V_1}{\partial x \partial y} + \frac{\partial^2 V_1}{\partial x^2} \right) + \frac{\alpha}{n_v} \eta_{bac} \frac{\partial \phi_1}{\partial x} + (\zeta_r - \frac{2}{3}) \eta_{bac} \frac{\partial^2 U_1}{\partial x \partial y} + (\zeta_r + \frac{1}{3}) \Gamma \frac{\Delta \rho}{\rho_l} \left(\eta_{bac} \frac{(1-n_v)}{n_v} \left(\Gamma \frac{\Delta \rho}{\rho_l} \frac{\partial^2 U_1}{\partial x \partial y} + \frac{\partial^2 U_1}{\partial y^2} + \Gamma \frac{\Delta \rho}{\rho_l} \frac{\partial^2 V_1}{\partial y^2} + \frac{\partial^2 V_1}{\partial x \partial y} \right) + \frac{\alpha}{n_v} \eta_{bac} \frac{\partial \phi_1}{\partial y} \right) \Gamma \frac{\Delta \rho}{\rho_l} + (\zeta_r + \frac{4}{3}) \eta_{bac} \frac{\partial^2 V_1}{\partial y^2} = -\frac{w_0}{U_0} \phi_1. \quad (\text{D.94})$$

Taking the Fourier transform of this expression gives

$$-i\tilde{p}_1 k_y + \eta_0 i^2 \tilde{U}_1 k_x k_y + \eta_0 i^2 \tilde{V}_1 k_x^2 + \eta_{bac} \frac{(1-n_v)}{n_v} \left(\Gamma \frac{\Delta \rho}{\rho_l} i^2 \tilde{U}_1 k_x^2 + i^2 \tilde{U}_1 k_x k_y + \Gamma \frac{\Delta \rho}{\rho_l} i^2 \tilde{V}_1 k_x k_y + i^2 \tilde{V}_1 k_x^2 \right) + \frac{\alpha}{n_v} \eta_{bac} i \tilde{\phi}_1 k_x + (\zeta_r - \frac{2}{3}) \eta_{bac} i^2 \tilde{U}_1 k_x k_y + (\zeta_r + \frac{1}{3}) \Gamma \frac{\Delta \rho}{\rho_l} \left(\eta_{bac} \frac{(1-n_v)}{n_v} \left(\Gamma \frac{\Delta \rho}{\rho_l} i^2 \tilde{U}_1 k_x k_y + i^2 \tilde{U}_1 k_y^2 + \Gamma \frac{\Delta \rho}{\rho_l} i^2 \tilde{V}_1 k_y^2 + i^2 \tilde{V}_1 k_x k_y \right) + \frac{\alpha}{n_v} \eta_{bac} i \tilde{\phi}_1 k_y \right) \Gamma \frac{\Delta \rho}{\rho_l} + (\zeta_r + \frac{4}{3}) \eta_{bac} i^2 \tilde{V}_1 k_y^2 = -\frac{w_0}{U_0} \tilde{\phi}_1. \quad (\text{D.95})$$

which simplifies to

$$-\tilde{p}_1 k_y + \eta_0 i \tilde{V}_1 k_x^2 + \eta_{bac} \frac{(1-n_v)}{n_v} \left(\Gamma \frac{\Delta \rho}{\rho_l} i \tilde{U}_1 k_x^2 + i \tilde{U}_1 k_x k_y + \Gamma \frac{\Delta \rho}{\rho_l} i \tilde{V}_1 k_x k_y + i \tilde{V}_1 k_x^2 \right) + \frac{\alpha}{n_v} \eta_{bac} \tilde{\phi}_1 k_x + (\zeta_r + \frac{1}{3}) \eta_{bac} i \tilde{U}_1 k_x k_y + (\zeta_r + \frac{1}{3}) \Gamma \frac{\Delta \rho}{\rho_l} \left(\eta_{bac} \frac{(1-n_v)}{n_v} \left(\Gamma \frac{\Delta \rho}{\rho_l} i \tilde{U}_1 k_x k_y + i \tilde{U}_1 k_y^2 + \Gamma \frac{\Delta \rho}{\rho_l} i \tilde{V}_1 k_y^2 + i \tilde{V}_1 k_x k_y \right) + \frac{\alpha}{n_v} \eta_{bac} \tilde{\phi}_1 k_y \right) \Gamma \frac{\Delta \rho}{\rho_l} + (\zeta_r + \frac{4}{3}) \eta_{bac} i \tilde{V}_1 k_y^2 = \frac{w_0}{U_0} \tilde{\phi}_1 \quad (\text{D.96})$$

This can be rewritten to isolate the variables which obtains

$$\begin{aligned}
& -\tilde{p}_1 k_y \\
& + \tilde{U}_1 i \left[\left(\zeta_r + \frac{1}{3} \right) \eta_{bac} k_x k_y + \eta_{bac} \frac{(1-n_v)}{n_v} \left(\Gamma \frac{\Delta \rho}{\rho_l} k_x^2 + k_x k_y \right) + \left(\zeta_r + \frac{1}{3} \right) \Gamma \frac{\Delta \rho}{\rho_l} \eta_{bac} \frac{(1-n_v)}{n_v} \left(\Gamma \frac{\Delta \rho}{\rho_l} k_x k_y + k_y^2 \right) \right] \\
& + \tilde{V}_1 i \left[\eta_{bac} k_x^2 + \left(\zeta_r + \frac{4}{3} \right) \eta_{bac} k_y^2 + \eta_{bac} \frac{(1-n_v)}{n_v} \left(\Gamma \frac{\Delta \rho}{\rho_l} k_x k_y + k_x^2 \right) + \left(\zeta_r + \frac{1}{3} \right) \Gamma \frac{\Delta \rho}{\rho_l} \eta_{bac} \frac{(1-n_v)}{n_v} \left(\Gamma \frac{\Delta \rho}{\rho_l} k_y^2 + k_x k_y \right) \right] \\
& = \tilde{\phi} \left[-\frac{\alpha}{n_v} \eta_{bac} k_x - \left(\zeta_r + \frac{1}{3} \right) \Gamma \frac{\Delta \rho}{\rho_l} \frac{\alpha}{n_v} \eta_{bac} k_y + \frac{w_0}{U_0} i \right]. \tag{D.97}
\end{aligned}$$

D.2.5 Bringing It All Together

The first order governing equations in Fourier space can be written as

$$\begin{aligned}
& \tilde{U}_1 i \left[\begin{array}{c} k_x \\ \left(\zeta_r + \frac{4}{3} \right) \eta_{bac} k_x^2 + \eta_{bac} k_y^2 + \left(\zeta_r + \frac{1}{3} \right) \Gamma \frac{\Delta \rho}{\rho_l} \eta_{bac} \frac{(1-n_v)}{n_v} \left(\Gamma \frac{\Delta \rho}{\rho_l} k_x^2 + k_x k_y \right) + \eta_{bac} \frac{(1-n_v)}{n_v} \left(\Gamma \frac{\Delta \rho}{\rho_l} k_x k_y + k_y^2 \right) \\ \left(\zeta_r + \frac{1}{3} \right) \eta_{bac} k_x k_y + \eta_{bac} \frac{(1-n_v)}{n_v} \left(\Gamma \frac{\Delta \rho}{\rho_l} k_x^2 + k_x k_y \right) + \left(\zeta_r + \frac{1}{3} \right) \Gamma \frac{\Delta \rho}{\rho_l} \eta_{bac} \frac{(1-n_v)}{n_v} \left(\Gamma \frac{\Delta \rho}{\rho_l} k_x k_y + k_y^2 \right) \end{array} \right] \\
& + \tilde{V}_1 i \left[\begin{array}{c} k_y \\ \left(\zeta_r + \frac{1}{3} \right) \eta_{bac} k_x k_y + \left(\zeta_r + \frac{1}{3} \right) \Gamma \frac{\Delta \rho}{\rho_l} \eta_{bac} \frac{(1-n_v)}{n_v} \left(\Gamma \frac{\Delta \rho}{\rho_l} k_x k_y + k_x^2 \right) + \eta_{bac} \frac{(1-n_v)}{n_v} \left(\Gamma \frac{\Delta \rho}{\rho_l} k_y^2 + k_x k_y \right) \\ \eta_{bac} k_x^2 + \left(\zeta_r + \frac{4}{3} \right) \eta_{bac} k_y^2 + \eta_{bac} \frac{(1-n_v)}{n_v} \left(\Gamma \frac{\Delta \rho}{\rho_l} k_x k_y + k_x^2 \right) + \left(\zeta_r + \frac{1}{3} \right) \Gamma \frac{\Delta \rho}{\rho_l} \eta_{bac} \frac{(1-n_v)}{n_v} \left(\Gamma \frac{\Delta \rho}{\rho_l} k_y^2 + k_x k_y \right) \end{array} \right] \\
& + \tilde{p}_1 \left[\begin{array}{c} \kappa_{bac} (k_x^2 + k_y^2) \\ -k_x \\ -k_y \end{array} \right] = \tilde{\phi}_1 \left[\begin{array}{c} -\frac{w_0}{U_0} (1 - \phi_{bac}) \frac{\beta}{\phi_0} \left(\frac{\phi_{bac}}{\phi_0} \right)^{\beta-1} k_y i \\ -\frac{\alpha}{n_v} \eta_{bac} \left(\left(\zeta_r + \frac{1}{3} \right) \Gamma \frac{\Delta \rho}{\rho_l} k_x + k_y \right) \\ -\frac{\alpha}{n_v} \eta_{bac} \left(k_x + \left(\zeta_r + \frac{1}{3} \right) \Gamma \frac{\Delta \rho}{\rho_l} k_y \right) + \frac{w_0}{U_0} i \end{array} \right]. \tag{D.98}
\end{aligned}$$

Matrix manipulation is used to find \tilde{U}_1 and \tilde{V}_1 which are then used to find the growth rate.

D.3 Growth Rate

Recall the equation found from the conservation of solid mass equation:

$$\frac{\partial s}{\partial t} - i \frac{\partial \omega}{\partial t} = (1 - \phi_{bac}) (k_x i \tilde{U}_1 + k_y i \tilde{V}_1) - \Gamma \frac{\Delta \rho}{\rho_l} \tag{D.99}$$

where the real component gives the growth rate.

D.3.1 Variable Bulk Viscosity

The growth rate for the variable bulk viscosity and isotropic expansion is found by substituting the equations for \tilde{U}_1 and \tilde{V}_1 found by solving eq D.98 into the equation for the growth rate. This yields the equation

$$\frac{\partial s}{\partial t} = \frac{\frac{\alpha}{n_v} \eta_{bac} \kappa_{bac} k^4 (6k_x k_y + \Gamma \frac{\Delta \rho}{\rho_l} k^2 (1 + 3\zeta_r)) (\phi_{bac} - 1)}{d_r} - \Gamma \frac{\Delta \rho}{\rho_l} \quad (\text{D.100})$$

where the denominator is given by

$$d_r = \frac{1-n_v}{n_v} \left(2\eta_{bac} \Gamma \frac{\Delta \rho}{\rho_l} \kappa_{bac} k_x k_y k^4 (4 + 3\zeta_r) + (k_x^6 + k_y^6) \psi_r + 3k_x^4 + k_x^2 k_y^2 (\sigma_r - 6) + k_x^4 (3 + \sigma_r) \right) + k^4 (3 + \eta_{bac} \kappa_{bac} k^2 (4 + 3\zeta_r)) \quad (\text{D.101})$$

and where $\sigma_r = \eta_{bac} \kappa_{bac} k_y^2 (8 - 3\zeta_r + (\Gamma \frac{\Delta \rho}{\rho_l})^2 (3 + 9\zeta_r))$ and $\psi_r = \eta_{bac} \kappa_{bac} (4 + (\Gamma \frac{\Delta \rho}{\rho_l})^2 + 3(1 + (\Gamma \frac{\Delta \rho}{\rho_l})^2) \zeta_r)$. For the strain rate independent case, $n_v = 1$, this simplifies to

$$\frac{\partial s}{\partial t} = \frac{\alpha \eta_{bac} \kappa_{bac} (6k_x k_y + \Gamma \frac{\Delta \rho}{\rho_l} k^2 (1 + 3\zeta_r)) (\phi_{bac} - 1)}{3 + \eta_{bac} \kappa_{bac} k^2 (4 + 3\zeta_r)} - \Gamma \frac{\Delta \rho}{\rho_l}. \quad (\text{D.102})$$

If no shear is applied to the system, i.e. $U_{bac} = U_{melt}$, the growth rate is found to be

$$\frac{\partial s}{\partial t} = \Gamma \frac{\Delta \rho}{\rho_l} \left(\frac{\alpha \eta_{bac} \kappa_{bac} k^2 (1 + 3\zeta_r) (\phi_{bac} - 1)}{3 + \eta_{bac} \kappa_{bac} k^2 (4 + 3\zeta_r)} - 1 \right). \quad (\text{D.103})$$

D.3.2 Constant Bulk Viscosity

The derivation outlined in this appendix is repeated for the constant bulk viscosity case including isotropic expansion. The Fourier transform of the governing equations for this case

are found to be

$$\begin{aligned}
& \tilde{U}_1 i \begin{bmatrix} k_x \\ (\zeta + \frac{4}{3}\eta_{bac})k_x^2 + \eta_{bac}k_y^2 + \frac{1}{3}\Gamma\frac{\Delta\rho}{\rho_l}\eta_{bac}\frac{1-n_v}{n_v}(\Gamma\frac{\Delta\rho}{\rho_l}k_x^2 + k_xk_y) + \eta_{bac}\frac{1-n_v}{n_v}(\Gamma\frac{\Delta\rho}{\rho_l}k_xk_y + k_y^2) \\ (\zeta + \frac{1}{3}\eta_{bac})k_xk_y + \eta_{bac}\frac{1-n_v}{n_v}(\Gamma\frac{\Delta\rho}{\rho_l}k_x^2 + k_xk_y) + \frac{1}{3}\Gamma\frac{\Delta\rho}{\rho_l}\eta_{bac}\frac{1-n_v}{n_v}(\Gamma\frac{\Delta\rho}{\rho_l}k_xk_y + k_y^2) \end{bmatrix} \\
& + \tilde{V}_1 i \begin{bmatrix} k_y \\ (\zeta + \frac{1}{3}\eta_{bac})k_xk_y + \frac{1}{3}\Gamma\frac{\Delta\rho}{\rho_l}\eta_{bac}\frac{1-n_v}{n_v}(\Gamma\frac{\Delta\rho}{\rho_l}k_xk_y + k_x^2) + \eta_{bac}\frac{1-n_v}{n_v}(\Gamma\frac{\Delta\rho}{\rho_l}k_y^2 + k_xk_y) \\ \eta_{bac}k_x^2 + (\zeta + \frac{4}{3}\eta_{bac})k_y^2 + \eta_{bac}\frac{1-n_v}{n_v}(\Gamma\frac{\Delta\rho}{\rho_l}k_xk_y + k_x^2) + \frac{1}{3}\Gamma\frac{\Delta\rho}{\rho_l}\eta_{bac}\frac{1-n_v}{n_v}(\Gamma\frac{\Delta\rho}{\rho_l}k_y^2 + k_xk_y) \end{bmatrix} \\
& + \tilde{P}_1 \begin{bmatrix} \kappa_{bac}(k_x^2 + k_y^2) \\ -k_x \\ -k_y \end{bmatrix} = \tilde{\Phi}_1 \begin{bmatrix} -\frac{w_0}{U_0}(1 - \phi_{bac})\frac{\beta}{\phi_0}\left(\frac{\phi_{bac}}{\phi_0}\right)^{\beta-1}k_y i \\ -\frac{\alpha}{n_v}\eta_{bac}\left(\frac{1}{3}\Gamma\frac{\Delta\rho}{\rho_l}k_x + k_y\right) \\ -\frac{\alpha}{n_v}\eta_{bac}\left(k_x + \frac{1}{3}\Gamma\frac{\Delta\rho}{\rho_l}k_y\right) + \frac{w_0}{U_0}i \end{bmatrix}. \tag{D.104}
\end{aligned}$$

By substituting the equations for \tilde{U}_1 and \tilde{V}_1 found from the above equation into the growth rate equation yields

$$\frac{\partial s}{\partial t} = \frac{\frac{\alpha}{n_v}\eta_{bac}\kappa_{bac}k^4(6k_xk_y + \Gamma\frac{\Delta\rho}{\rho_l}k^2)(\phi_{bac} - 1)}{d_c} - \Gamma\frac{\Delta\rho}{\rho_l} \tag{D.105}$$

where the denominator is found to be

$$\begin{aligned}
d_c = & \frac{1-n_v}{n_v}(8\eta_{bac}\Gamma\frac{\Delta\rho}{\rho_l}\kappa_{bac}k_xk_yk^4 + (k_x^6 + k_y^6)\Psi_c + k_x^2k_y^2(\sigma_c - 6) + k_x^4(3 + \sigma_c) + 3k_y^4) \\
& + k^4(3 + k^2\kappa_{bac}(4\eta_{bac} + 3\zeta)) \tag{D.106}
\end{aligned}$$

and where $\sigma_c = \kappa_{bac}k_y^2(\eta_{bac}(8 + 3(\Gamma\frac{\Delta\rho}{\rho_l})^2) - 3\zeta)$ and $\Psi_c = \kappa_{bac}(\eta_{bac}(4 + (\Gamma\frac{\Delta\rho}{\rho_l})^2) + 3\zeta)$. For the strain rate independent viscosity case the growth rate is given by

$$\frac{\partial s}{\partial t} = \frac{\alpha\eta_{bac}\kappa_{bac}(\phi_{bac} - 1)(6k_xk_y + \Gamma\frac{\Delta\rho}{\rho_l}k^2)}{3 + \kappa_{bac}k^2(4\eta_{bac} + 3\zeta)} - \Gamma\frac{\Delta\rho}{\rho_l}. \tag{D.107}$$

When no applied shear is present the growth rate can be expressed as

$$\frac{\partial s}{\partial t} = \Gamma\frac{\Delta\rho}{\rho_l} \left(\frac{\alpha\eta_{bac}\kappa_{bac}k^2(\phi_{bac} - 1)}{3 + \kappa_{bac}k^2(4\eta_{bac} + 3\zeta)} - 1 \right). \tag{D.108}$$

D.4 Oscillation Frequency

The equation found from the conservation of solid mass equation is given by

$$\frac{\partial s}{\partial t} - i \frac{\partial \omega}{\partial t} = (1 - \phi_{bac})(k_x i \tilde{U}_1 + k_y i \tilde{V}_1) - \Gamma \frac{\Delta \rho}{\rho_l}. \quad (\text{D.109})$$

The imaginary component yields the oscillation frequency.

D.4.1 Variable Bulk Viscosity

The oscillation frequency for the variable bulk viscosity case is given by

$$\frac{\partial \omega}{\partial t} = \frac{w_0}{U_0} (1 - \phi_{bac}) \frac{n_f}{d_r} \quad (\text{D.110})$$

where the numerator is

$$n_f = 3\kappa_{bac} k_y k^4 - \kappa_{bac} \frac{1-n_v}{n_v} (k_x^4 - k_y^4) (3k_y + \Gamma \frac{\Delta \rho}{\rho_l} k_x (1 + 3\zeta_r)) + 3\kappa_1 k_y (k^4 + \frac{1-n_v}{n_v} (k_x^2 - k_y^2)^2) (\phi_{bac} - 1) \quad (\text{D.111})$$

The strain-rate independent case is given by

$$\frac{\partial \omega}{\partial t} = 3k_y (1 - \phi_{bac}) \frac{w_0}{U_0} \frac{\kappa_{bac} + \kappa_1 (\phi_{bac} - 1)}{3 + \eta_{bac} \kappa_{bac} k^2 (4 + 3\zeta_r)}. \quad (\text{D.112})$$

D.4.2 Constant Bulk Viscosity

The oscillatory frequency for the constant bulk viscosity case is given by

$$\frac{\partial \omega}{\partial t} = (1 - \phi_{bac}) \frac{w_0}{U_0} \frac{n_o}{d_c} \quad (\text{D.113})$$

where the numerator is

$$n_o = 3\kappa_{bac} k_y k^4 - \kappa_{bac} \frac{1-n_v}{n_v} (\Gamma \frac{\Delta \rho}{\rho_l} k_x + 3k_y) (k_x^4 - k_y^4) + 3\kappa_1 k_y (k^4 + \frac{1-n_v}{n_v} (k_x^2 - k_y^2)^2) (\phi_{bac} - 1). \quad (\text{D.114})$$

. The strain-rate independent case has the oscillation frequency of

$$\frac{\partial \omega}{\partial t} = 3k_y (1 - \phi_{bac}) \frac{w_0}{U_0} \frac{\kappa_{bac} + \kappa_1 (\phi_{bac} - 1)}{3 + \kappa_{bac} k^2 (4\eta_{bac} + 3\zeta)}. \quad (\text{D.115})$$